AFFDL-TR-74-108

[redacted]

REVIEW OF METHODS OF SOLUTION OF AFTERBODY/EXHAUST NOZZLE FLOW FIELDS

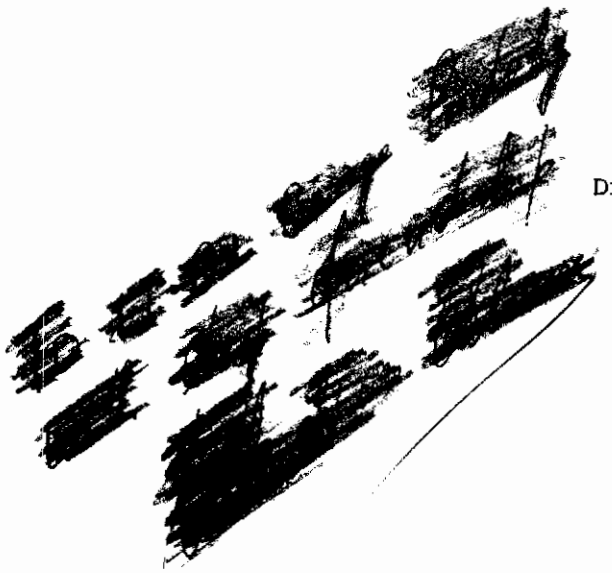

Dr. Wladimiro Calarese

FOREWORD

This report was prepared by Dr. Wladimiro Calarese of the Analysis Group, Flight Mechanics Division, Air Force Flight Dynamics Laboratory, Wright-Patterson Air Force Base, Ohio. The work was performed in-house in support of Project Nr. 14760204 and covers work conducted between January and June 1973.

This Technical Report has been reviewed and is approved.

PHILIP P. ANTONATOS
Director
Flight Mechanics Division

ABSTRACT

The present work consists of a review of methods of solution of afterbody/exhaust nozzle flow fields for different flight regimes. For the transonic regime airfoil solutions are also presented. A comparison between various theories and experiments is made wherever considered necessary to show the state-of-the-art. Most of the available theories are selected and correlated.

TABLE OF CONTENTS

TABLE OF CONTENTS (Continued)

LIST OF FIGURES

LIST OF FIGURES (Continued)

LIST OF FIGURES (Continued)

LIST OF FIGURES (Continued)

LIST OF FIGURES (Continued)

LIST OF SYMBOLS

A	Area
A_{BT}	Boattail Frontal Area
A_M	Afterbody Maximum Area
C	Chord
C_D	Pressure Drag Coefficient Based on Maximum Cross-Sectional Area
$\hat{C}_D$	Total Drag Coefficient (pressure and friction)
C_f	Skin Friction Coefficient
C_L	Lift Coefficient
C_p	Pressure Coefficient
C_T	Thrust Coefficient
d	Discriminating Streamline
D	Diameter
E	Energy per Unit Volume
jb	Jet Boundary Streamline
K	Transonic Simularity Parameter: $(1-M_\infty^2)/(M_\infty^2\tau)^{2/3}$
ℓ	Body Length
L	Length
M	Mach Number
MFR	Jet to Free Stream Momentum Flux Ratio $\gamma_j p_j A_j M_j^2/\gamma_\infty p_\infty A_\infty M_\infty^2$
p	Pressure
p_o	Total Pressure
q	Dynamic Head
r	Radial Distance from Body Surface, Perpendicular to Body Surface

LIST OF SYMBOLS (Continued)

R	Radial Distance from Body or Flow Axis, $\sqrt{Y^2+Z^2}$
$\mathcal{R}$	Gas Constant
Rl	Radius
Re	Reynolds Number
$S_l(X)$	Cross Sectional Area
t	Time
T	Temperature
T_o	Total Temperature
u	Perturbation Velocity Component in the X Direction
U	Velocity
v	Perturbation Velocity Component in the Y Direction
$\dot{w}$	Mass Flow Rate
x	Boundary Layer Coordinate in the Longitudinal Direction
X	Cartesian Coordinate in the Longitudinal Direction
y	Boundary Layer Coordinate in the Normal Direction
Y	Cartesian Coordinate in the Normal Direction
Z	Cartesian Coordinate in the Peripheral Direction
α	Angle of Attack
β_l	Boattail Angle
γ	Specific Heat Capacity Ratio
δ	Boundary Layer Thickness
Δ	Increment
δ^*	Boundary Layer Displacement Thickness
θ	Boundary Layer Momentum Thickness, Flow Deflection Angle, or Divergence Half Angle

LIST OF SYMBOLS (Continued)

$\lambda, \lambda_{pa}, \lambda_{pe}$	Transonic Parameters Defined in Equations 4,6, and 11 Respectively
μ	Viscosity
ξ	Dummy Variable
ρ	Density
$\hat{\rho}$	Radius of Curvature
τ	Thickness Ratio: D_M/ℓ
ϕ	Perturbation Velocity Potential
Φ	Velocity Potential
ω	Peripheral Angle (ω = o Being a Meridian Plane)

SUBSCRIPTS

α	Angle of Attack
a	Primary Stream Within the Two Stream Mixing Region, or Free Stream Adjacent to Mixing Region
A	Three-Dimensional Transonic
am	Ambient
b	Secondary Stream Within the Two Stream Mixing Region, Free Stream Adjacent to Mixing Region
B	Base
BT	Boattail (Afterbody + Nozzle)
C	Based on Chord
d	Discriminating Streamline
e	Local External Flow
eb	Equivalent Body
I	Internal
i	Incompressible
imp	Impingement Point
inc	Incipient Separation
j	Jet
jb	Inviscid Jet Boundary Streamline
m	Minimum Pressure Point
M	Maximum
N	Nozzle
n	Nose
p	Pitot
pl	Plateau
R	Partial Derivative with Respect to R

SUBSCRIPTS (Continued)

s	Separation Point
sb	Origin of Shock Wave-Boundary Layer Interaction
T	Transition
t	Partial Derivative with Respect to t
tk	Thickness
w	Wall Conditions
x	Based on x
X	Partial Derivative with Respect to X
Y	Partial Derivative with Respect to Y
Z	Partial Derivative with Respect to Z
1	Internal Point Ahead of Separation or Initial Conditions
2	Two-Dimensional
∞	Free Stream Conditions

SUPERSCRIPTS

*	Sonic Conditions
','','''	Ordinary Derivatives with Respect to the Specified Argument
~	Virtual Origin

ABBREVIATIONS

AFT-END	Afterbody + Nozzle + Base
C-D	Convergent-Divergent
C-F-L	Courant, Friedricks, Lewey
1-D	One-Dimensional
2-D	Two-Dimensional
3-D	Three-Dimensional
IMS	Integral Mean Slope
L.E.	Leading Edge
MOC	Method of Characteristics
PR	Nozzle Pressure Ratio $P_{o_N}/p_\infty = p_{oj}/p_\infty$
T.E.	Trailing Edge
V-T	Viscous Transonic

I. INTRODUCTION

Advanced tactical and strategic military aircraft are required to perform efficiently in the subsonic, transonic, and supersonic speed regimes, consequently the installed nozzle performance becomes increasingly important. Large decreases in aircraft performance may be attributed directly to the afterbody/exhaust nozzle flow field. This flow field is formed by a complicated interaction of the nozzle internal flow, the afterbody/nozzle external flow, and the jet plume, and also the interference effect of this combined flow on adjacent aerodynamic surfaces. It is important that the afterbody/exhaust nozzle flow field be accurately predicted to assess and optimize aircraft exhaust nozzle performance.

The use of improved computers has enabled engineers to develop new analytical techniques and improve existing ones. This technical report presents and reviews various state-of-the-art analytical techniques to predict the afterbody/exhaust nozzle flow field in the subsonic, transonic, and supersonic speed regimes and a qualitative analysis of transonic airfoil solutions. The analytical techniques are evaluated with respect to the theoretical basis and areas of application in a short summary presented at the end of each speed regime.

This technical report is based on the AFFDL report of Reference 1.

II. CRITICAL REVIEW

A. Subsonic Flow

1. External Flow

The external subsonic flow field over airfoils and bodies of revolution has been evaluated quite accurately using potential flow theory. At low free stream Mach numbers, the incompressible irrotational flow field is governed by the Laplace's equation for a velocity potential and the use of a gradient form of boundary conditions makes the problem one of the Neumann kind. Laplace's equation is easily solved, giving the flow field pressure and velocity components over specified boundaries. However the number of solutions available is small because of the difficulty of satisfying the boundary conditions. Some conformal transformations of the boundaries have been used to obtain more solutions. The inverse problem has also been solved, i.e. for a given distribution of known singularities, e.g. sources, sinks, etc., the flow field and the stream function are computed and any resulting streamline can be used as a boundary surface. This procedure is difficult in 3-D because of the nonexistence of a simple stream function (Ref. 2). "Exact" numerical methods, i.e. finite difference approximation of exact equations, or approximate methods, i.e. exact solution of approximate equations (slender body approximation), have been used.

The subsonic potential flow over arbitrary boundaries can be obtained as the solution of a Fredholm integral equation of the second kind for the source-density distribution over the boundary

surface. The advantage of this method is to reduce the dimensionality of the problem by one.

Goebel and Divita (Ref. 3) use this integral method. The subsonic external flow is calculated with a reduced version of the Douglass-Neumann Code (Refs. 4-5). The code can handle both 2-D and axisymmetric bodies. The inviscid low speed flow is corrected for compressibility effects by means of Gothert's rule, which consists of transforming the body contour into an equivalent incompressible body by multiplying the coordinate in the radial direction by $(1-M_\infty^2)^{1/2}$, solving the flow field for this new contour, and then dividing the pressure coefficients obtained by $(1-M_\infty^2)$. Solid and nonsolid boundaries can be used in the program. The body is represented by surface sources and sinks and can be placed at an angle of attack. Since linear algebraic equations are considered, the superposition principle is used to account for angle of attack effects. Velocity and pressure distributions can be obtained on the body surface and also in the flow field. The surface pressure distribution is shown in Figure 1. The agreement with the experimental data of Reference 6 is good up to the body plume junction where a slope discontinuity exists. This discontinuity results in a very high pressure rise in this region.

Lockheed-California Company (Ref. 7) and Rudman and Maise (Ref. 8) use the same method of solution but combine the inviscid solution with boundary layer computations. In so doing, they account for the displacement thickness effect and are able to avoid the high pressure rise at the body plume junction by smoothing out the boundary layer displacement streamline and extrapolating it

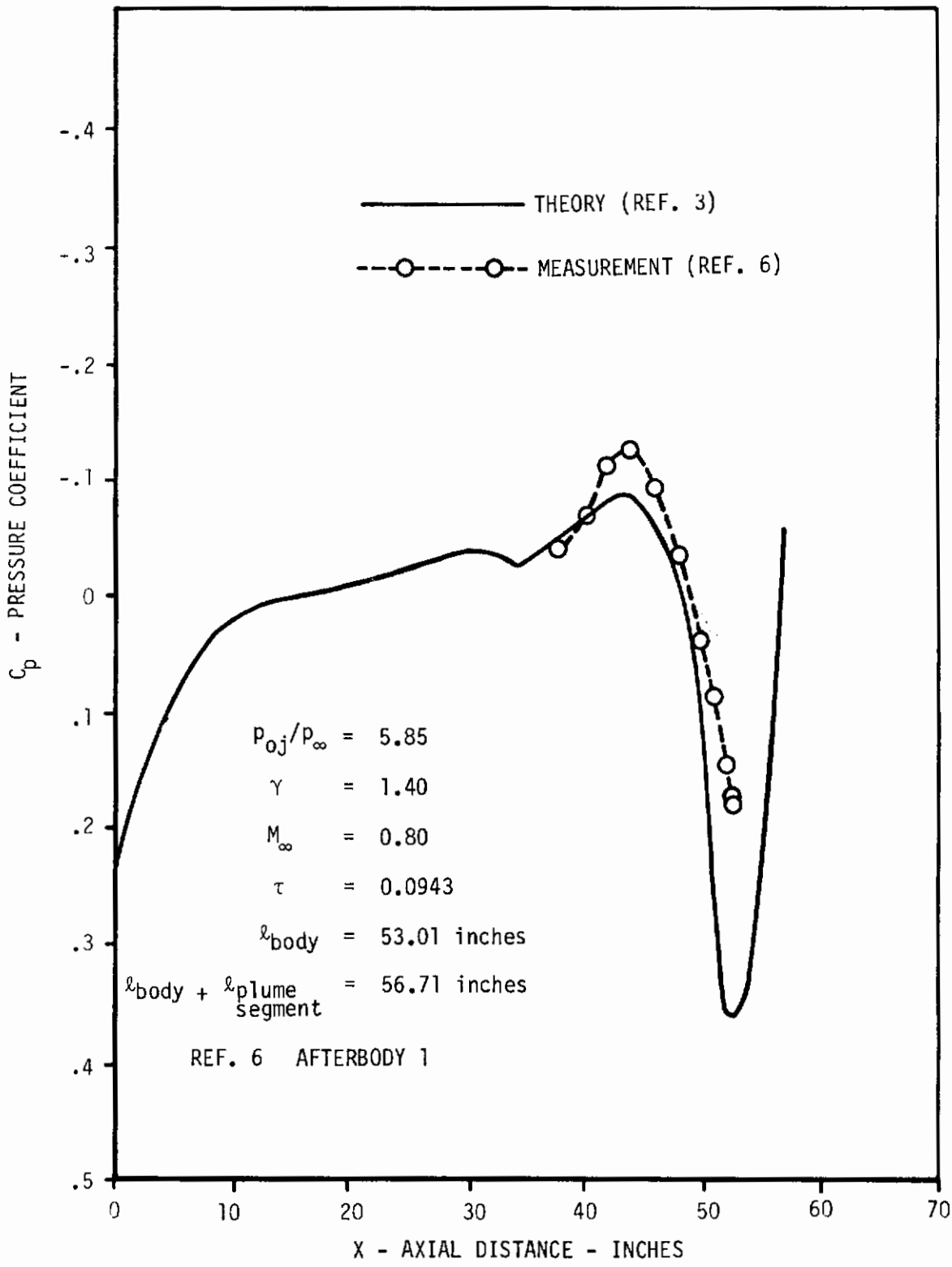

Figure 1. Pressure Distribution Over Body and Plume Segment (From Ref. 3)

downstream into the plume starting from the minimum slope point. The theory and the experimental data of Reference 9 are compared in Figure 2.

A different method to solve the subsonic flow over boattails and airfoils is devised by Moretti (Ref. 10) and Grossman (Refs. 11-12) and consists of using time dependent techniques in 2-D or axisymmetric cases. These techniques consist of writing the partial differential equations of motion in a suitable frame of reference and then, using mapping functions, transforming the region of computation into a square or a cube on which a rectangular mesh can be used with equally spaced mesh points. The differential equations are written as finite difference equations valid at discrete mesh points and integrated numerically for large values of time, since it is assumed that a bounded, steady state solution exists in the limit as time goes to infinity. Different provisions are made for interior points, rigid wall points, symmetry lines, and arbitrary boundaries. In Reference 10 the equations of motion which are expressed upon transformation in new independent variables are of the form

$$f_t + \alpha f_X + \beta f_Y + \varepsilon = 0 \qquad (1)$$

where X,Y are space variables and t is the time variable. α and β are matrices which depend on the mapping function and on the coefficients of the original equations of motion. f is any vector whose components are the unknown variables and ε is a vector which includes viscous effects (identically equal to zero for inviscid cases expressed in Cartesian coordinates). The unknown variables are

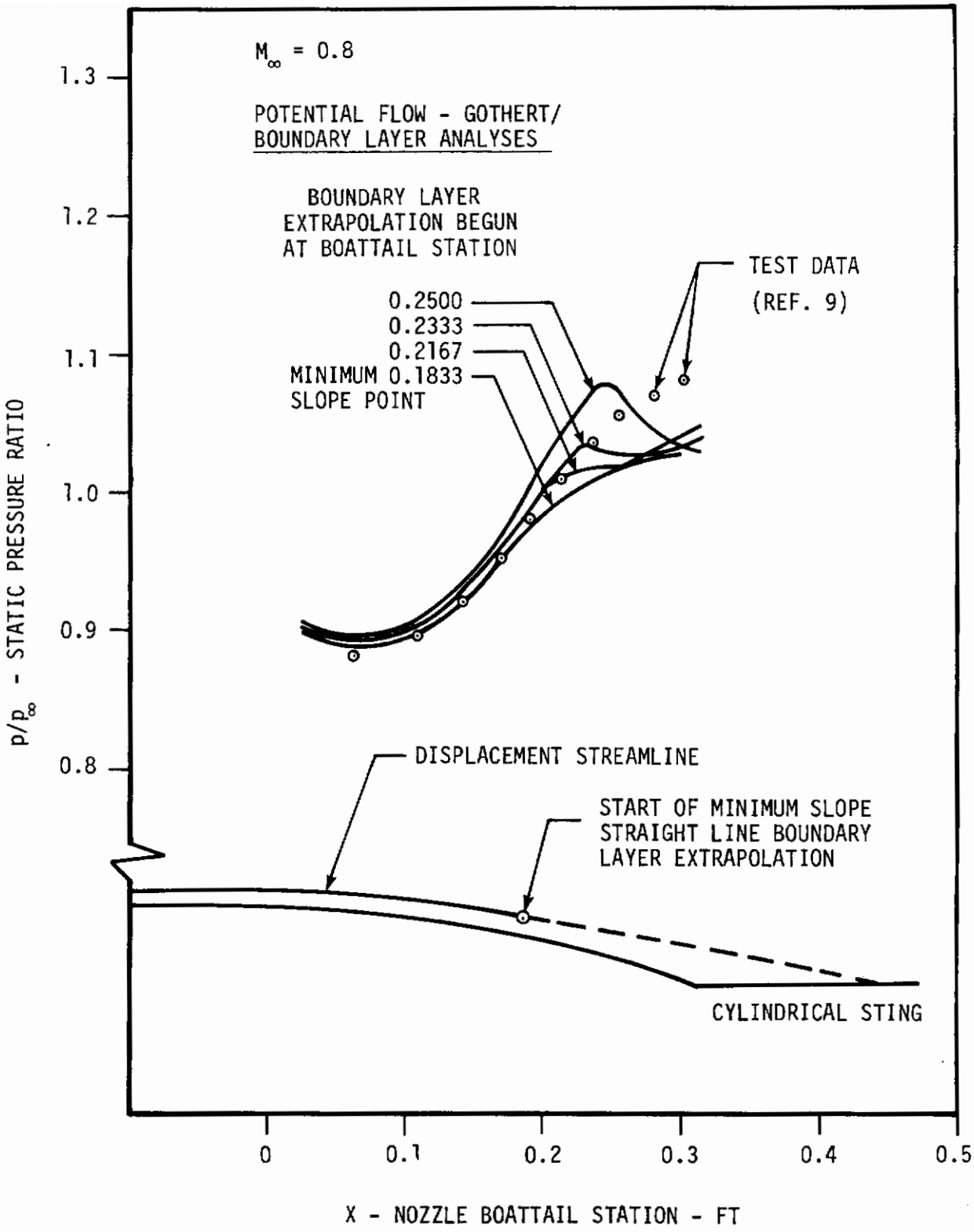

Figure 2. Effect of Boundary Layer Extrapolation Starting Point on Pressure Distribution (From Ref. 7)

density, velocity components u and v, and entropy all expressed as nondimensional quantities. Time is also nondimensionalyzed. In order to insure stability, the well-known Courant-Friedrichs-Lewy (C-F-L) criterion (Ref. 13) is applied, which states that a point being computed must lie inside the Mach cone generated by the nodal points used to compute it. The points on rigid boundaries are calculated in a way to include directly the boundary conditions, i.e. the velocity component normal to the wall is set equal to zero.

The technique just outlined can be used for subsonic, transonic, and supersonic flows over boattails and inside nozzles. In computing the afterbody drag, one simplifying assumption is that the jet is considered as a straight long pipe which simulates a perfect expansion nozzle. Figure 3 shows a comparison between the theoretical and experimental pressure coefficient over a 15° conical boattail.

The inviscid subsonic flow is also analyzed with various relaxation techniques. These techniques consist of successive approximation schemes for the solution of ordinary or partial differential equations. The assumption that a steady state solution exists near the boundary conditions is required. Finite difference formulas are used to reduce the differential equations to a system of algebraic equations that must be solved simultaneously. Rigorous analysis of relaxation techniques is required to insure that convergence is obtained on the basis of certain eigenvalue criteria.

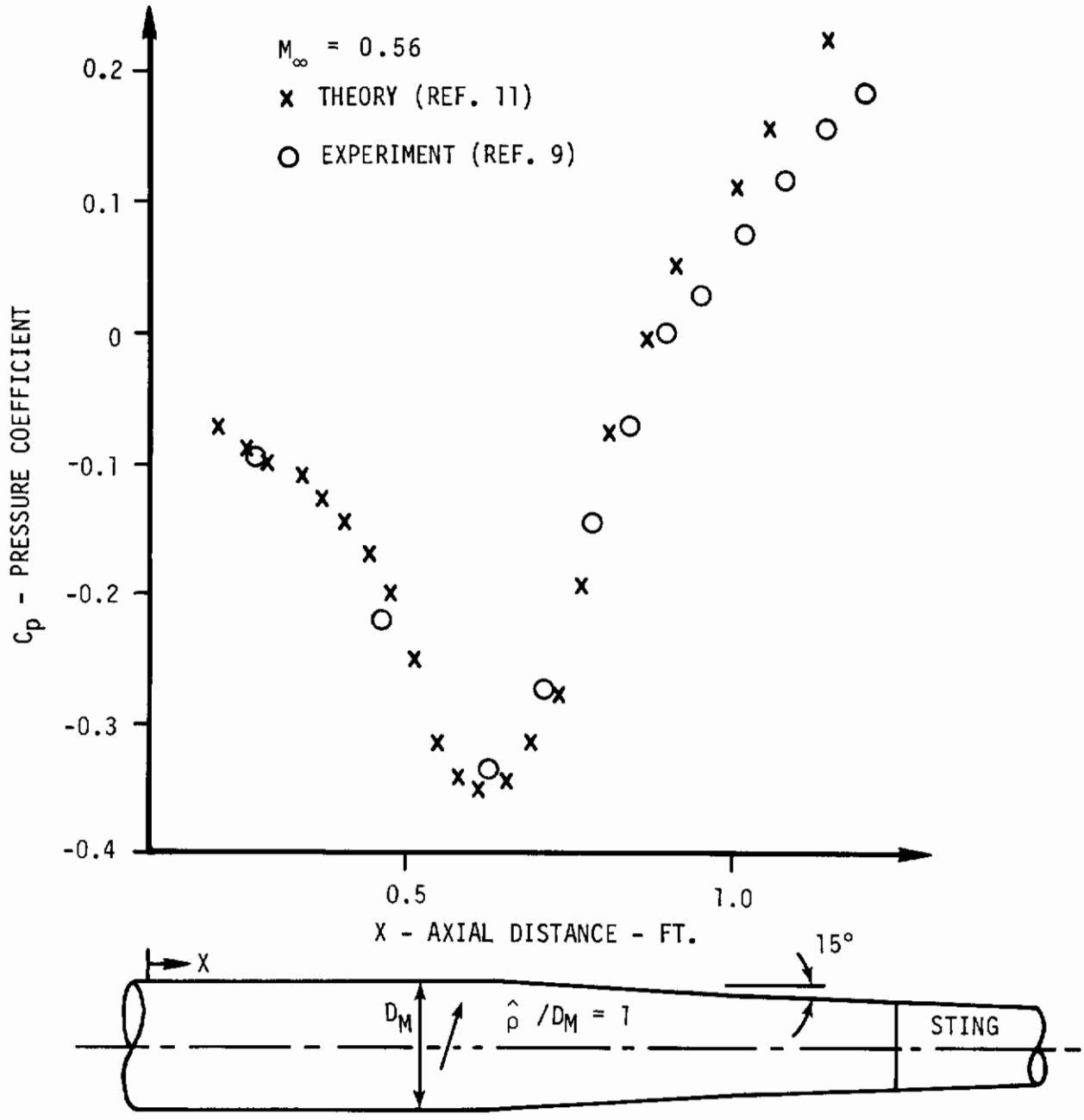

Figure 3. Pressure Distribution, Conical Boattail (From Ref. 11)

Steger and Lomax (Ref. 14) use central schemes to solve numerically the equation of motion for 2-D subsonic flow written in terms of a perturbation potential in body coordinates. The boundary condition of tangent velocity on the body surface is applied. The relaxation parameter, i.e. the parameter that reduces the error at each successive iteration, is taken as slightly less than two. For airfoils at angle of attack, an iterative solution for the proper circulation is superimposed on the relaxation procedure. Values of the circulation and the relaxation parameters are changed as the relaxation proceeds. Convergence is achieved when the residuals, i.e. the errors, are smaller than a certain prescribed value for a continuous pressure at the trailing edge of the airfoil.

This technique can be easily extended to axisymmetric and 3-D bodies without conceptual difficulties and therefore can be used for the solution of axisymmetric boattail flowfields.

Circular arc and conical boattail pressure drag coefficients are obtained theoretically with the various methods described above. Some authors (Ref. 15) do not attempt to calculate the boattail drag analytically and prefer to use reliable experimental data, e.g. the data of Silhan and Cubbage (Ref. 16).

The potential flow theory used to solve subsonic flow fields is very attractive due to its validity even at high subsonic Mach number where compressibility effects are significant. Simple corrections for these effects yield very good results when

the theory is compared with real flow experimental data. Time-dependent and relaxation techniques are very valuable since they can be applied to mixed flow transonic cases. A particular effort should be made to improve them for better accuracy and rate of convergence.

The friction drag over boattails is obtained using well known boundary layer theories for laminar and turbulent flow (Refs. 17-20) which are valid for subsonic and supersonic flows. Reference 17 refers to laminar boundary layer. Similar solutions are used and a set of third order ordinary differential equations is obtained for the momentum and energy equations through a transformation of independent variables. These equations are solved simultaneously by means of an iteration procedure. References 18-20 are integral techniques for turbulent flow. Sasman and Cresci theory (Ref. 20) consist of an integral method where the momentum and moment of momentum equations are transformed to give coupled ordinary differential equations and are solved simultaneously with a Runge-Kutta procedure. The Ludwieg-Tillman (Ref. 21) skin friction relation is used to get the skin friction coefficient, and the reference enthalpy method (Ref. 22) to account for compressibility. The Crocco relation is used to relate total temperature and velocity profiles and a power law velocity profile is assumed. This analysis applies to the entire Mach number range and can be used in both 2-D and axisymmetric configurations. As a representative example of the accuracy that these boundary layer methods can achieve at different speed regimes, the boundary layer theory of

Wazzan and Ball for supersonic flow (Ref. 18), used by Goebel and Divita (Ref. 3) in their investigation, is compared with the data of Reference 23 in Figures 4-6.

Flow separations usually occur on boattails and they are triggered by the upstream influence of the base pressure, boundary layer properties, adverse pressure gradients due to the presence of the jet flow, and geometrical characteristics of the aft-end. The accurate analysis of these separated flow regions, the mixing between the diverted dissipative boundary layer and the isentropic external flow is of utmost importance for the prediction of the afterbody drag. In subsonic flow empirical relations are obtained and used for the determination of the surface pressure in presence of flow separation. Goldschmied (Ref. 24) has obtained the following equation

$$C_{p_s} = 200 C_{f_{\infty m}} + C_{p_m} \qquad (2)$$

which states that the pressure rise due to separation at the minimum pressure point is a function of the skin friction at that point. Benson et al (Ref. 15) assume instead that the surface pressure of the separated region is equal to the free stream pressure when sharp trailing edges are considered. This assumption must influence the value of the boattail drag since it disregards the small but still finite pressure recovery in the separated region, which gives a higher than free stream pressure.

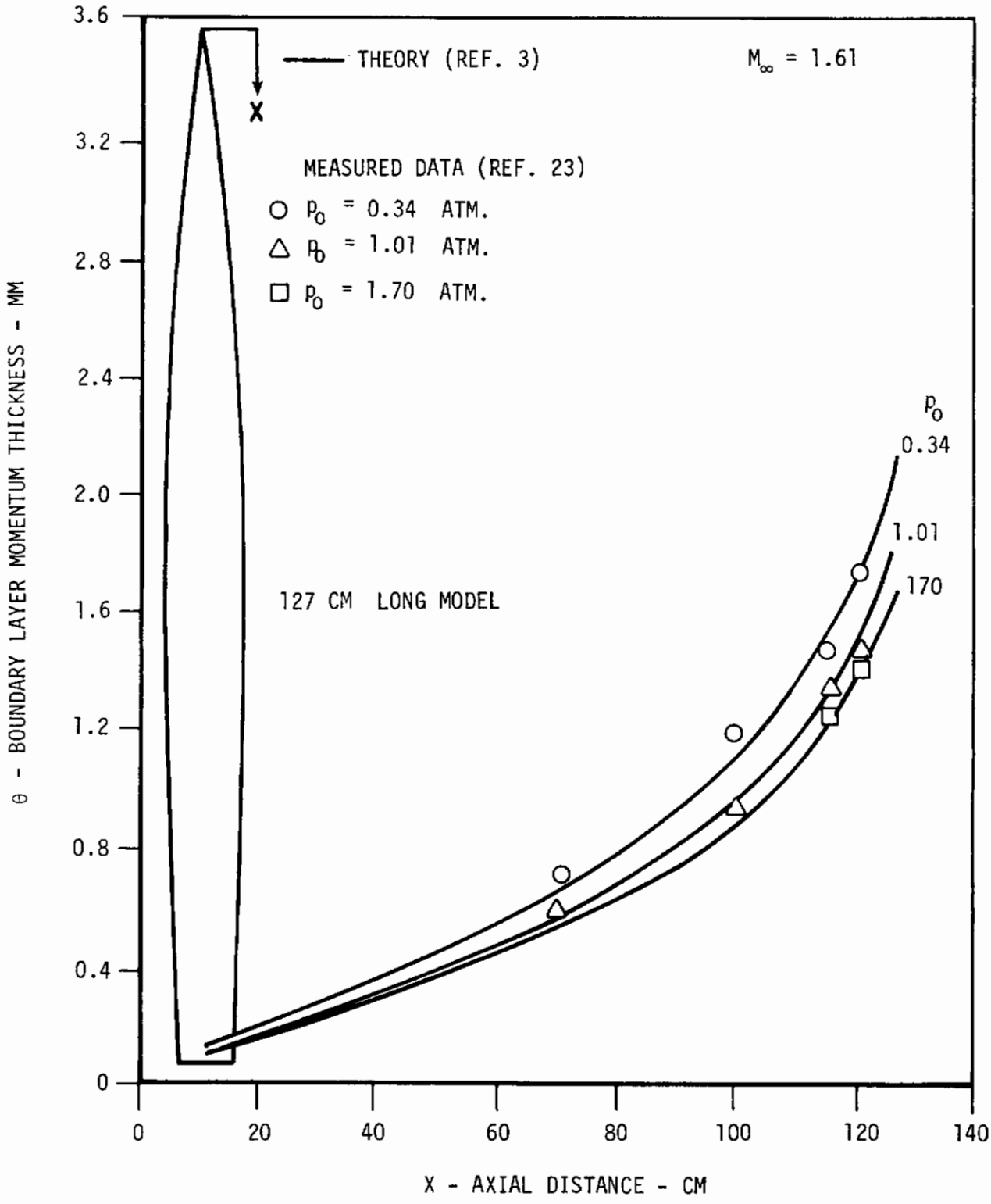

Figure 4. Boundary Layer Momentum Thickness (From Ref. 3)

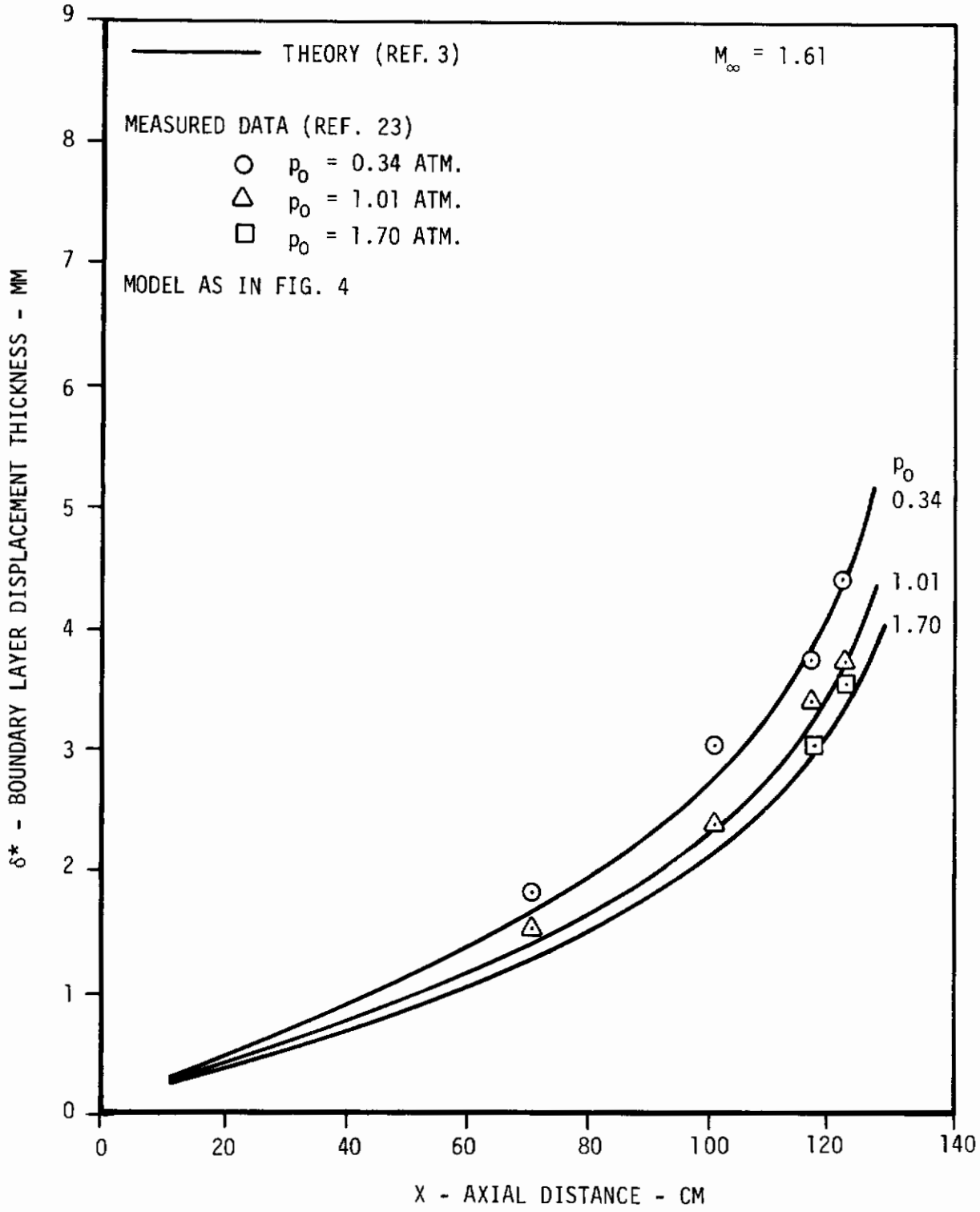

Figure 5. Boundary Layer Displacement Thickness (From Ref. 3)

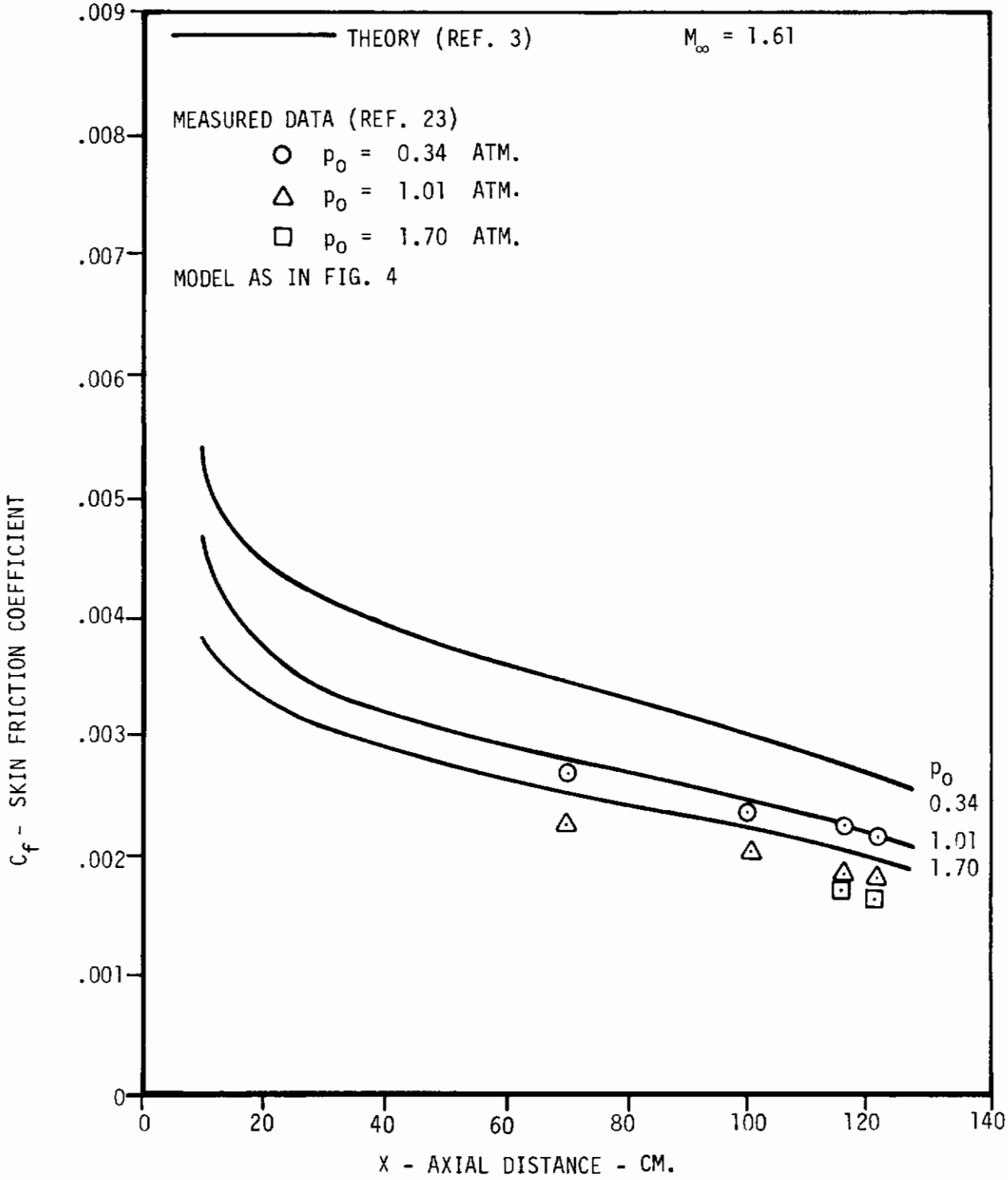

Figure 6. Local Skin Friction Coefficient (From Ref. 3)

The methods outlined for the determination of the skin friction coefficient over the boattails seem to be reliable. The boundary layer properties are reproduced quite accurately. The method of Goldschmied for the subsonic external separation pressure has been substantiated for low Mach number 2-D flows, i.e. flows which might be considered incompressible. Nevertheless References 3 and 7 have used the criterion at high subsonic Mach numbers for 2-D and axisymmetric bodies. No comparison with experimental data is presented, and so it is not possible to check the validity of the criterion. Nevertheless its use has been recommended in Reference 25 at subcritical speeds on the basis that a review of Goldschmied's paper did not indicate any obvious limitation due to compressibility effects.

2. Internal Flow

Various types of nozzles have been analyzed by many authors to find the configuration that maximizes the performance of the aircraft. The analysis include convergent, C-D, C-D ejector, plug, blow-in-door nozzles.

The subsonic internal flow is solved with 1-D flow theory. This solution is valid for convergent nozzles and for the convergent part of C-D and C-D ejector nozzles. If the flow is formed by more than one stream, the total mass, momentum, and energy of the flow is considered as the sum or superposition of the masses, momentums, and energies of the individual streams, thus obtaining an equivalent 1-D stream. Benson et al (Ref. 15) use this equivalence principle in the computation of the flow of a blow-in-door nozzle (See Ref. 1 for details).

Time-dependent techniques, of the Lax-Wendroff type (Ref. 13), are also used successfully.

Nozzle flow separation is predicted empirically. Based on experimental evidence (Ref. 26) it is assumed that the flow will separate from the wall when the local pressure ratio $p/p_\infty \leq 0.85$, which differs from $p/p_\infty \leq 0.28$ as assumed in supersonic flow (Refs. 15, 27-30).

The internal flow theories discussed are considered adequate when compared to experimental data. There is no appreciable

difference between them (Fig. 7). As far as nozzle flow separation is concerned, it seems that the pressure ratio correlation might only be valid in certain specific cases since the value of the separation pressure depends also on nozzle geometry and boundary layer characteristics. For widely different nozzle and boundary layer characteristics there is no evidence that the same pressure ratio would still be valid.

3. Jet Plumes

Plumes and plume effects on afterbodies have received particular attention in the past for their primary importance on the performance of aircraft and missiles (see Refs. 31-36). At high thrust levels plumes can cause either separation or changes in the flow field which can affect the lift, stability, and control of the vehicle. The jet effects on the afterbody are such that the static loads, because of fluctuations, cause fatigue stresses on the structures and temperature beyond permissible limits. These detrimental effects can occur at any altitude and over the entire Mach number range. However, by increasing thrust and nozzle pressure ratios, some beneficial effects could be obtained from the jet plume since afterbody and nozzle boattails would be pressurized with consequent decrease in drag. The thrust increase produces also a reversal in the base pressure behavior which goes from a decrease to a favorable increase.

Thrust levels and nozzle pressure ratios are not the only parameters to be considered when jet plumes are studied. Obviously

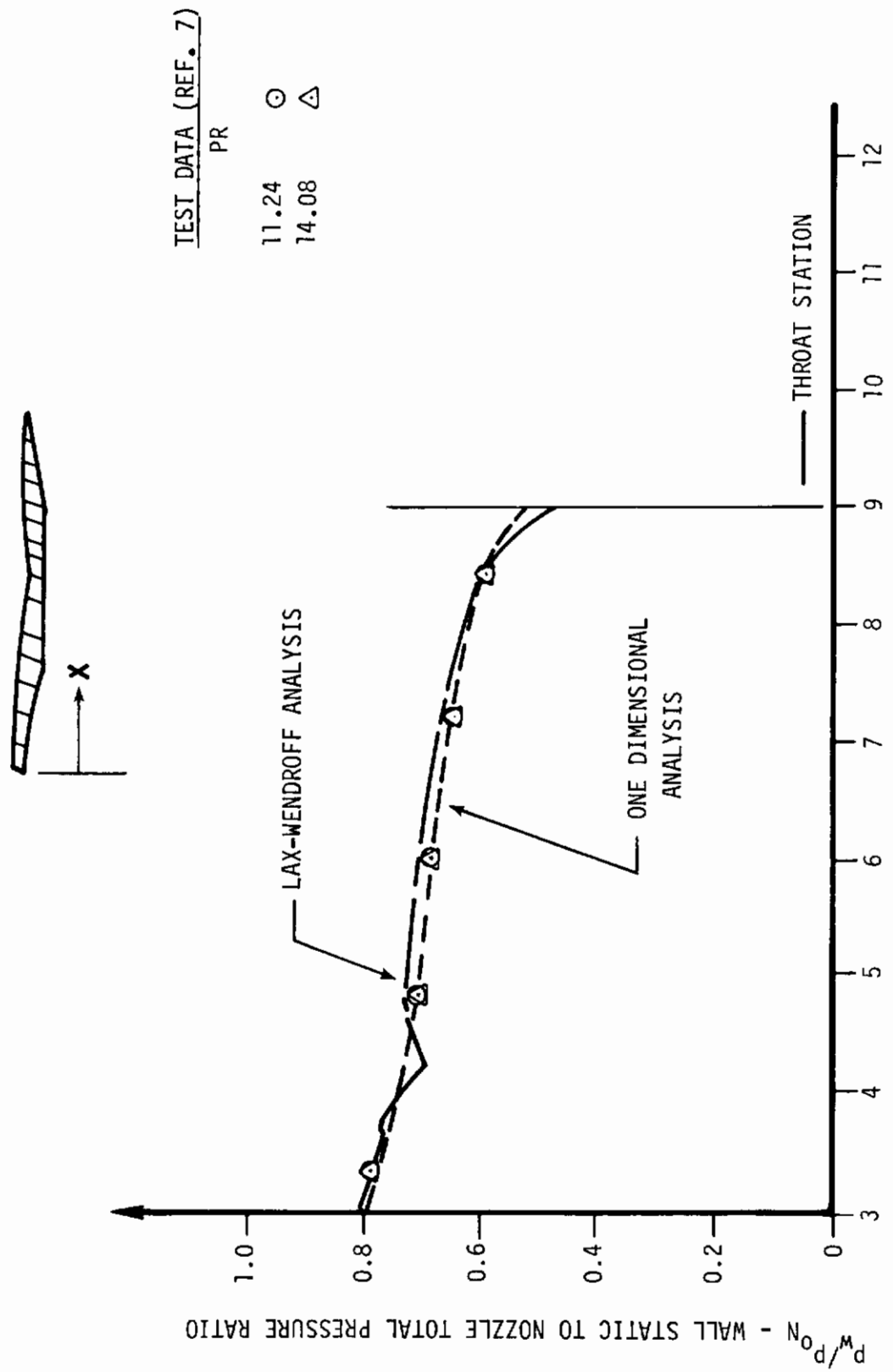

Figure 7. Nozzle Predicted and Experimental Pressure Profiles (From Ref. 7)

viscous effects control the interaction of the plume with the external flow. The approaching boundary layer properties must be known, together with separation conditions, free shear layer and jet plume mixing in the confluence region.

Jet plumes must be carefully analyzed since they have such a strong effect on the afterbody and base drag levels. Therefore it is of prime importance to develop methods that give accurately the shape of the jet boundary. Plumes are usually supersonic, but plumes with subsonic internal flow are treated with 1-D analysis, with the requirement that the internal and external pressures and flow directions are matched on the jet boundary. Once the jet boundary is obtained, a problem arises in subsonic flow. Due to the jet boundary a body slope discontinuity exists at the trailing edge and therefore the inviscid pressure distribution is also discontinuous. Rudman and Maise (Ref. 8) for example, solve the problem by assuming a continuous pressure distribution at the trailing edge. The inviscid flow field can therefore be determined.

There is very little in the literature about subsonic plumes. The one-dimensional technique used can be assumed adequate if a parallel is drawn from supersonic plume performances where the 1-D analysis gives average values of the more accurate method of characteristics.

4. Base Flow

The base flow and pressure depend on the mechanics of the wake and the vortex pattern. The subsonic wake behavior is not fully understood and a satisfactory theoretical approach that would give reasonable pressure estimates has not yet been developed. Experimental data, as that of Reference 37, is generally used for the base pressure but also some empirical and semiempirical correlations (Ref. 38,39) which take into consideration the effect of the propulsive jet. McDonald and Hughes (Ref. 39) calculated the base drag variation due to jet effects for different boattail angles (Fig. 8). A correlation of sting effects and free stream Mach number on base pressure variation was obtained in order to compare wind tunnel to free flight tests.

Brazzel and Henderson (Ref. 38) developed a power-on base drag correlation for isolated jets valid in supersonic flow. Lockheed California (Ref. 7) modified the correlation to make it applicable to subsonic flow. It was found that the base pressure is a weak function of jet to free stream momentum flux ratio and boattail to maximum area ratio (Figs. 9-10). The correlation is consistent with experimental data but a lot of scatter is present for low area ratios.

5. Summary

The various techniques presented to analyze the subsonic flow regime are effective and adequate up to the body/plume junction. Time-dependent and relaxation methods are very promising and their use should be continued. The body slope discontinuity presents

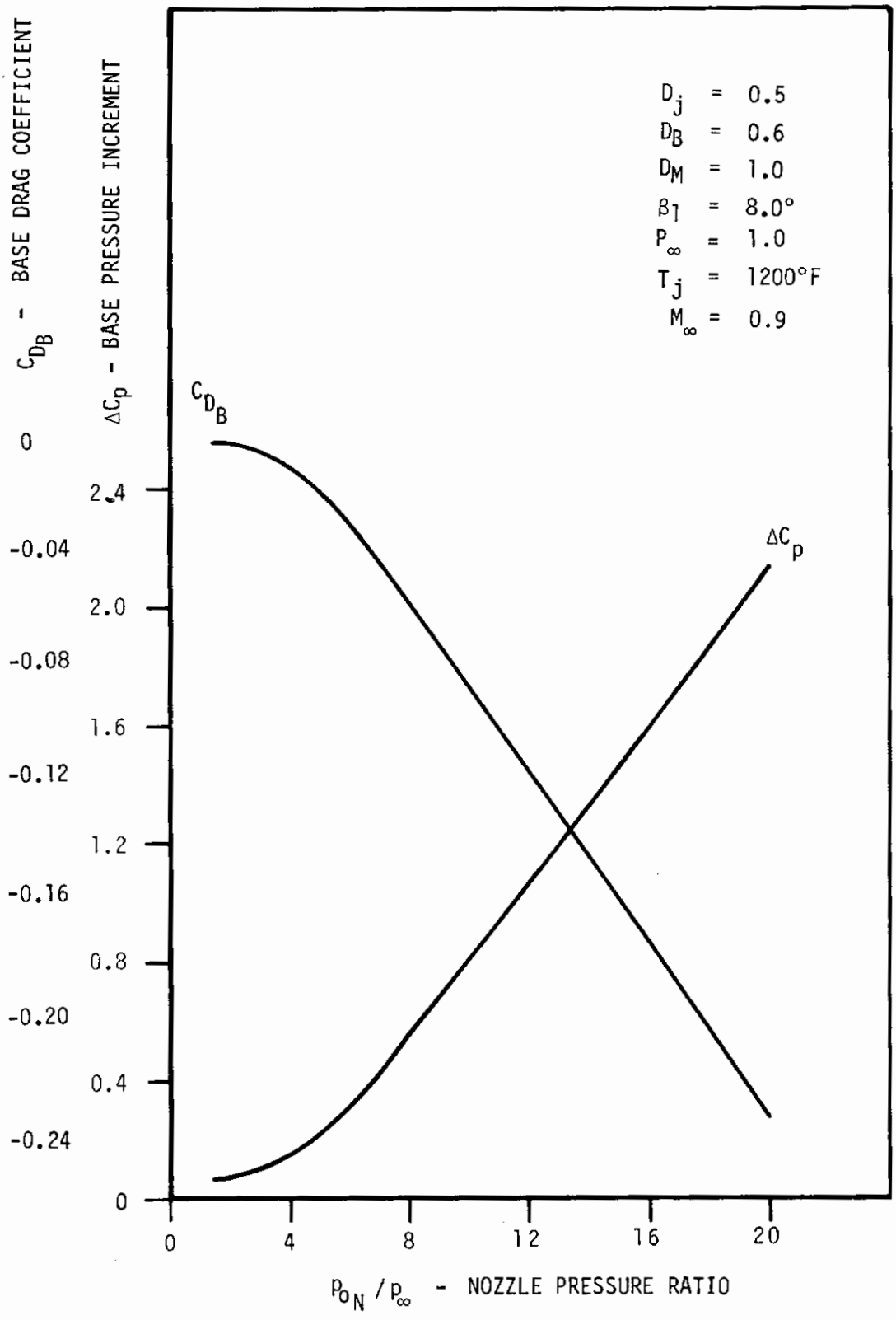

Figure 8. Base Drag Correlation (Ref. 39); Effect of Nozzle Pressure Ratio on Base Pressure Increment and Base Drag Coefficient (From Ref. 3)

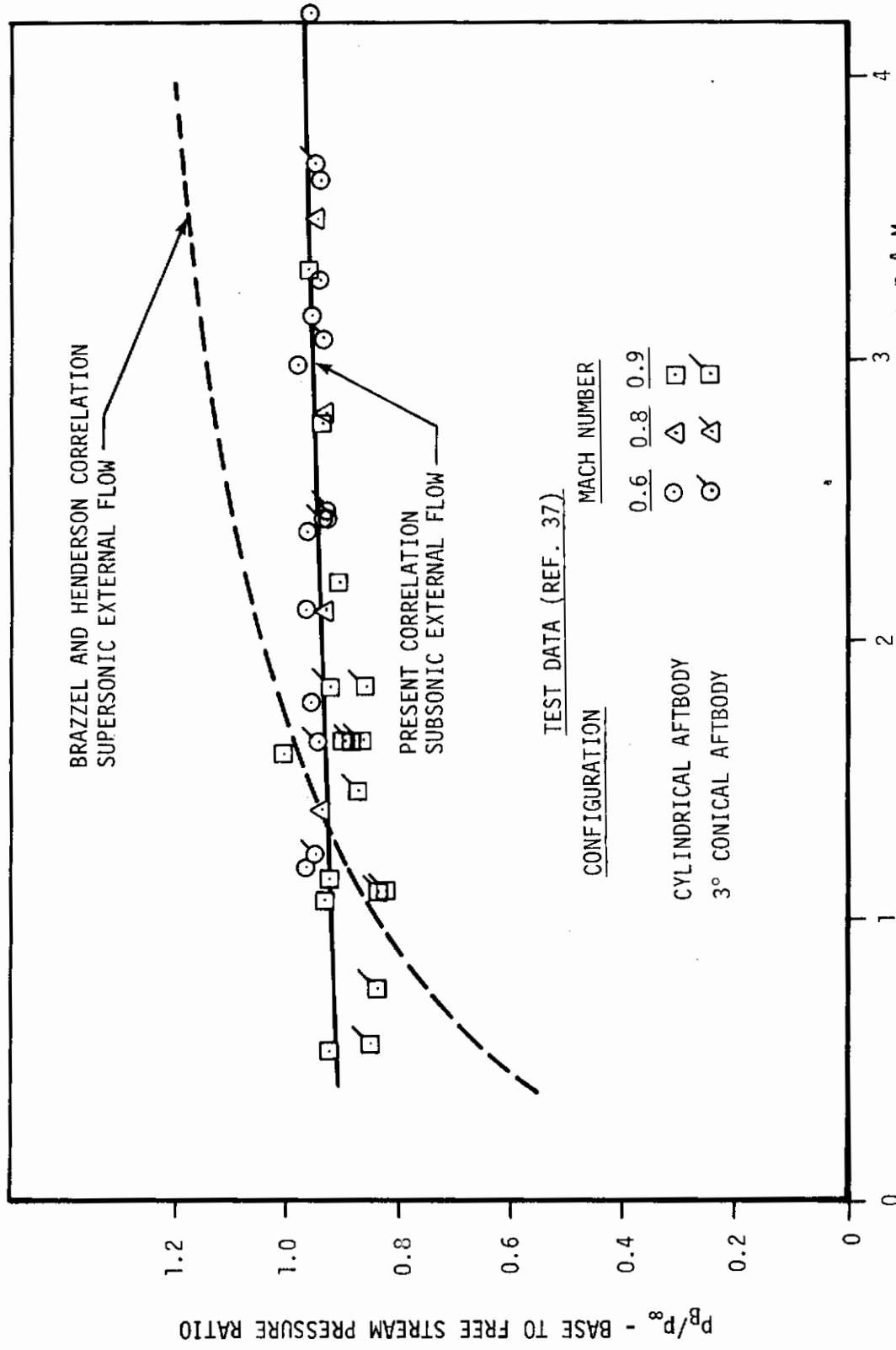

Figure 9. Annular Base Pressure Correlation for Cylindrical and 3-Degree Conical Afterbodies (From Ref. 7)

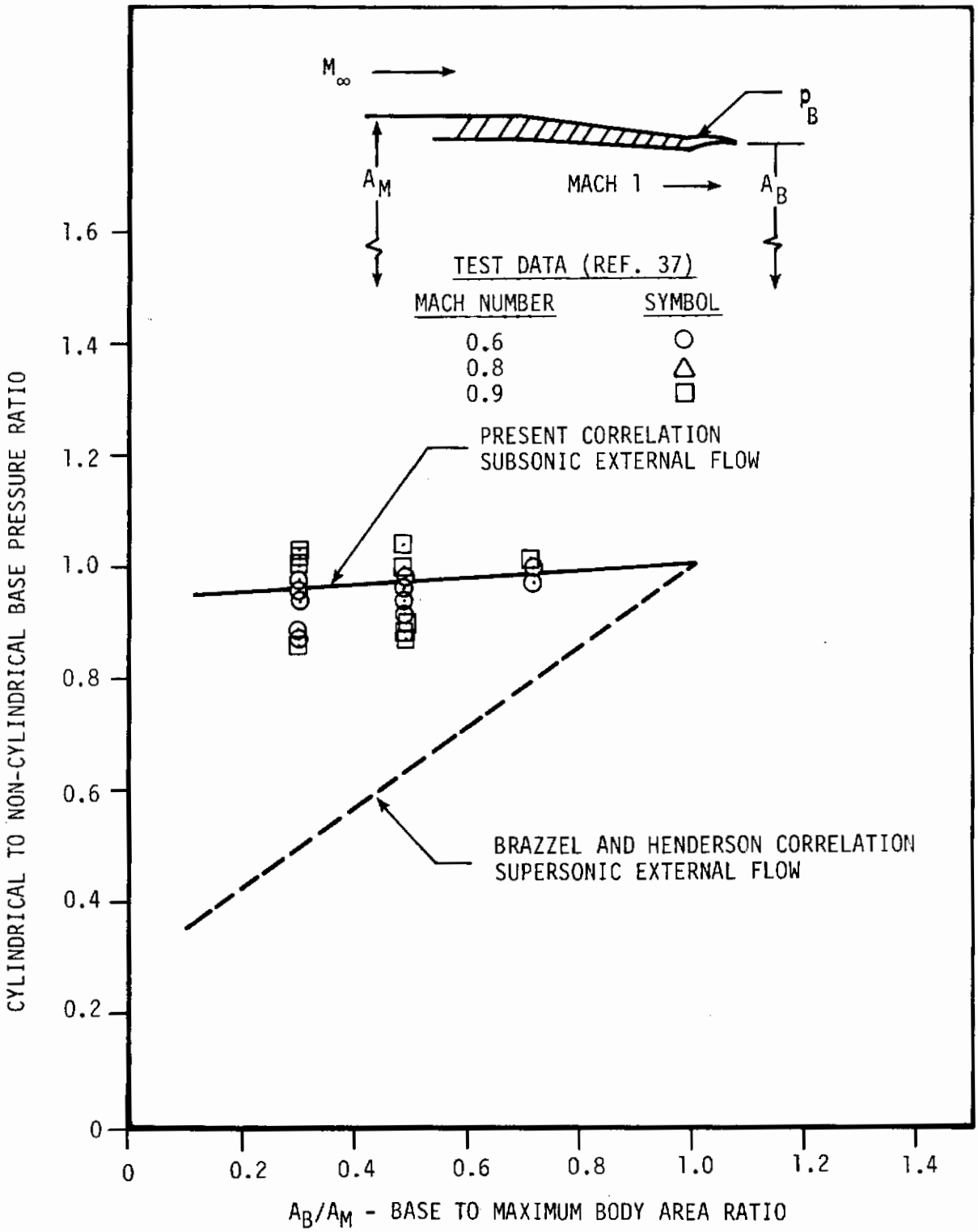

Figure 10. Annular Base Pressure Correction for Non-Cylindrical Afterbodies (From Ref. 7)

a problem in the external flow analysis and displacement streamline extrapolations or arbitrary streamline smoothing achieve only partial success. Consequently afterbody drag is usually underestimated. Internal and external flow separations are predicted empirically. The correlations are based on some experimental evidence, but the criterion for external flow separation has been proven valid only for incompressible flow. The paucity of investigations on subsonic plumes is justified by the fact that plumes are usually supersonic. Nevertheless the use of 1-D theory should be experimentally checked. The base drag correlations are consistent with experimental results when cylindrical afterbodies are analyzed; for noncylindrical afterbodies the amount of scatter present in the experimental results suggests the necessity of finding a correlating parameter other than the area ratio A_B/A_M; e.g. the boattail angle.

B. Transonic Flow

1. External Flow

The external transonic inviscid flow field has been treated by many investigators and many different techniques have been used to solve it. The success of these techniques has been different but a common problem has been to ascertain exactly the shock location on the body and the factors affecting its stability. The nonlinearity of the flow field is such that a small change in any of the flow parameters or any small error in their evaluation produces drastic differences in the final outcome of the calculations.

Spreiter and Alksne (Refs. 40,41) devised a technique called "Method of Local Linearization" applied to the small perturbation equation for a perturbation potential in order to solve the flow field over airfoils and slender bodies at $M_\infty \simeq 1$. The 2-D governing equation is:

$$(1-M_\infty^2)\phi_{XX}+\phi_{YY} = \frac{M_\infty^2(\gamma+1)}{U_\infty}\,\phi_X\phi_{XX} \tag{3}$$

For M_∞ close to but different from 1, we set

$$\lambda = 1-M_\infty^2 - \frac{M_\infty^2(\gamma+1)}{U_\infty}\,\phi_X \quad \begin{matrix} > 0 \text{ subsonic} \\ < 0 \text{ supersonic} \end{matrix} \tag{4}$$

and the governing equation becomes:

$$\lambda\,\phi_{XX} + \phi_{XX} = 0 \tag{5}$$

The assumption is that the variation of λ is small, that its value never becomes infinity or zero, and that therefore λ can be considered locally constant. In this manner the equation of motion is linearized and the problem is reduced to the solution of an elliptic equation in subsonic flow and a hyperbolic equation in supersonic flow. In the particular case of $M_\infty=1$ the value of λ is set as

$$\lambda_{pa} = \frac{(\gamma+1)}{U_\infty}\,\phi_{XX} > 0 \tag{6}$$

and the equation of motion becomes

$$\phi_{YY} = \lambda_{pa}\phi_X \tag{7}$$

which is parabolic and of the same form as the 1-D equation for transient heat conduction. The solutions for the different forms of the equation of motion are known and enable us to calculate velocity and pressure distributions over sharp-nosed airfoils and bodies of revolution. Three different solutions are used for axisymmetric mixed flow, i.e. subsonic, transonic, and supersonic; and the three different regions are joined by matching the velocity and the velocity gradients (Ref. 3).

The solutions valid in the supersonic region and the rear subsonic region have logarithmic singularities when the local Mach number is equal to 1. Therefore the matching of the two solutions, which do not overlap, is done with the numerical and graphical method of isoclines.

This transonic theory gives numerical difficulties at the rear sonic point near the junction of the body with the jet plume (Ref. 3). Figure 11 shows that the analytical results underestimate the recompression taking place, probably because no provisions are made for the presence of a shock in this region. Therefore the pressure distribution over the jet plume boundary cannot be obtained.

A recommended method for the calculation of the transonic boattail drag is the use of a correlation called Integral Mean Slope (IMS) (Refs. 7,42,43). The Integral Mean Slope is the average value of the rate of change of cross-sectional area with length.

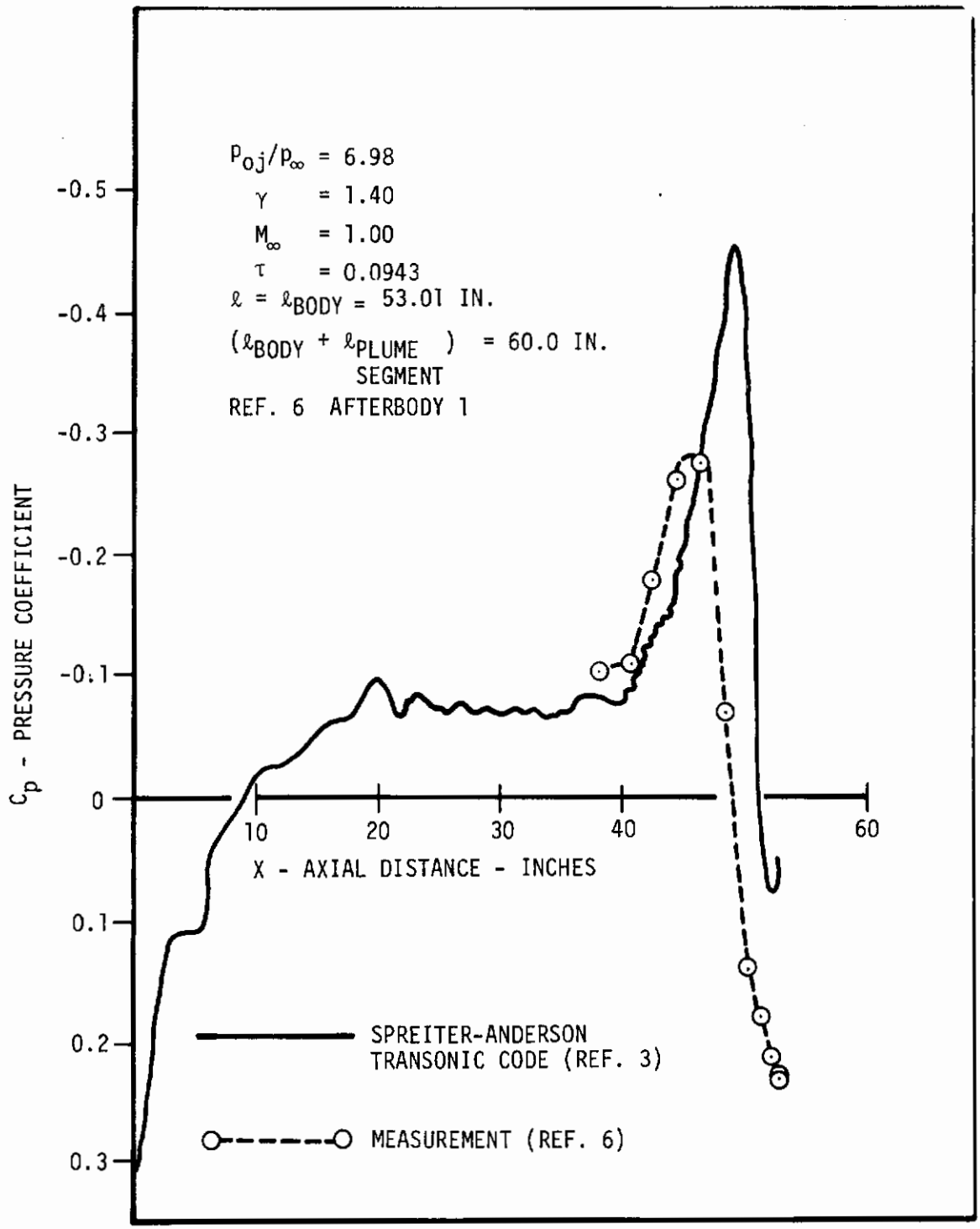

Figure 11. Body Plus Estimated Plume Smoothed to Fair Out Discontinuities in S_1' Versus X. C_p Versus X (From Ref. 3)

$$IMS = \frac{1}{\left(1 - \frac{A_{BT}}{A_M}\right)} \int_{\frac{A_{BT}}{A_M}}^{1} \frac{d\left(\frac{A}{A_M}\right)}{d\left(\frac{X}{D_M}\right)} \quad d\left(\frac{A}{A_M}\right) \tag{8}$$

From linearized theory the boattail pressure drag is a function of the IMS and the free stream Mach number, and therefore it is readily evaluated. The range of applicability of the IMS correlation goes from a free stream Mach number of 0.6 to 1.6. Some corrections are needed to account for nozzle pressure ratio effects not directly included in the correlation. The correlation is useful especially for obtaining quick estimates and preliminary design criteria of boattail geometries and can be used for both isolated and twin boattails. (Fig. 12).

In order to analyze twin jet aircraft, a 3-D transonic theory was needed and References 43 and 44 developed a theory described in detail in Reference 45. Assuming small perturbations and following the Spreiter and Alksne analysis of local linearization (Ref. 41), the transonic potential flow equation for axisymmetric bodies is:

$$(1-M_\infty^2)\ \phi_{XX} + \frac{1}{R}\phi_R + \phi_{RR} = \frac{M_\infty^2\ (\gamma+1)}{U_\infty}\ \phi_X\ \phi_{XX} \tag{9}$$

For approaching subsonic flow its solution is:

$$\phi = -\frac{U_\infty}{4\pi} \int_0^{\ell} \frac{S_1'(\xi)\ d\xi}{\sqrt{(X-\xi)^2+\lambda R^2}} \tag{10}$$

where λ is defined in Equation (4). Upon differentiation, the compressible perturbation velocity distribution in the longitudinal direction is obtained.

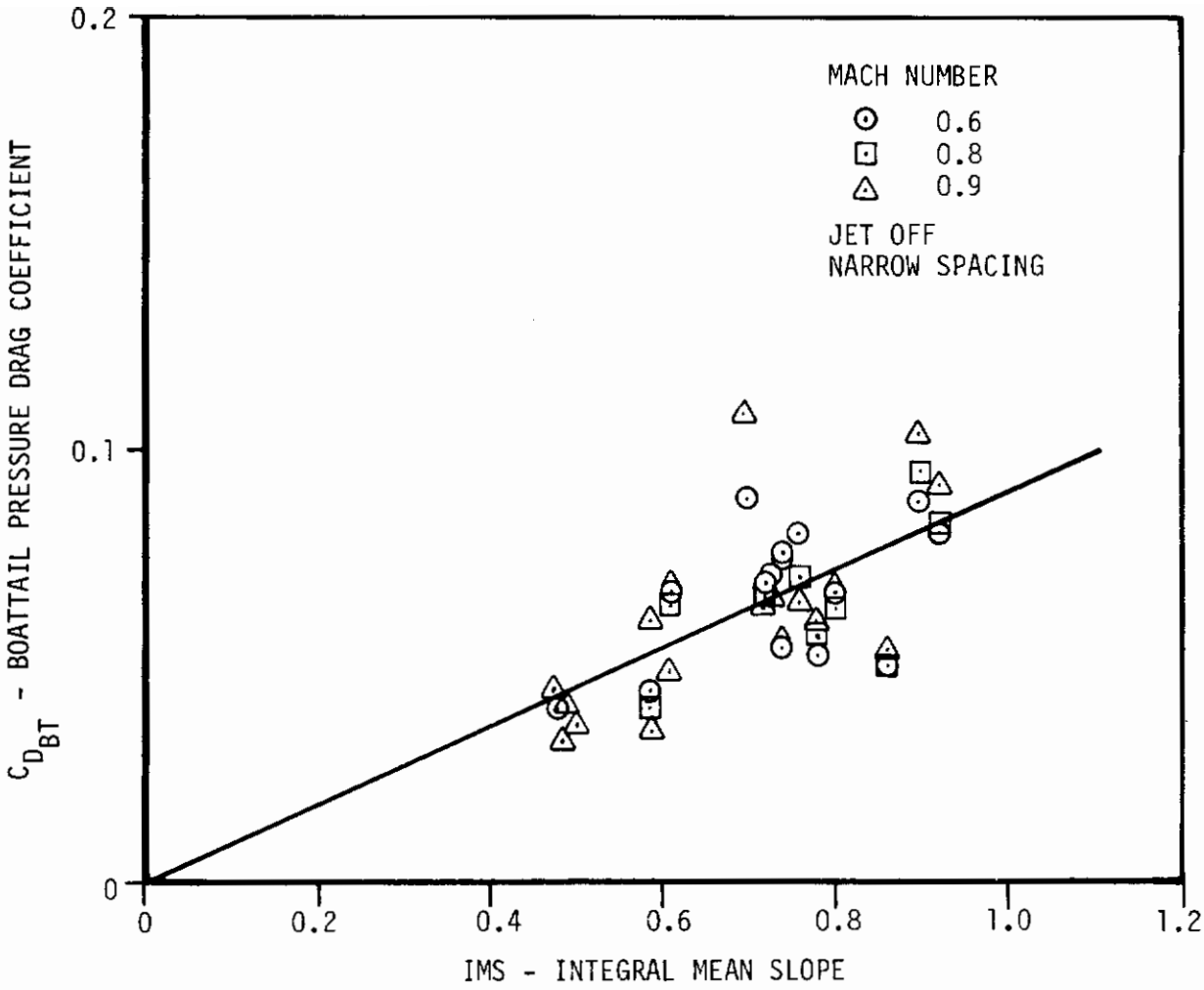

Figure 12. Correlation of Twin-Jet Drag Data With IMS - Subsonic (From Ref. 43)

Presz et al (Ref. 45) modify the Spreiter and Alksne result by introducing an expression for the local perturbation velocity for incompressible flow, u_i, obtained from slender body theory without the Spreiter and Alksne simplifying assumptions. The equation for u_i gives better results for bodies without an analytical cross-sectional area distribution. For approaching supersonic flow, Spreiter and Alksne's solution is used. For approaching transonic flow, the Oswatitsch and Keune approach (Ref. 46) is used. It consists of assuming the term

$$\lambda_{pe} = M_\infty^2 \frac{\gamma+1}{U_\infty} \phi_{XX} \tag{11}$$

constant as in the 2-D case so that the governing equation becomes

$$\frac{\phi_R}{R} \rightarrow \phi_{RR} - \lambda_{pe}\phi_X = (M_\infty^2-1)\ \phi_{XX} \tag{12}$$

The solution for the local perturbation velocity distribution is therefore obtained.

These various solutions are connected at appropriate axial locations and allow the calculations of potential flow over axisymmetric bodies.

Presz et al superimpose the viscous effect, due to the presence of the boundary layer, on the inviscid solution. The displacement thickness is calculated in first approximation using

the inviscid pressure distribution obtained from the inviscid equations and then the flow field is recalculated over the displaced body. Iterations are necessary to obtain convergence. The boundary layer theory of Reshotko and Tucker (Ref. 19) is used.

The axisymmetric body theory presented, corrected for viscous effects, represents the basis of the Presz et al 3-D theory. The argument here is that the flow field over a 3-D body is equivalent to the flow field over an axisymmetric body of equivalent cross-sectional area distribution plus the cross flow difference between the actual body and the equivalent body. The cross flow, i.e. the flow in a plane normal to the body longitudinal axis, can be calculated independently of the flow in the longitudinal direction, and it is proven to be independent of Mach number. Therefore the cross flow difference between the 3-D body and its equivalent body of revolution can be calculated using incompressible flow theory. Laplace's equation is solved for the two different bodies and the usual boundary conditions of zero normal velocity on the surface and flow regularity at infinity are used. A sample calculation for a typical twin jet aircraft is compared to experimental data in Figure 13.

Spreiter and Stahara (Ref. 47) present an investigation of 3-D transonic flow fields using an extension of the method of local linearization. The fundamental 3-D equation of motion for a perturbation potential ϕ is used in inviscid, irrotational, isentropic, transonic flow with the assumption of small disturbances. The equation is valid when the X axis is aligned with

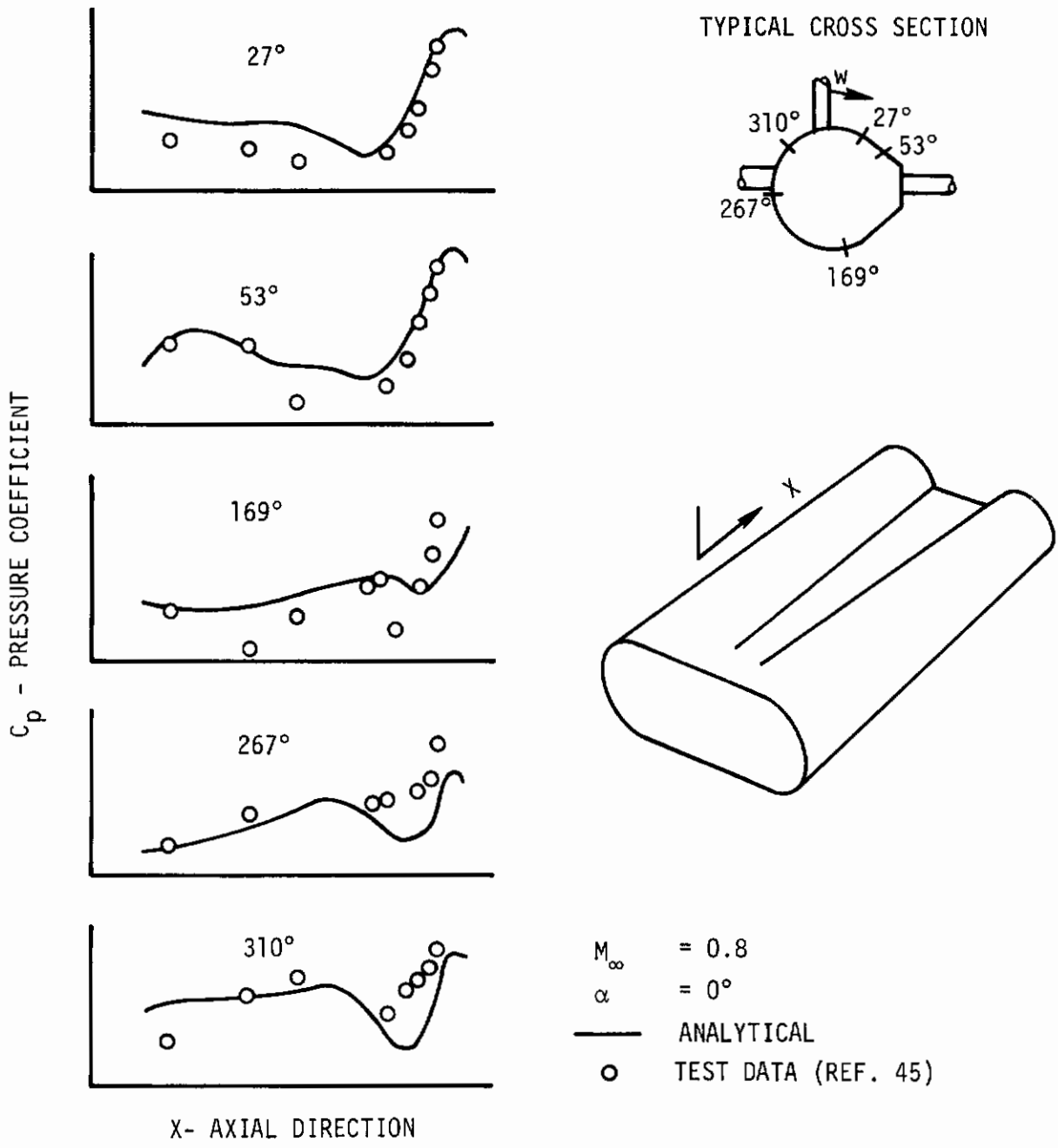

Figure 13. 3-D Boattail Pressures (From Ref. 45)

the free stream direction or inclined a small angle to it. The pressure coefficient is therefore:

$$C_p = -\frac{2}{U_\infty}(\phi_X + \alpha\phi_Y) - \frac{1}{U_\infty^2}(\phi_Y^2 + \phi_Z^2) \tag{13}$$

The boundary conditions require that the velocity be uniform far from the body and that the velocity component normal to the body surface be zero.

The transonic equivalence rule is used to make the transonic flow more amenable to analytical investigation. Therefore ϕ in the vicinity of a slender body of arbitrary cross section can be expressed as follows

$$\phi = \phi_2(X,Y,Z) + g(X) \tag{14}$$

where ϕ_2 is the solution of the 2-D Laplace's equation

$$\phi_{YY} + \phi_{ZZ} = 0 \tag{15}$$

at each X station and g(X) is the contribution to the velocity potential which depends on M_∞ and $S_1(X)$ but not on the cross-sectional shape. Therefore g(X) can be obtained solving the axisymmetric flow over the equivalent body of revolution having the same longitudinal cross-sectional area of the original body.

$$\phi_2 = \phi_{2,\alpha} + \phi_{2,tk} \tag{16}$$

$$g(X) = -\phi_{2eb} + \phi_A \tag{17}$$

$\phi_{2,\alpha}$ is the 2-D incompressible flow solution of the Laplace's equation

for translation of the cross section and $\phi_{2,tk}$ is the solution for growth of the cross section. ϕ_{2eb} refers to the 2-D incompressible flow solution of the Laplace's equation for the growth of the cross section of the equivalent body, and ϕ_A is the 3-D solution of the full transonic equation. Figure 14 illustrates the transonic equivalence rule.

The pressure coefficients obtained by this method are valid in purely subsonic flow, in transonic accelerating flow, and in purely supersonic flow.

Results obtained by using the above technique are quite accurate and compare well with experimental data up to 70% of the chord length. From this point on the analysis deviates considerably from the experimental data in as much as the presence of a rear shock and viscous interactions are not considered (Fig. 15). It is also true, as the authors remark in their paper, that the experimental data might be partially erroneous because of the wind tunnel wall interference.

Grund et al (Ref. 48) present an analysis to predict the airframe/exhaust nozzle interaction at transonic Mach numbers. The analysis involves a modification of the Spreiter-Alksne method and applies to arbitrary, slender, axisymmetric fuselages and after-bodies. The inviscid solution is coupled with the turbulent boundary layer solution of Reshotko and Tucker (Ref. 19) to take into consideration the viscous effects. Convergent, fully expanded nozzle jet flow

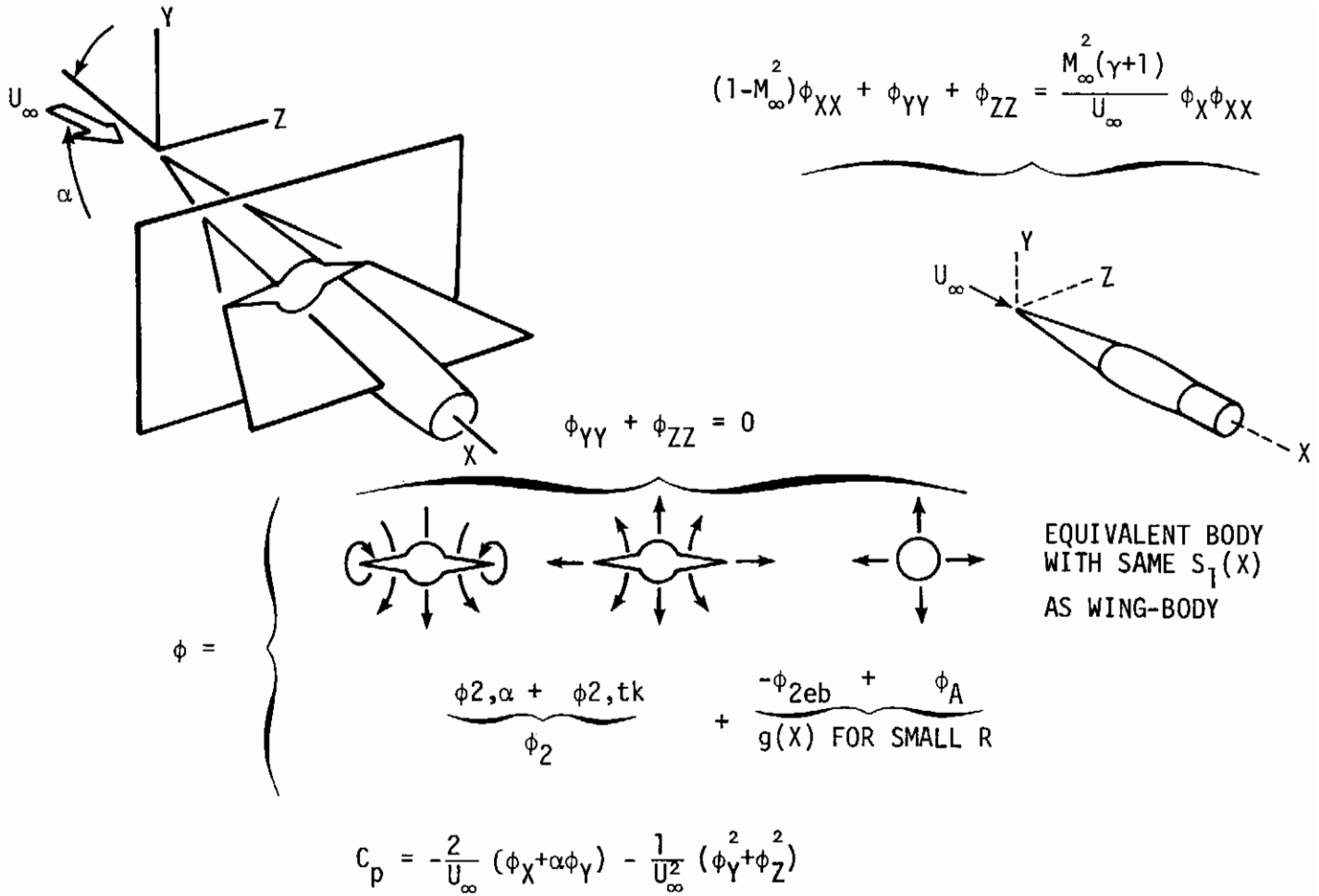

Figure 14. Transonic Equivalence Rule for Slender Wing-Body Combinations (From Ref. 47)

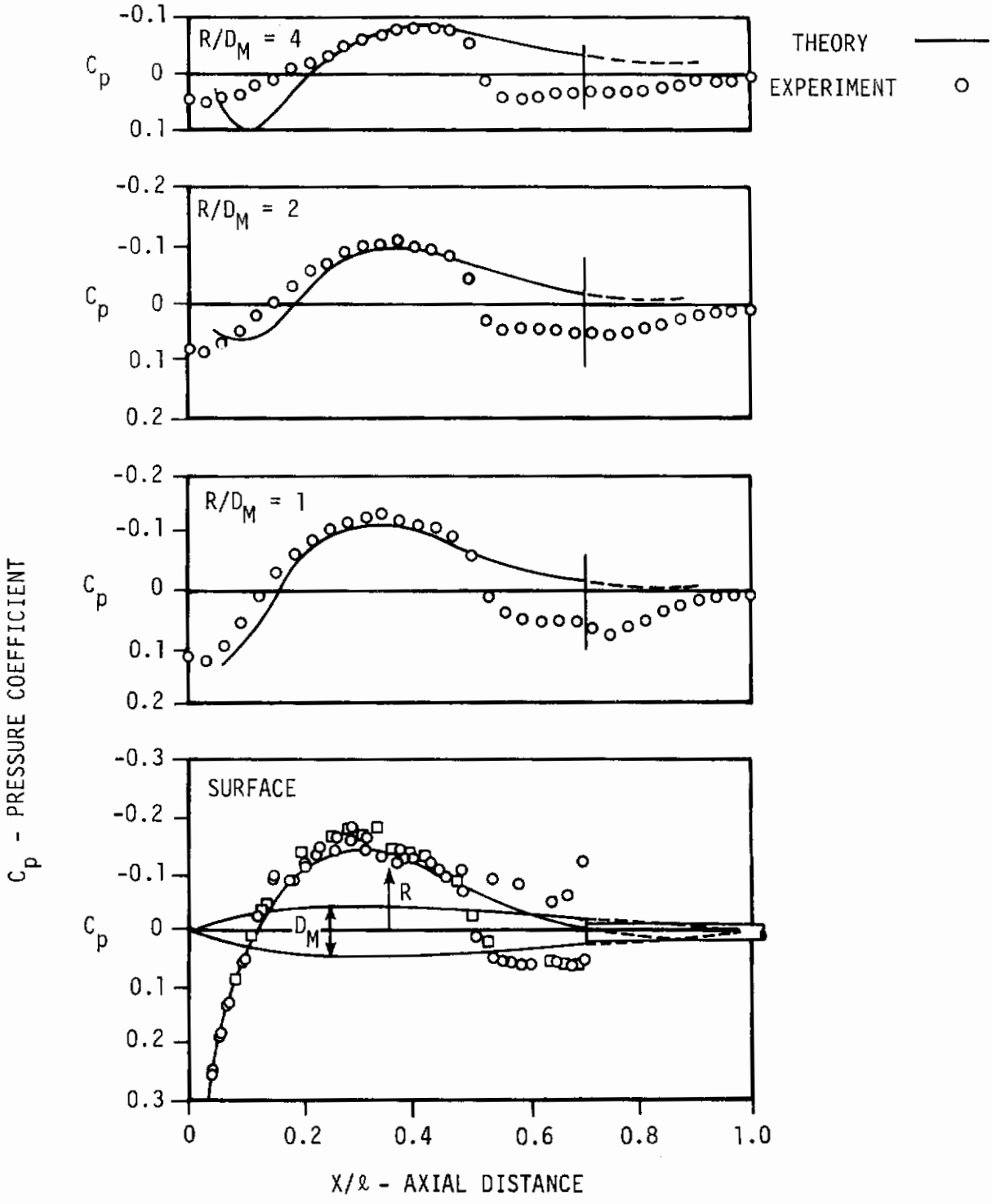

Figure 15. Theoretical and Experimental Surface and Flow Field Pressure Distributions at $M_\infty = 1$; $\tau = 1/12$; Maximum Thickness at $X/\ell = 0.3$ (From Ref. 47)

for a pressure ratio of approximately two is simulated by a cylindrical section starting at the exit station. The small perturbation transonic axisymmetric flow equation for the perturbation potential ϕ is used and the solution for the perturbation velocity is obtained. The function $G(M_\infty, \gamma, \text{shape})$, related to the perturbation velocity at different free stream Mach numbers, piecewise linear in the method of Spreiter and Alksne (Ref. 41), is modified in the present analysis (Fig. 16). The equations derived by Grund et al are similar to the Spreiter and Alksne equations (Ref. 41). The main difference is that the local linearization principle is applied only to a compressibility term instead of the full flow equation.

The equations are integrated with the well known Runge-Kutta numerical method. The analysis is applied to different boattail configurations and jet pressure ratios, and the pressure coefficients and pressure drags for parabolic arc fuselages and circular arc afterbodies are obtained and compared with the experimental data of References 9,48,49 (Figs. 17-20). Also the boundary layer effects on the afterbody drag and forebody/afterbody interactions are considered. The comparison is satisfactory up to and including the surface discontinuity at the jet exit station. Unfortunately the restrictions of the analysis limit somewhat its use; the bodies analyzed must be slender, mixing and boundary layer effects must be of second order, and the flow must not separate. In fact, in the case of flow separation on the boattail, viscous effects affect significantly the afterbody drag.

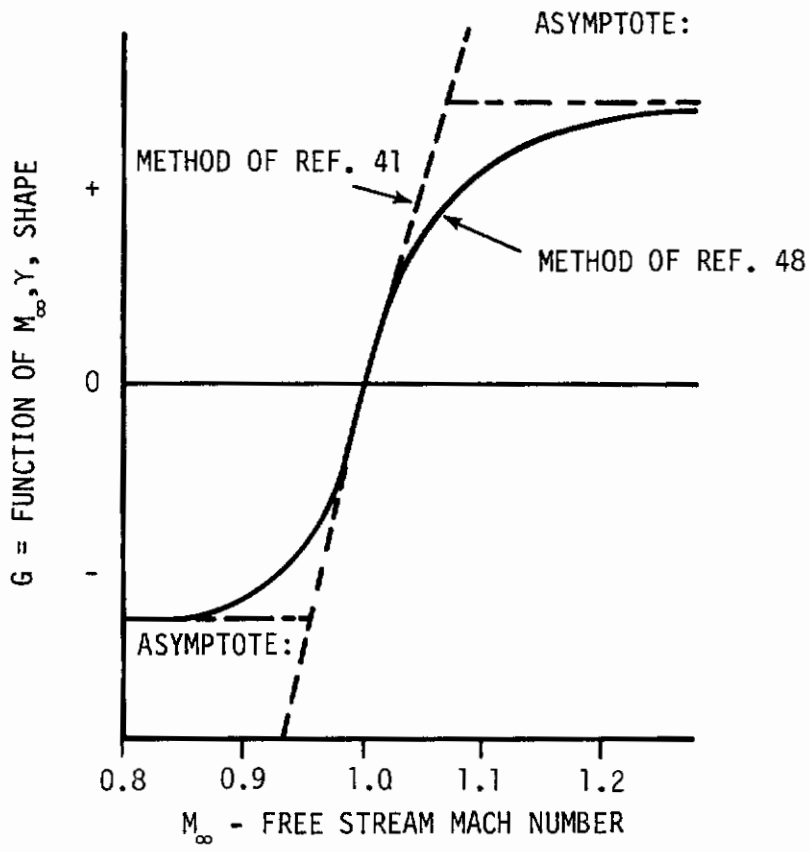

Figure 16. Variation of the Function G With Mach Number (From Ref. 48)

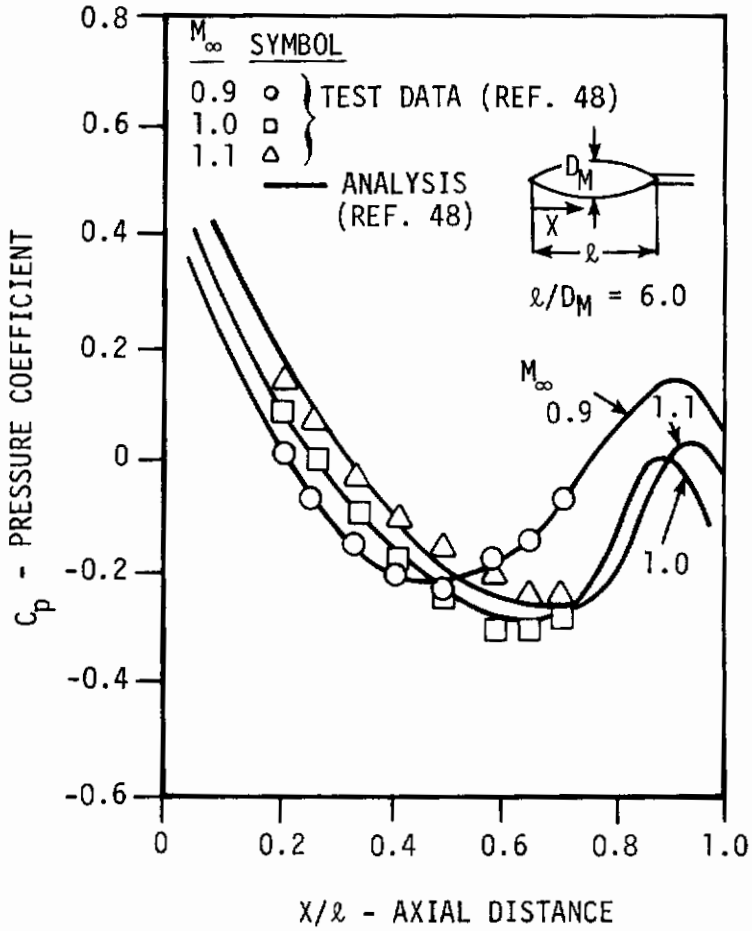

Figure 17. Pressure Coefficients for Parabolic Arc Fuselage (From Ref. 48)

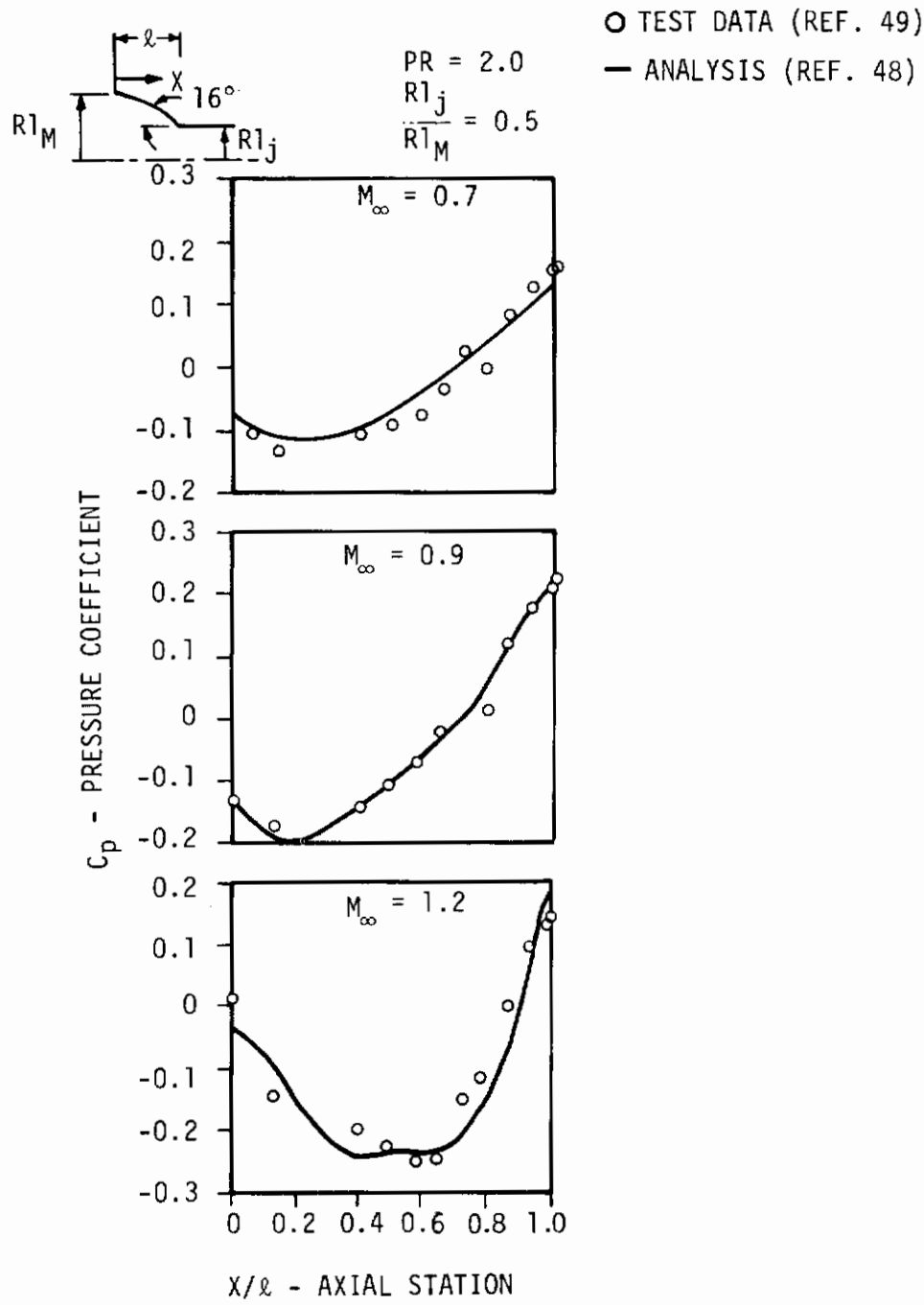

Figure 18. Pressure Coefficients for Circular Arc Afterbody (From Ref. 48)

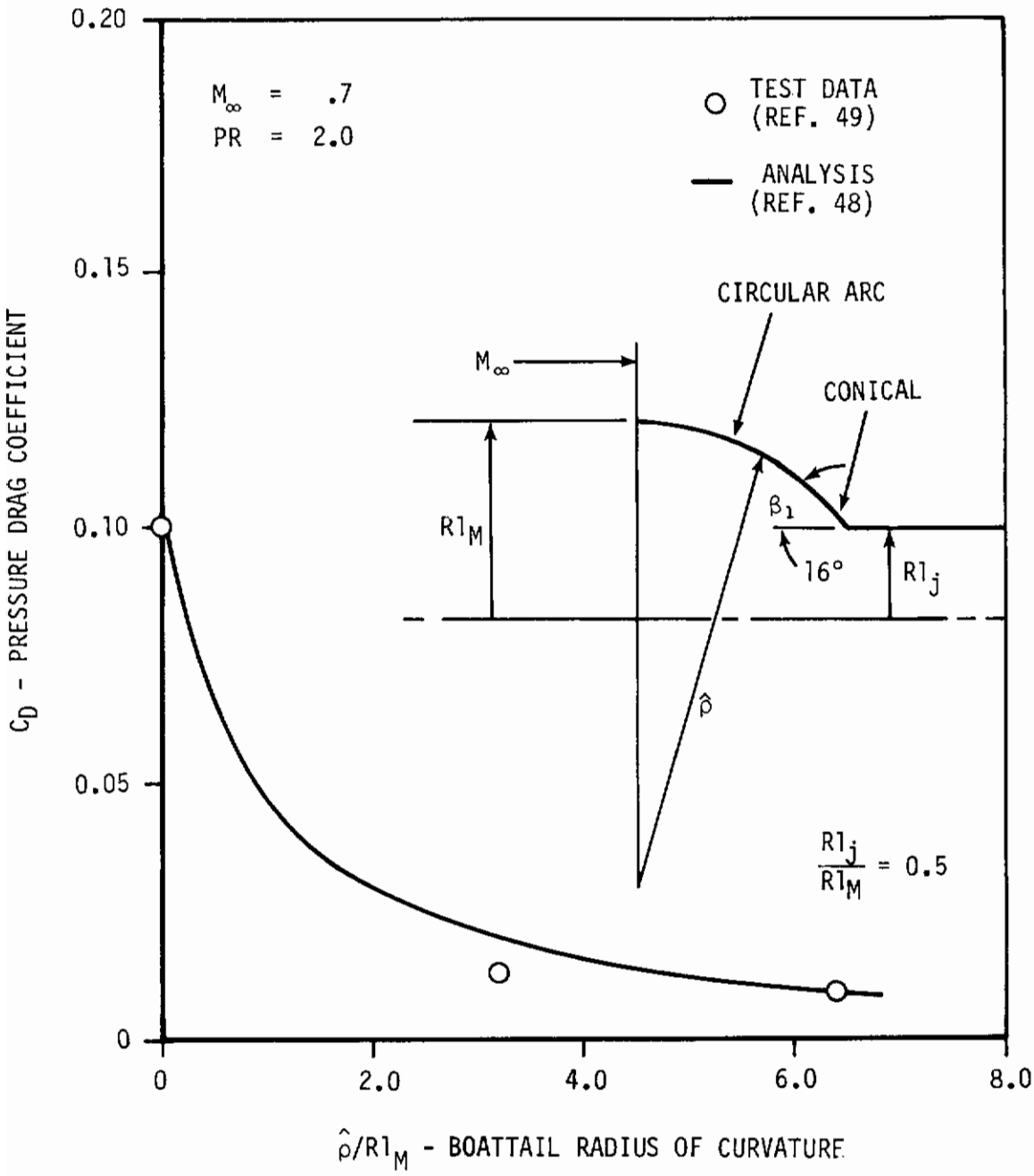

Figure 19. Pressure Drag for Axisymmetric Boattails (From Ref. 48)

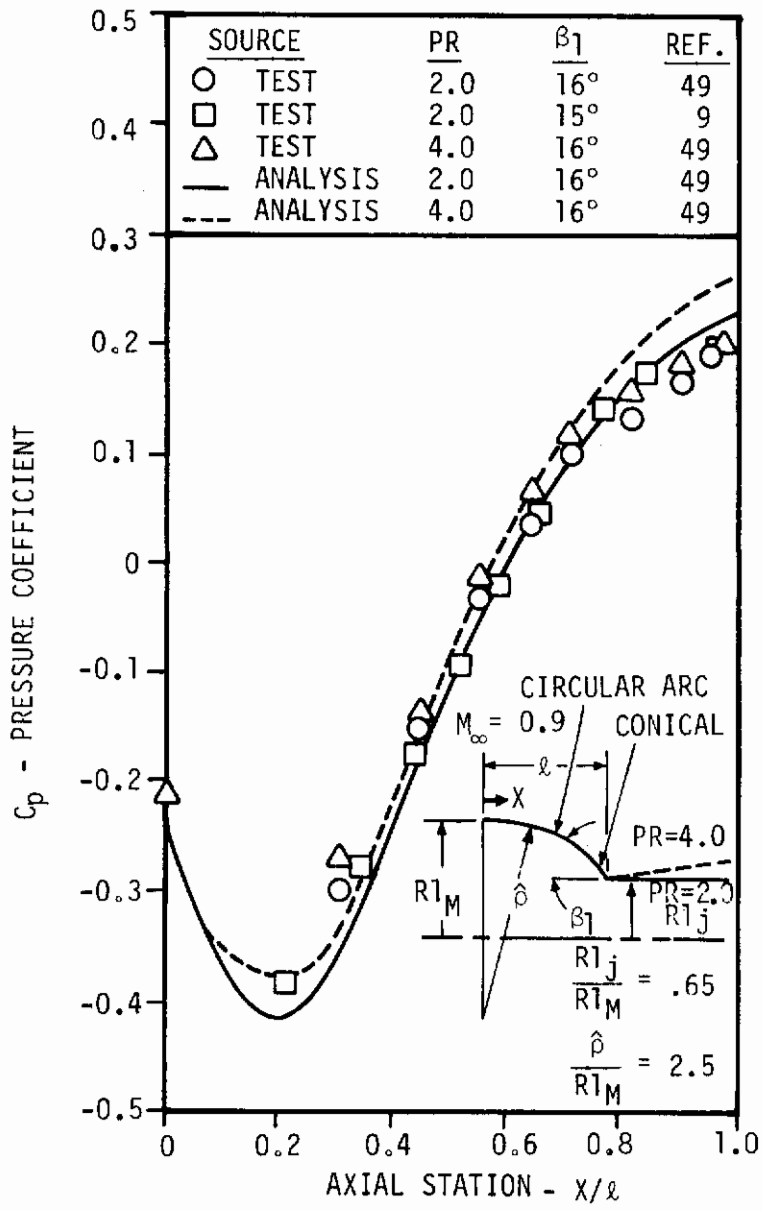

Figure 20. Pressure Ratio Effects on Afterbody Pressures (From Ref. 48)

Wu et al (Ref. 50) solve the transonic flow equation for a slender ogive at a small angle of attack with a parabolic method. The assumption is that the complete nonlinear solution for a velocity potential Φ consists of the sum of the linear solution ϕ of Oswatitsch and Keune type (Ref. 46) and a correction function g (Ref. 51) which satisfies the following equation

$$g_X(X;R,g) = -\left[\phi_X - \frac{1-M_\infty^2}{M_\infty^2(\gamma+1)}\right] \pm \sqrt{Y(X)} \tag{18}$$

where

$$Y(X) = \left[\phi_X - \frac{1-M_\infty^2}{M_\infty^2(\gamma+1)}\right]^2 - 2\int_{X^*}^{X} \phi_{XX}\left(\frac{\lambda_{pe}}{M_\infty^2(\gamma+1)}\right)\phi_X dX \tag{19}$$

and $\lambda_{pe} = \dfrac{M_\infty^2(\gamma+1)}{U_\infty}\,\phi_{XX}$ represents the acceleration term which is held constant. X* is the parabolic point where the coefficient of Φ_{XX} in the nonlinear transonic equation vanishes. The end result is that

$$\Phi_X = \frac{1-M_\infty^2}{M_\infty^2(\gamma+1)} \pm \sqrt{Y(X)} \tag{20}$$

The linearized velocity potential ϕ is formed by the sum of an axial component and a cross flow component. The boundary conditions are the usual flow tangency at the body surface and vanishing of flow perturbations at infinity. Once this solution is obtained, the boundary layer properties are determined through the use of the Navier-Stokes equations, and iterated with the inviscid flow solution until convergence is reached.

This method of approach is valid if the flow is not separated, since the nonlinear and the boundary layer corrections are

second order effects and therefore the growth of the displacement thickness must be small compared to the body dimensions. Figures 21,22 show the pressure distribution on an ogive at 2° angle of attack and $M_\infty \simeq 1$. The theory is consistent with experimental data obtained from the U. S. Army Missile Command and the shock location is predicted quite accurately. The flow field calculation is not carried out to the plume/body junction where the flow is very sensitive to the jet plume effects and where the slope discontinuity usually creates serious instabilities. Wu et al in their report perform a preliminary study of the rear shoulder effect on the transonic flow solution and recommend that further detailed analysis is warranted in this area.

2. Airfoils

Some transonic airfoil analyses should be presented at this point as they give a qualitative description of transonic flow field solutions that can eventually be extended to axisymmetric and 3-D flow fields and applied to afterbody/nozzle flow fields and wings.

Crown (Ref. 52) uses an integral method which accounts for the presence of shocks normal to the surface of thick airfoils. The exact 2-D inviscid flow equations are integrated analytically by means of the spline fit technique. When compared to the thin airfoil theory, the thick airfoil theory gives a correction factor proportional to M_∞^2 and therefore it is more important at higher free stream Mach numbers. Nevertheless the improvement in the computation of the pressure coefficient on an airfoil is negligible and does not compare

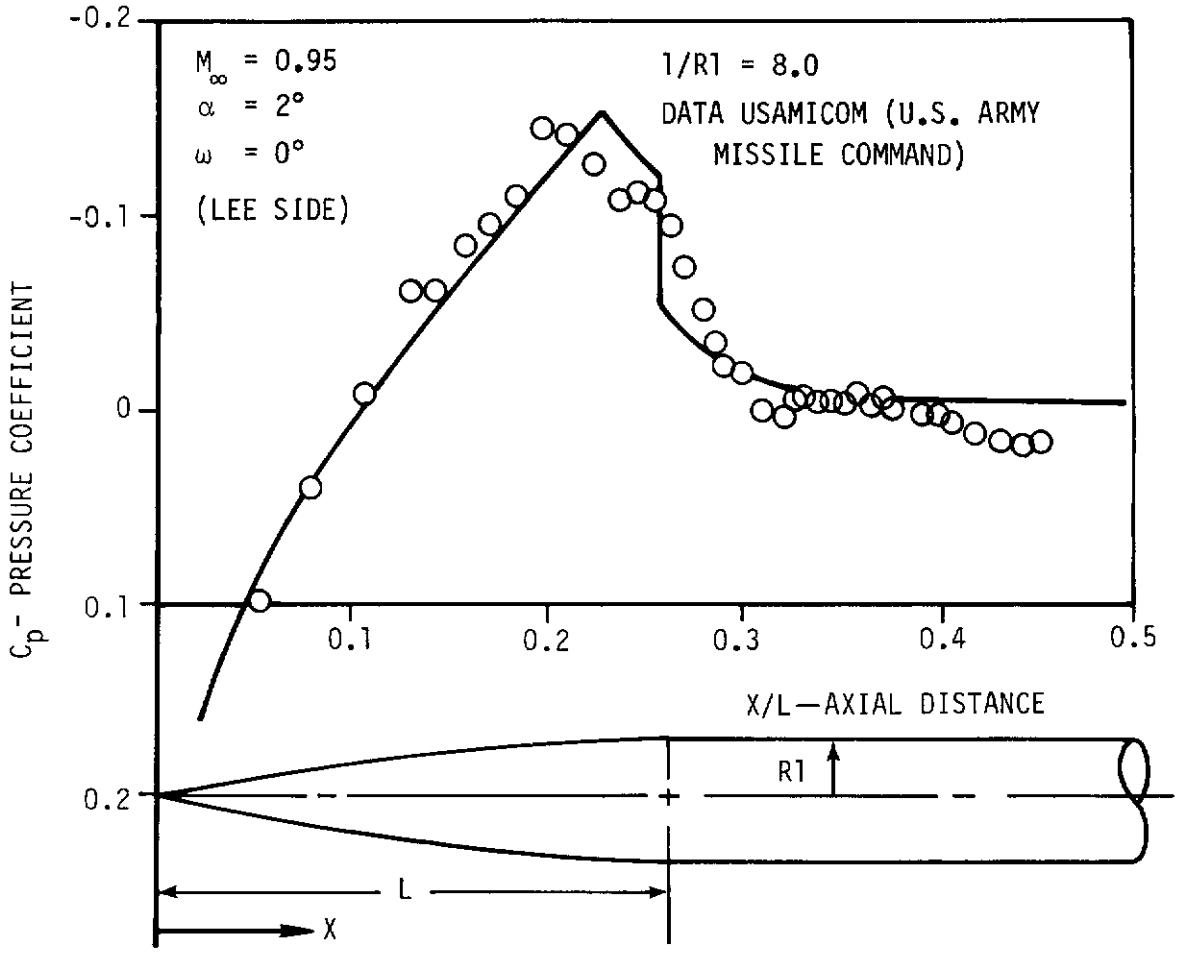

Figure 21. Comparison of Theory With Experiments on Leeward Side for 2° Angle of Attack at M_∞ = 0.95 (From Ref. 50)

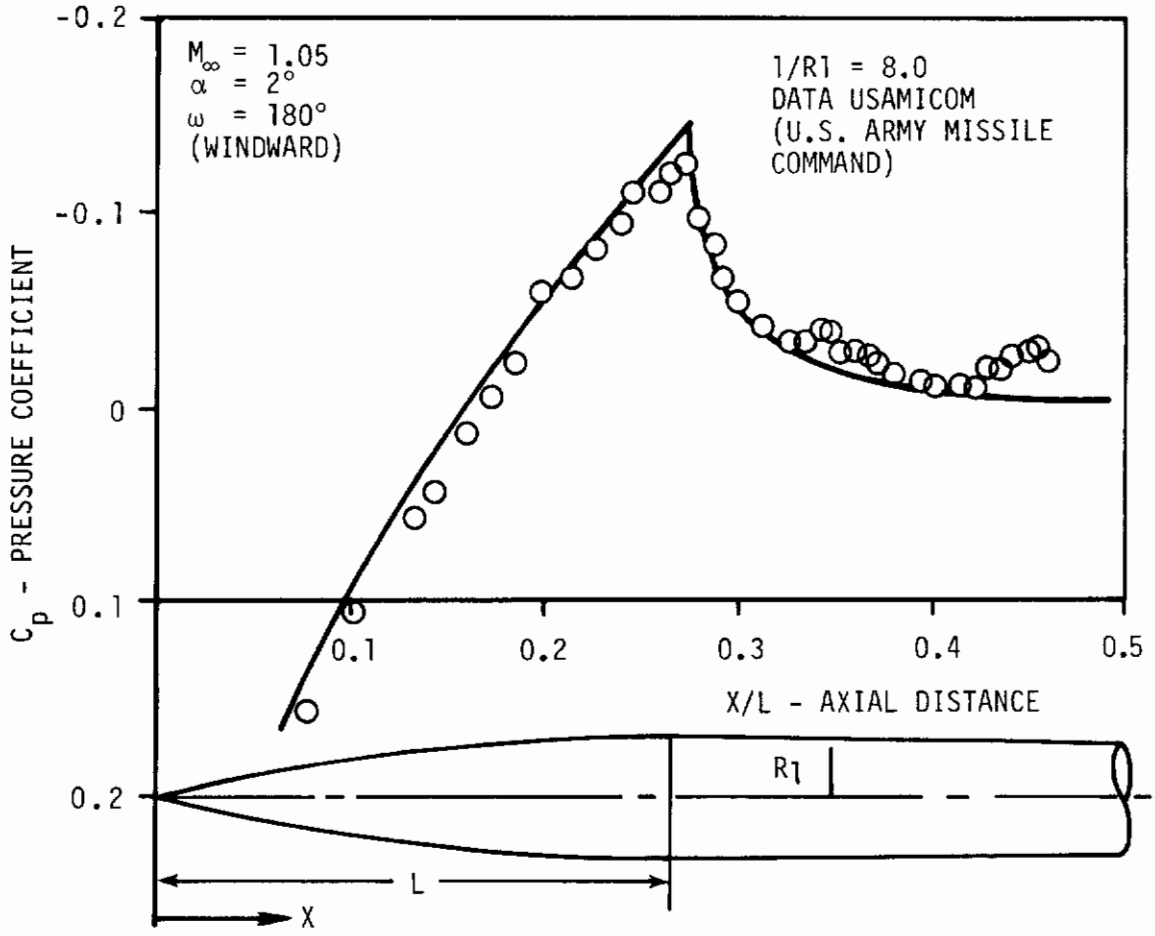

Figure 22. Comparison of Theory With Experiements on Windward Side for 2° Angle of Attack at M_∞ = 1.05 (From Ref. 50)

accurately with experimental results even in the case of thin airfoils (Fig. 23). This is probably due to the fact that the shock-boundary layer interaction and viscous effects are not included in the analysis. Furthermore, when applied to thick airfoils, the theory runs into convergence difficulties. However, the analysis predicts the flow deceleration just ahead of the shock and the flow acceleration just behind it. This is consistent with previous theoretical and experimental results.

Erdos et al (Ref. 55) analyze the transonic viscous flow around 2-D lifting airfoils using a new approach which accounts for the singularity existing at the point where the shock interacts with the surface of finite curvature. This new approach involves the solution of an indirect problem, i.e. from a specified pressure distribution that can be obtained from experimental data the airfoil contour is determined. The pressure distribution must therefore satisfy both the inviscid flow and boundary layer, which implies that it must be selected in such a way to give a correct placement of the shock wave and to be compatible with boundary layer requirements at the separation and reattachment points. If these requirements are met, no iterations will be required between the inviscid and viscous numerical solutions, and the individual stability conditions for the inviscid and viscous flow will be sufficient to yield a physically acceptable airfoil contour.

The inviscid flow is solved using the transonic flow equation for a perturbation potential written in conservation form. This equation contains the correct jump conditions and

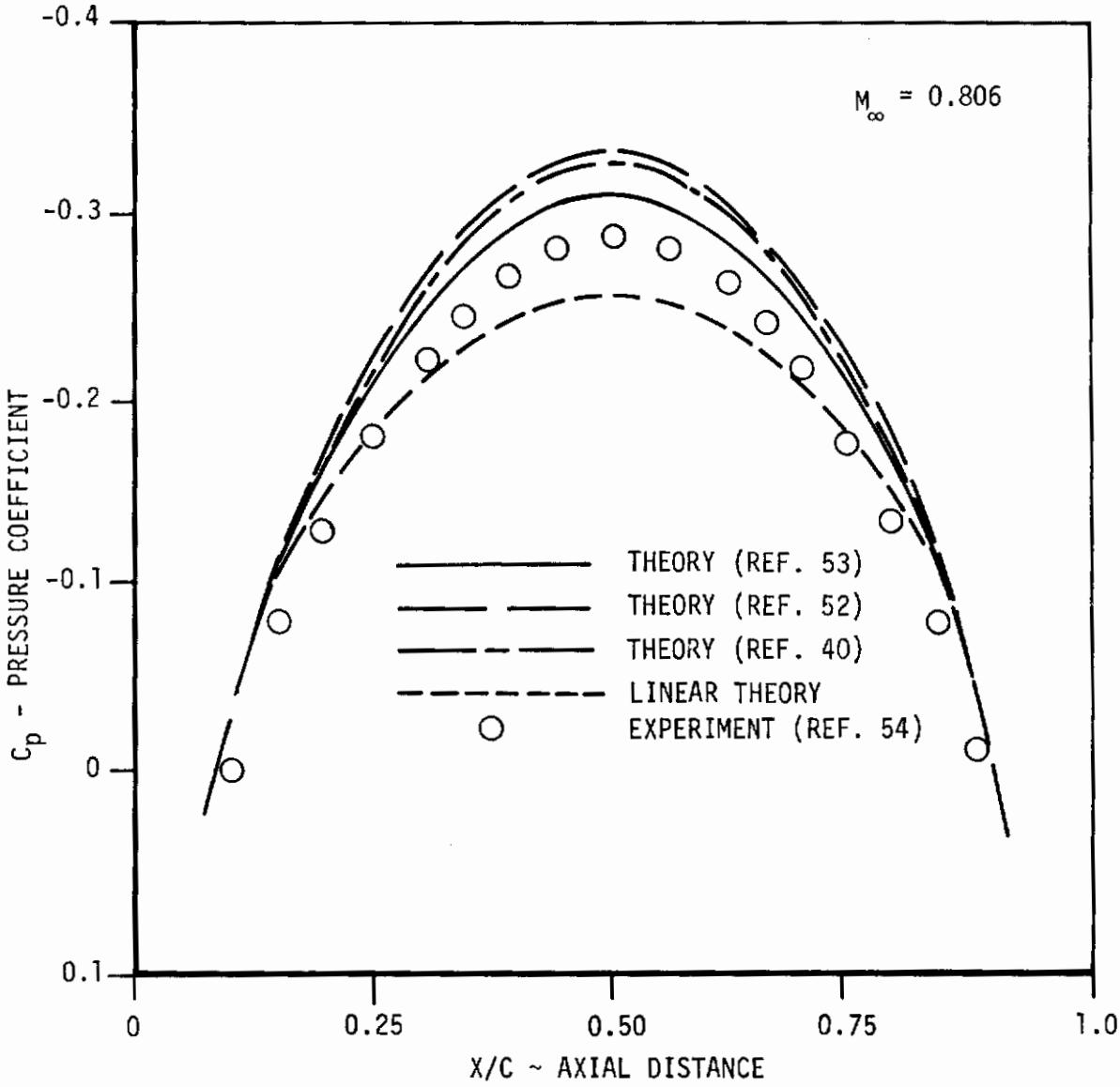

Figure 23. Comparison of Pressure Distribution at the Critical Mach Number over a 6% Thick Circular Arc Airfoil from Various Sources (From Ref. 52)

therefore it can be integrated across embedded shock waves. The appropriate value of the perturbation potential at infinity and the boundary conditions at the surface are used, together with a Kutta slice at the trailing edge of the airfoil across which ϕ_y is continuous but ϕ jumps by the value of the circulation. The boundary conditions are a combination of surface slope and surface pressure.

The transonic flow nonlinear equation of motion is of the parabolic type near the sonic line, but becomes elliptic or hyperbolic depending on the Mach number and the local value of the perturbation velocity. It is solved numerically with a relaxation procedure.

The viscous flow is solved with an integral method that yields a differential equation of parabolic type. The value of u can be determined from a set of initial values for u, if C_p is known and $u \geq 0$. If $u<0$, as in the separated recirculating region, upstream and downstream conditions must be used to avoid the infinity of solutions that would occur if only upstream conditions were specified, due to the parabolic nature of the equation. The boundary layer solution therefore takes on an elliptic-type character in the separated region even though the governing equation is parabolic. This implies that, in the case of negative velocities, the time-like direction points upstream. An implicit numerical method is used to solve the boundary layer equation because of its unconditional stability and second order accuracy.

The method for both the direct and indirect problems is applied to 2-D supercritical airfoils at an angle of attack and compares quite well with either the experimental data of Knechtel (Ref. 54) or the airfoil shape. (See Figs. 24-26).

Due to the positive results obtained, it is felt that the authors should extend the present approach to include 3-D flow fields, since this extension does not present any conceptual difficulty.

Viscous effects on the external transonic flow field can be nonnegligible when curved shock waves impinge on the airfoil surface. To this effect Sichel (Ref. 56) and others derived a so-called V-T (viscous-transonic) equation. This viscous-transonic equation solves only partially the problem of determining the correct jump conditions across a weak shock adjacent to a curved boundary. The flow in a region of this sort is a non-Hugoniot flow, i.e. a flow where the Rankine-Hugoniot relations do not hold. In order for the conventional oblique shock relations to hold, the ratio of shock thickness to shock radius of curvature must be of second order with respect to the perturbation potential. Sichel uses the 2-D small perturabation transonic flow equation to prove that the term $(1-M^2)\phi_{XX}$ for $M \to 1$ is comparable to a dissipative term. He then expands the perturbation velocity components, density, pressure and temperature in powers of a small quantity ε and substitutes them in the Navier-Stokes equations retaining only the largest terms. Together with the irrotationality condition, justified in

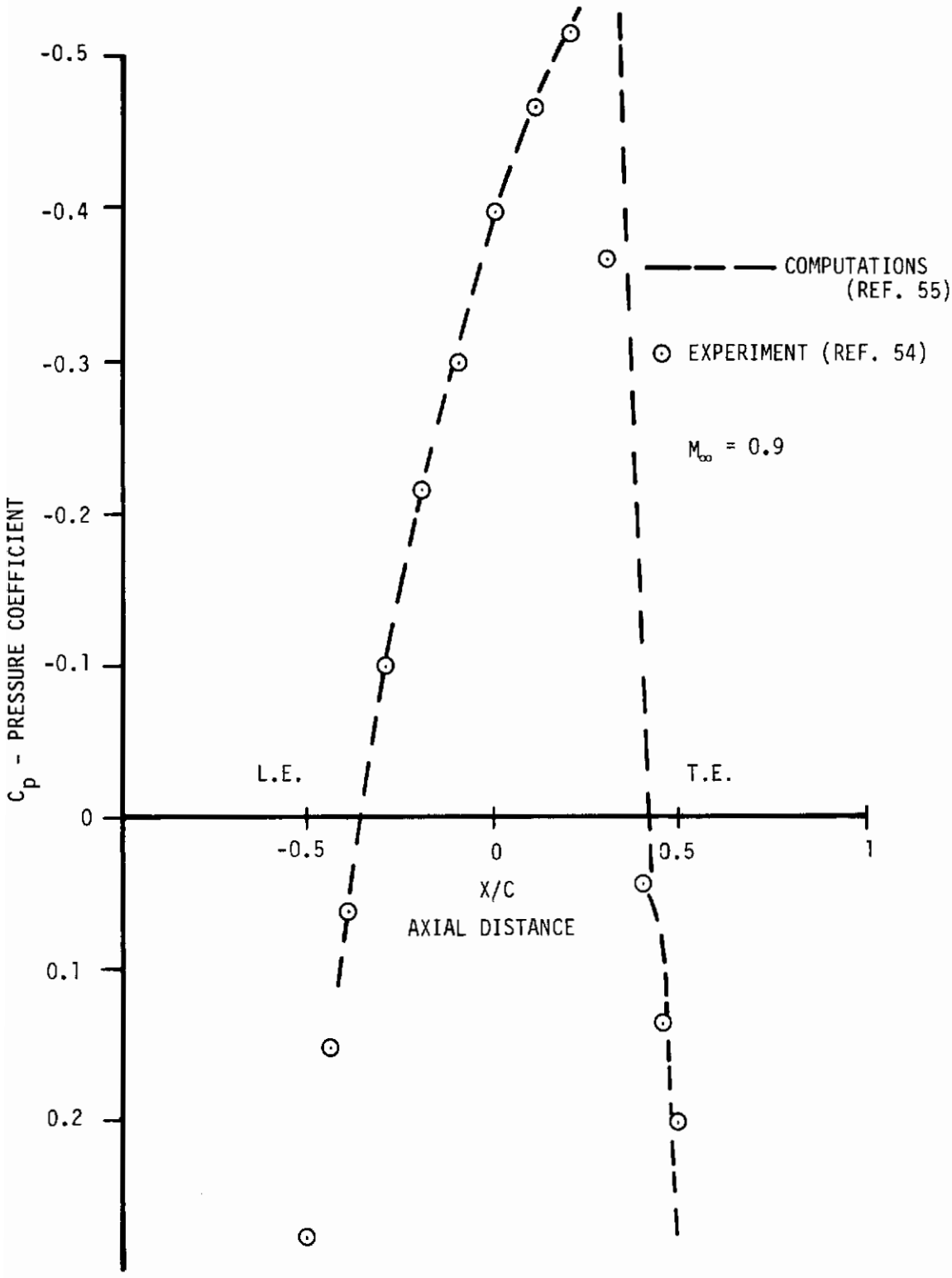

Figure 24. Pressure Distribution for Supercritical Circular Arc Airfoil With Geometry Prescribed (From Ref. 55)

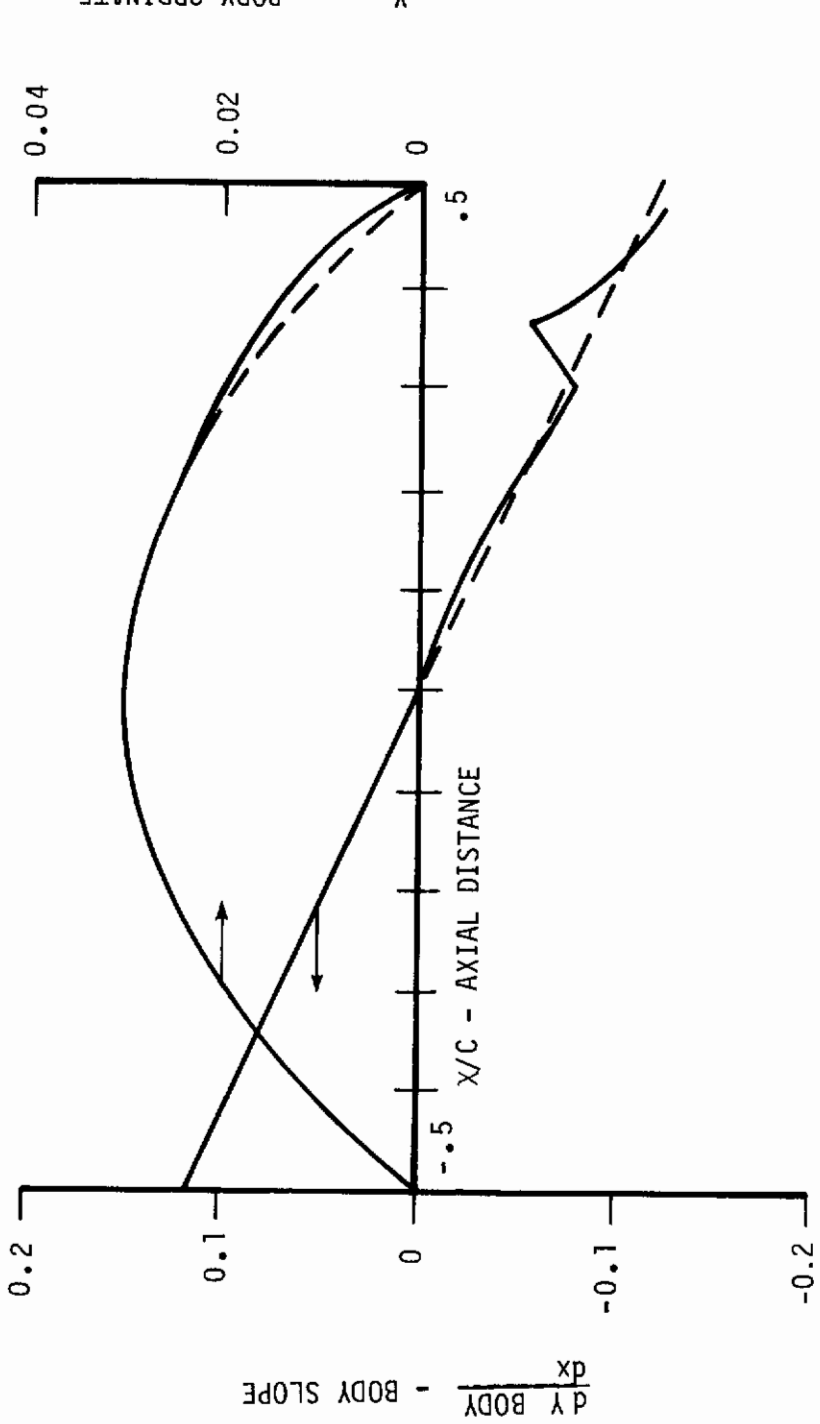

Figure 25. Body Shape for Supercritical Airfoil With Mixed Boundary Conditions (Dashed Line Represents Arc Airfoil) M_∞ = 0.9 (From Ref. 55)

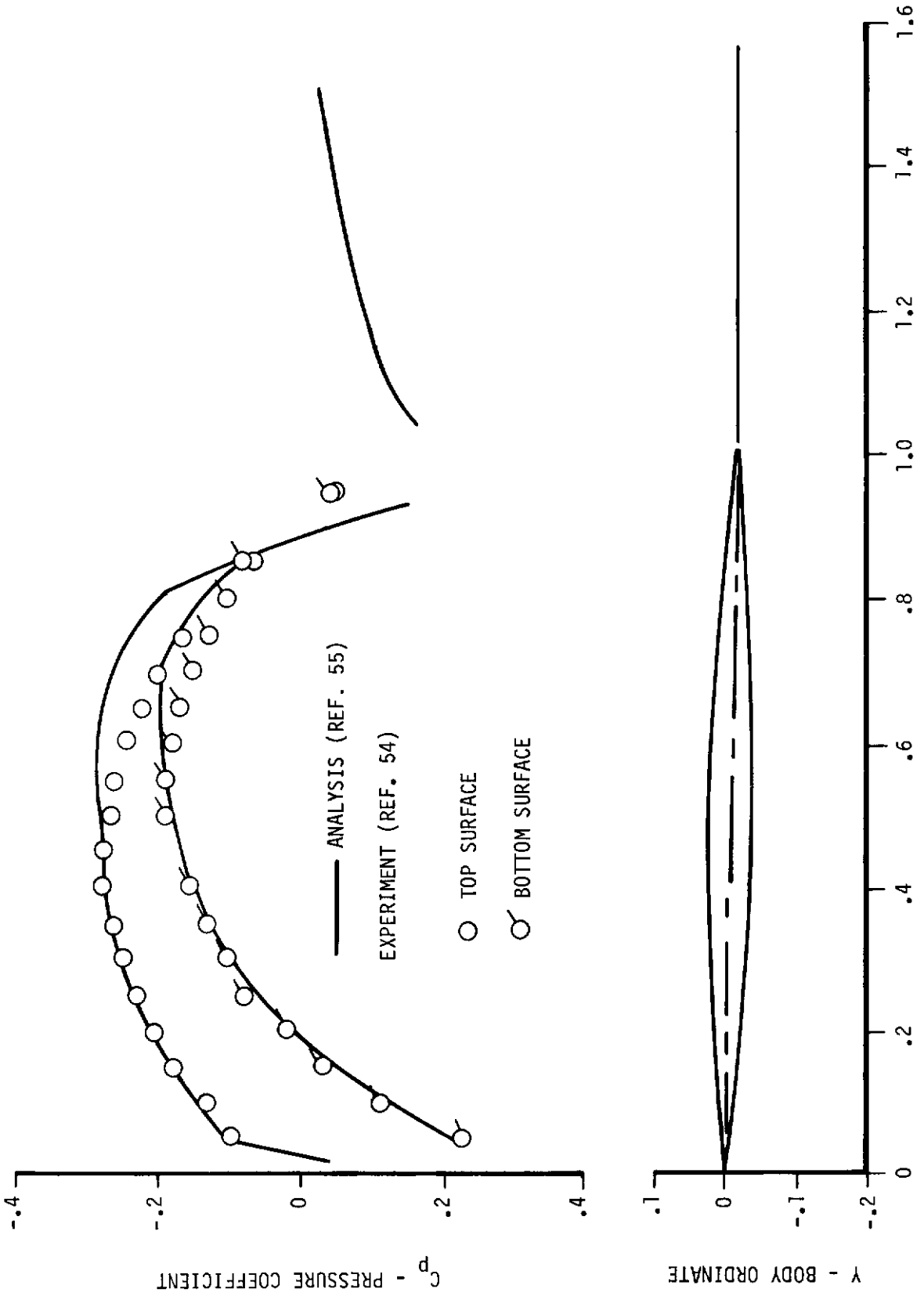

Figure 26. 6% Thick Circular Arc Airfoil at 1° Angle of Attack and M_∞ = 0.7 (From Ref. 55)

transonic flow since entropy changes are of higher order, and eliminating redundant second order expansion terms, he obtains a V-T equation in terms of a perturbation potential. This equation includes Reynolds and Prandtl numbers effects and is singular in nature for vanishing shock thickness, i.e. when the V-T equation tends to the inviscid transonic flow equation. This fact accounts for the instabilities in inviscid transonic flow when the shock discontinuity hits the surface, giving an infinite curvature to the inviscid streamline. The V-T equation can be reduced to a Riccati type equation, second order linear, with definite advantages, like close form solutions, and it may shed some light on the controversy of shockless transonic flows, smooth pockets of supersonic flow imbedded in outer subsonic flow.

Lock et al (Ref. 57) try to find approximate second order methods for an airfoil at angle of attack to improve solutions at critical Mach numbers. For subcritical Mach numbers the exact numerical solution using the full compressible flow equations is obtained through conformal mapping and the use of the Gauss-Seidel relaxation method (Ref. 58). But at critical Mach numbers we need approximate methods to deal with airfoils in real viscous flows and also for possible extension to 3-D investigations. Therefore the authors modify a second order Van Dyke solution (Ref. 59) of the small perturbation equation. They include a parameter that takes care of the necessary distortion of the shape of the pressure distribution near the leading edge of the airfoil as the Mach

number increases. Figures 27-28 show a comparison between exact and approximate solution and Figure 29 shows the correction for viscous effects.

Another approximate method is due to Labrujere et al (Ref. 63). This method consists of applying a rule similar to Gothert's rule to transform the linearized compressible potential flow equation into an incompressible flow equation. In order to take care of nonlinear compressibility effects, correction factors are used. Viscous effects are also considered by modifying the 2-D airfoil profile by superposing the value of the displacement thickness.

Garabedian and Korn (Ref. 64) have developed a Hodograph method based on complex characteristics which enables the determination of supercritical airfoil shapes which are shockless for the design free stream Mach number and angle of attack. The method consists of using conformal mapping to map the flow exterior to the airfoil into the unit circle and to solve the flow field along characteristic directions by means of overrelaxation procedures. The use of logarithmic singularities distributed in the interior of the airfoil enables to reach convergence for subsonic free stream Mach numbers up to $M_\infty \simeq 0.8$. Figures 30-31 show a comparison of the theoretical and experimental pressure distributions over a supercritical airfoil and the agreement is satisfactory if the experimental Mach number and angle of attack are slightly greater than the theoretical ones. For higher free stream Mach numbers it seems

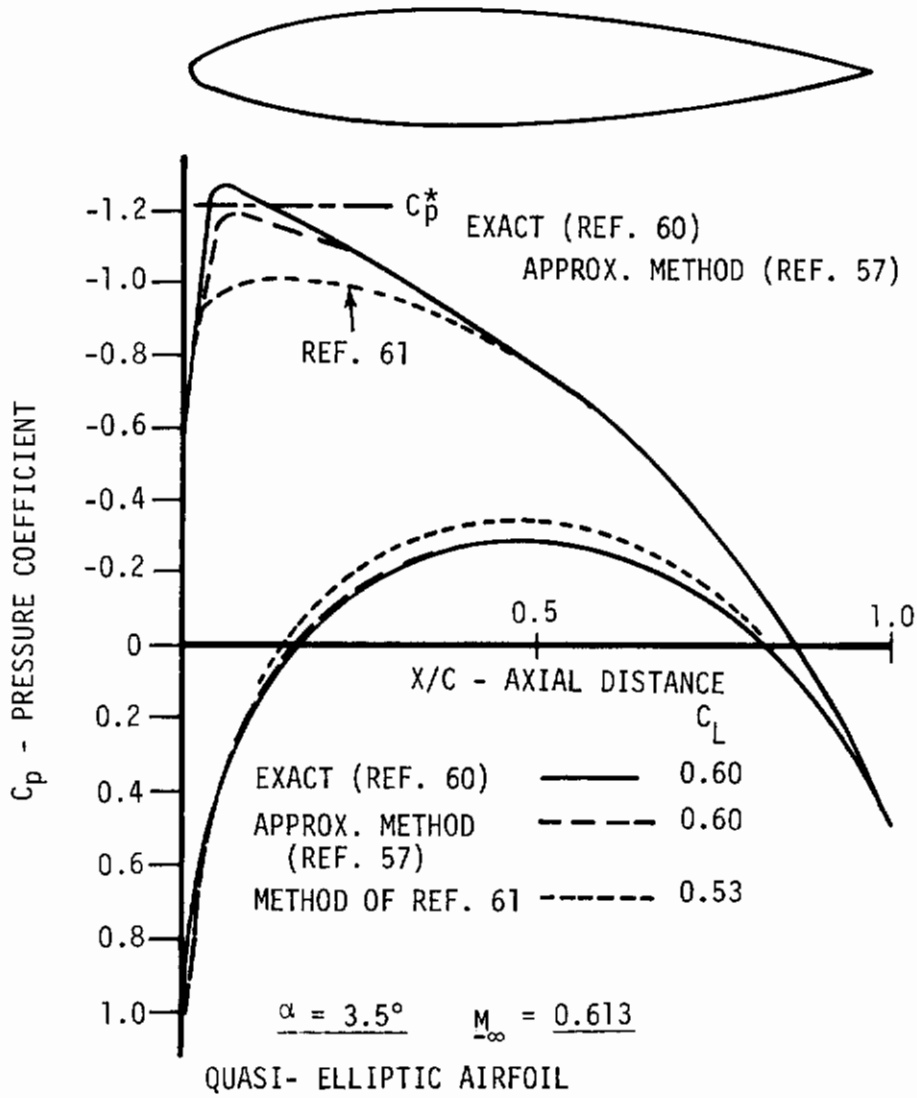

Figure 27. Inviscid Pressure Distributions (From Ref. 57)

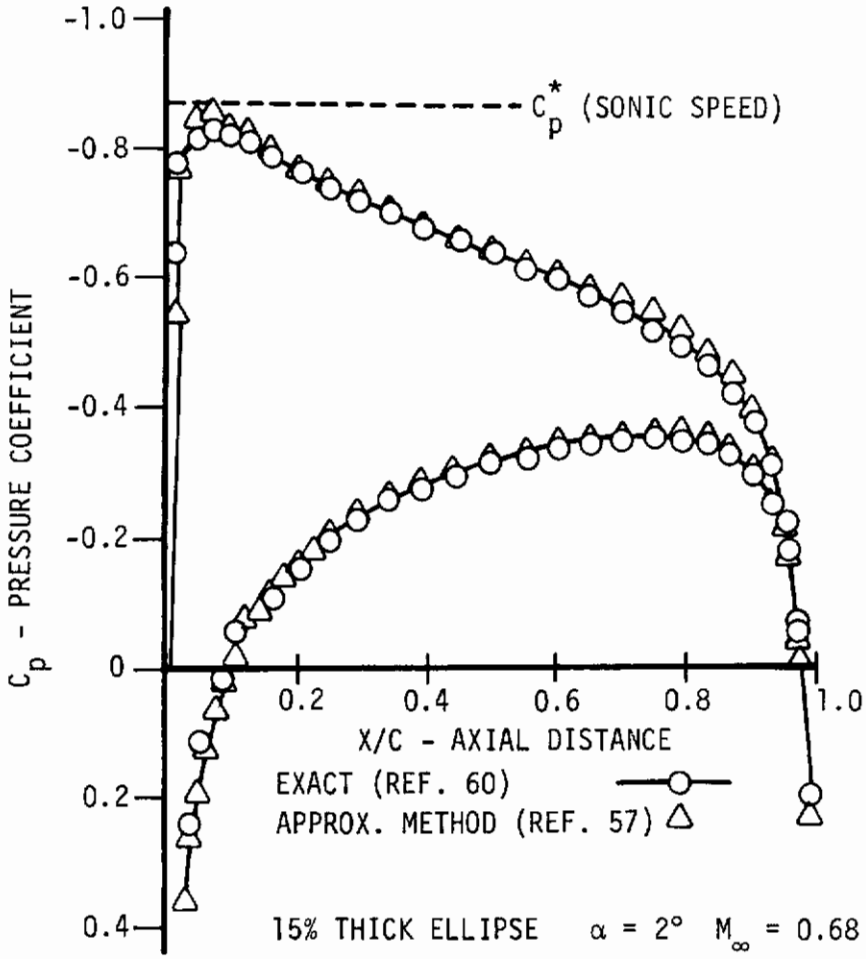

Figure 28. Load Distribution on an Ellipse at Incidence (From Ref. 57)

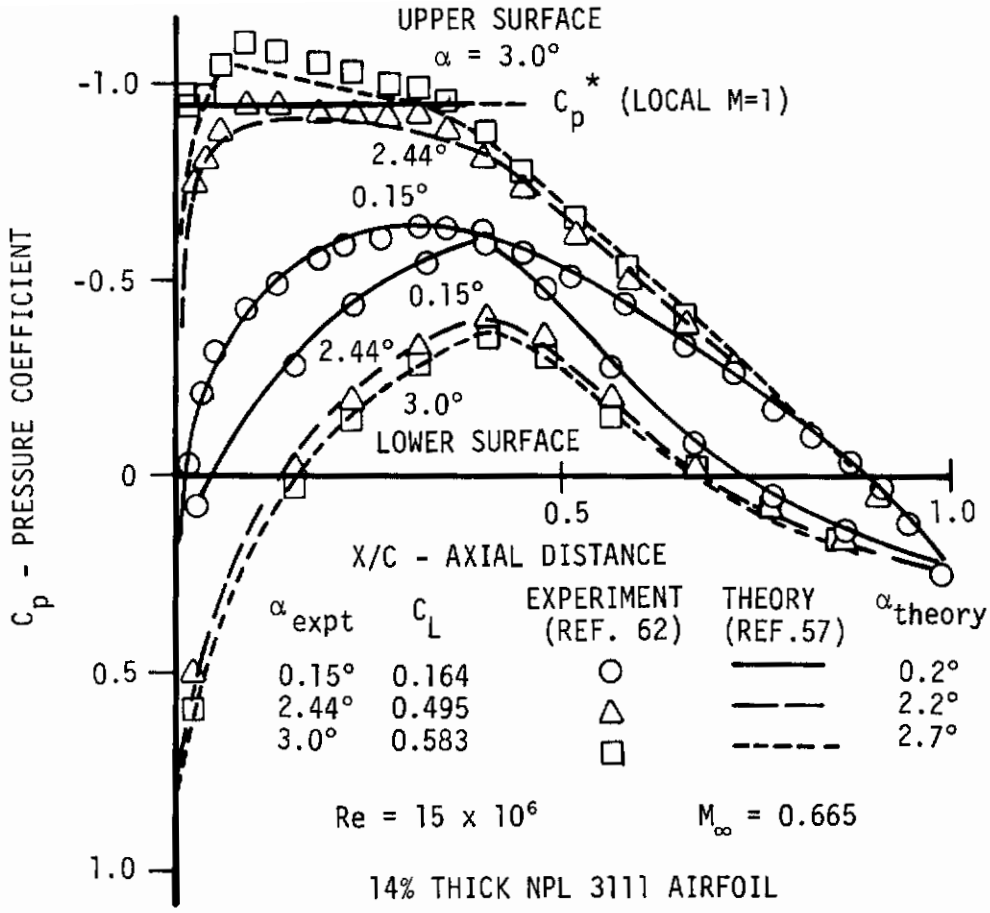

Figure 29. Pressure Distributions in Viscous Flow (From Ref. 57)

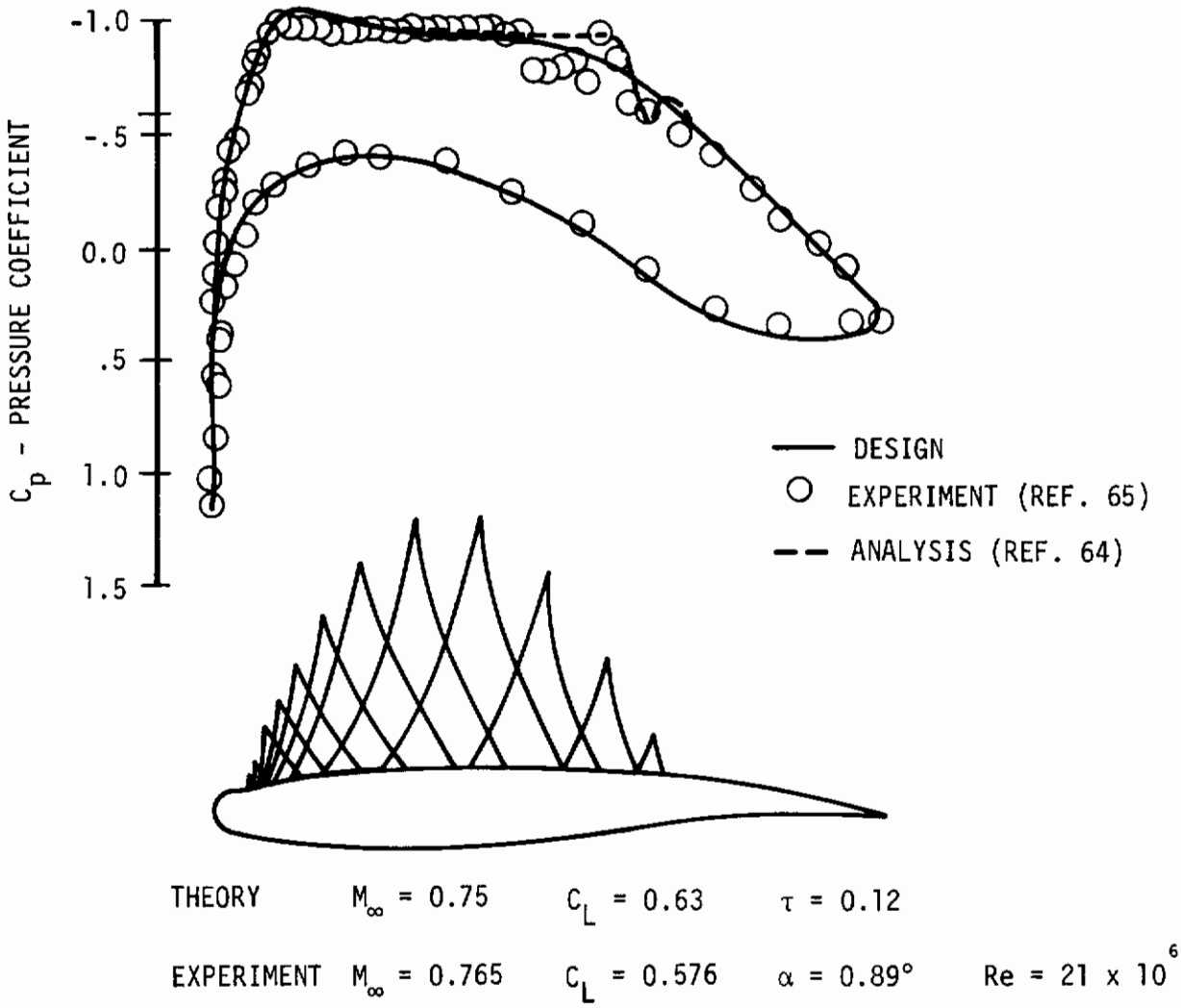

Figure 30. Shockless Flow Pressure Distribution (From Ref. 64)

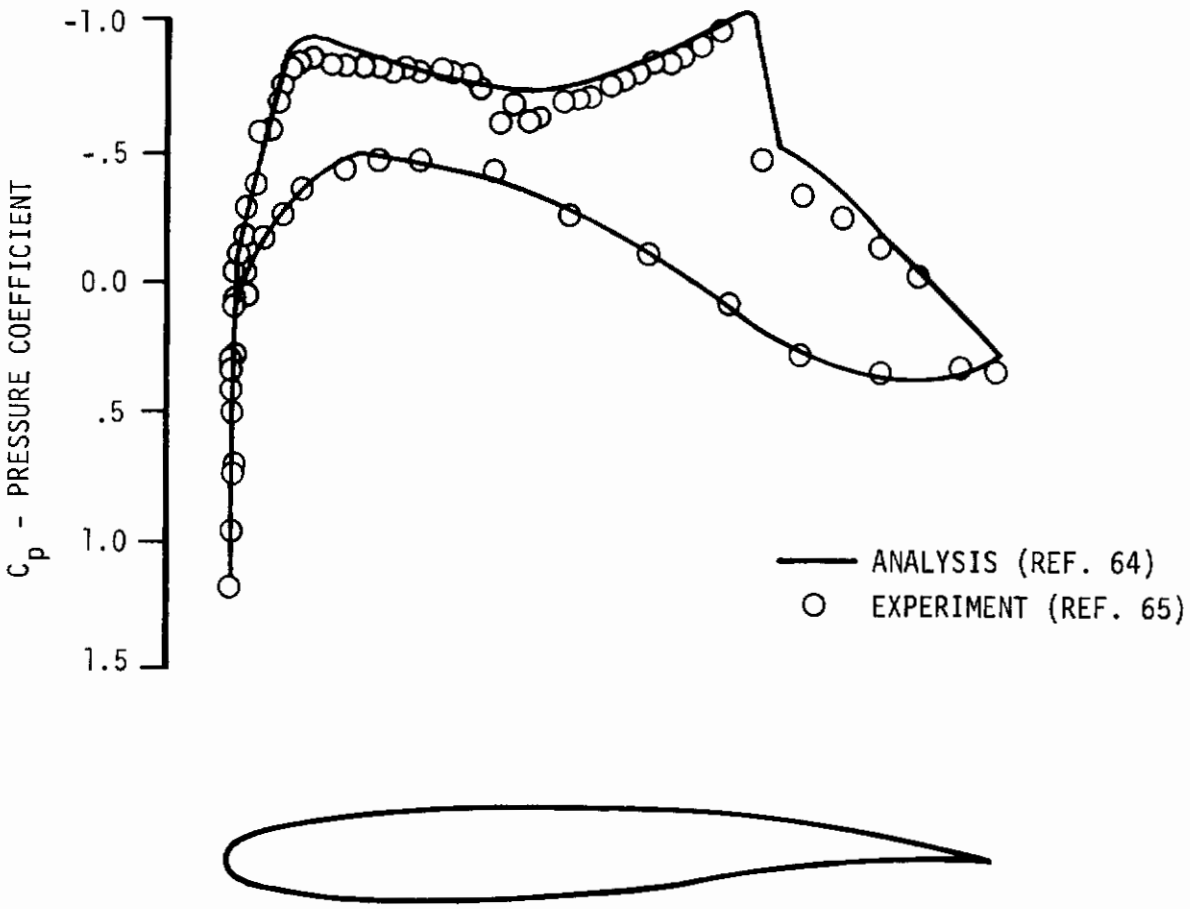

THEORY	$M_\infty = 0.757$	$C_L = 0.54$	$\alpha = -0.45°$	$\tau = 0.12$
EXPERIMENT	$M_\infty = 0.772$	$C_L = 0.48$	$\alpha = 0.44°$	$Re = 20 \times 10^6$

Figure 31. Off-Design Airfoil Pressure Distribution With 2 Weak Shocks (From Ref. 64)

that the relaxation procedure runs into difficulties since some instabilities are generated in the flow field.

Other authors have worked extensively in transonic flow problems. Some have used nonlinear integral methods (Ref. 66), others have used time-dependent techniques (Ref. 67) (Fig. 32), or relaxation techniques in 2-D, with some extensions to 3-D, over lifting and nonlifting airfoils and wings (Refs. 14, 69-71) (Figs. 33-35). Klunker (Ref. 72) obtained an analytical expression for the far field value of the velocity potential that considerably facilitates the numerical computation.

The relaxation techniques presented are very effective in transonic flow. It is felt that every effort should be done to improve their rate of convergence without loss of accuracy especially for extension to 3-D lifting schemes where the computer time necessary for convergence is considerable.

3. Separation and Shock-Boundary Layer Interaction

The transonic theories presented assume at most the presence of weak shocks, i.e. isentropic conditions over the airfoils. Obviously if stronger shocks were present they would effect the boundary layer growth and might possibly cause flow separation in the shock region. It is interesting to analyze such an occurrence. In the case of separation, the pressure distribution on the airfoil is drastically changed. Laminar and turbulent separations affect the flow field differently (Fig. 36) and Reynolds number effects are evident in the anomalous behavior of the shock location (Fig. 37).

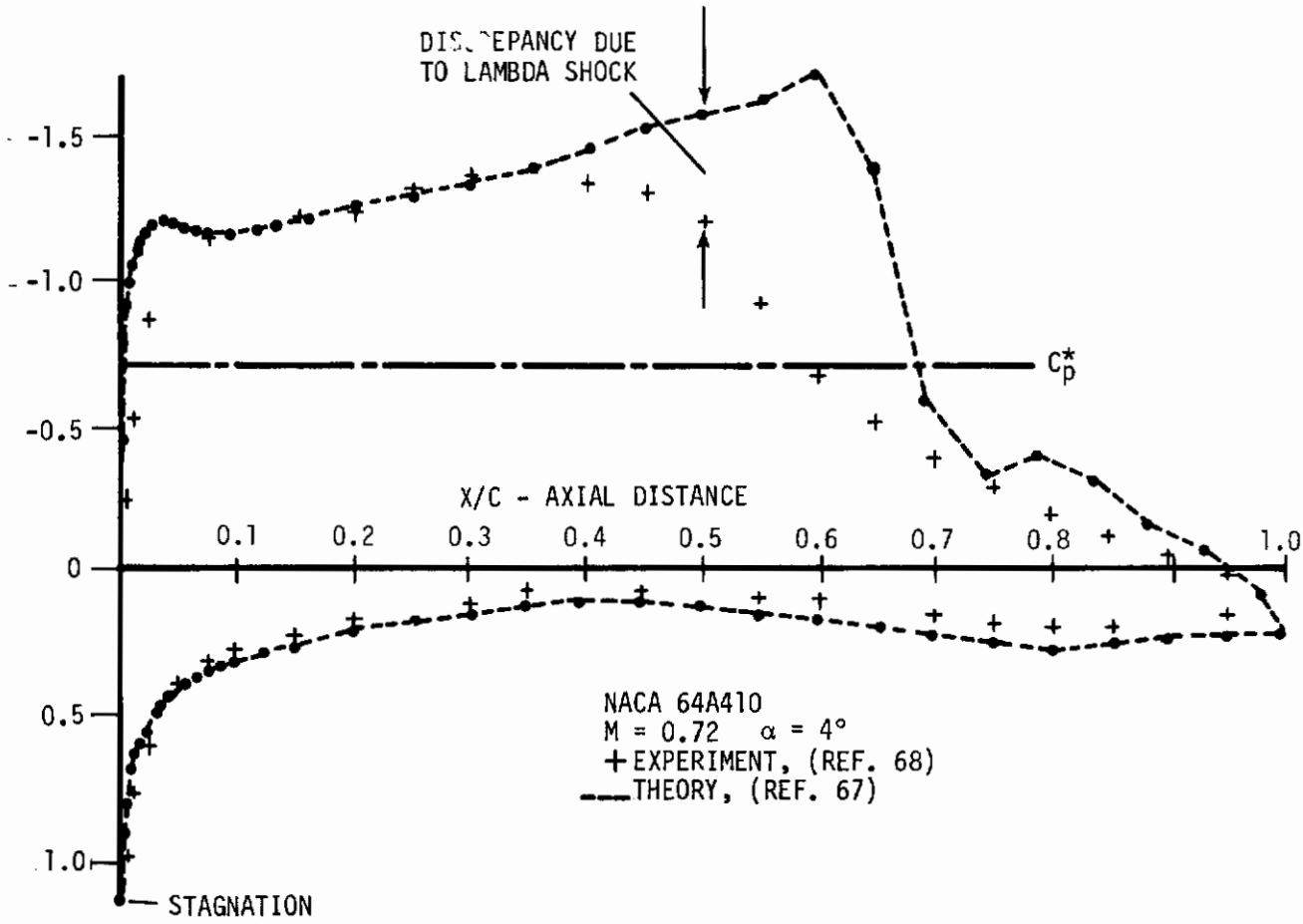

Figure 32. Comparison of Theory With Experiments (From Ref. 67)

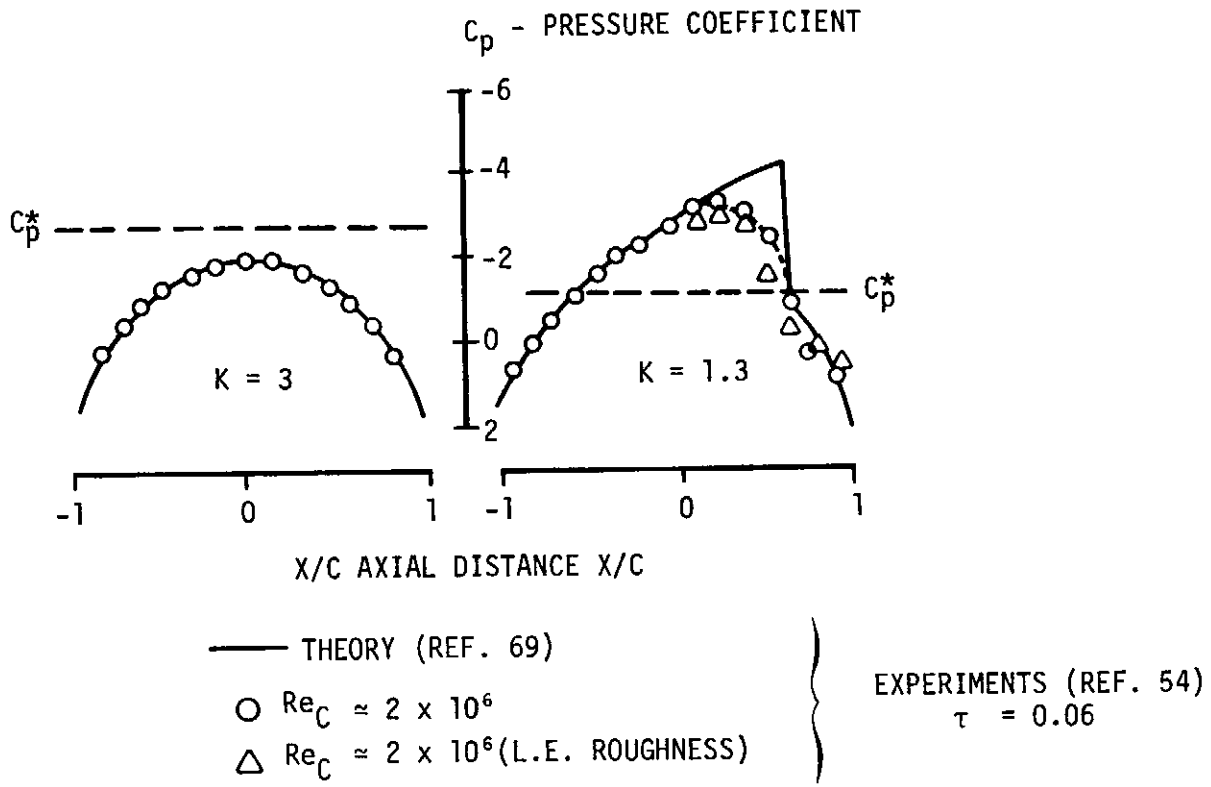

Figure 33. Pressure Distribution for Circular Arc Airfoil (From Ref. 69)

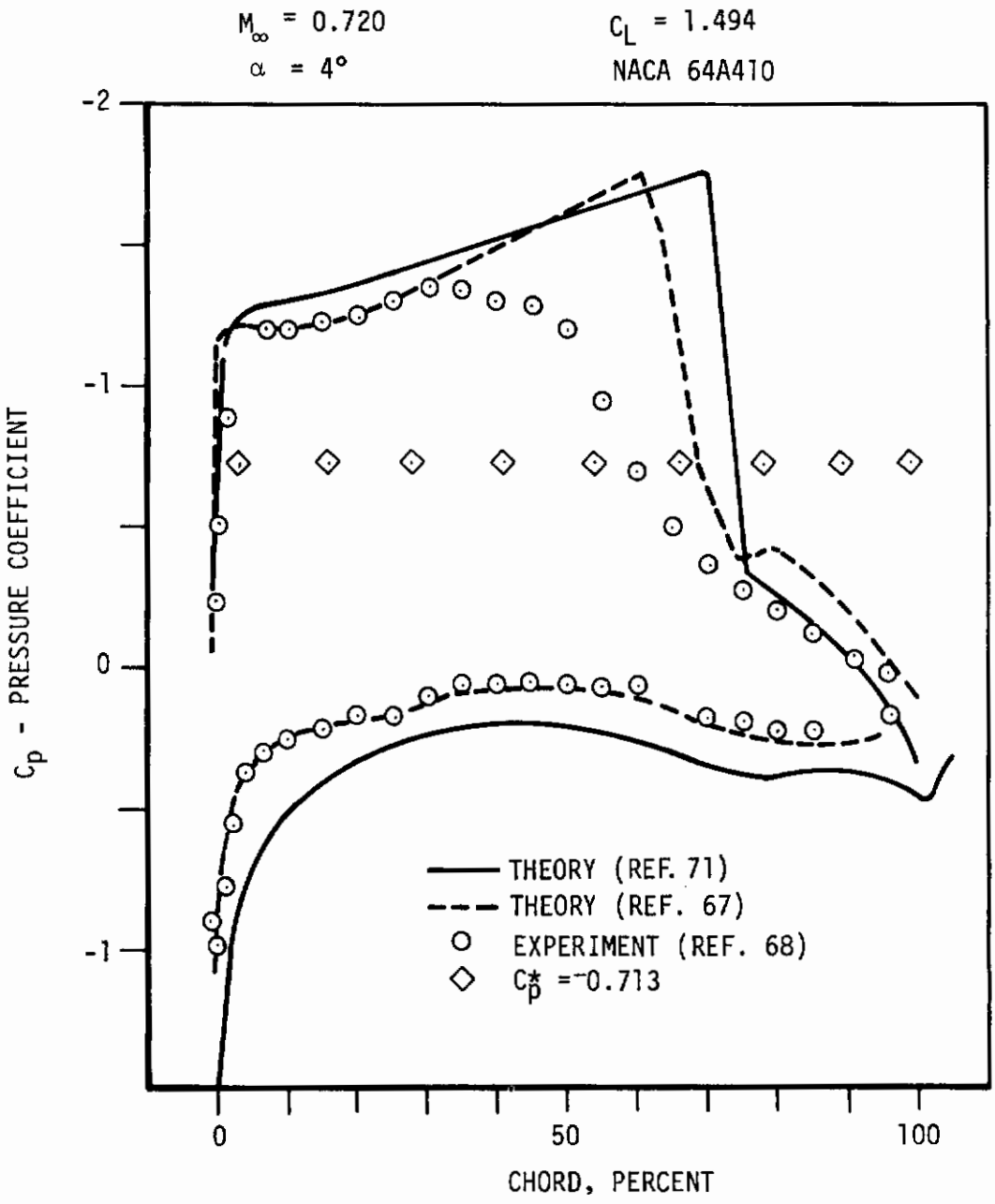

Figure 34. Comparison of Theories With Experiment (From Ref. 71)

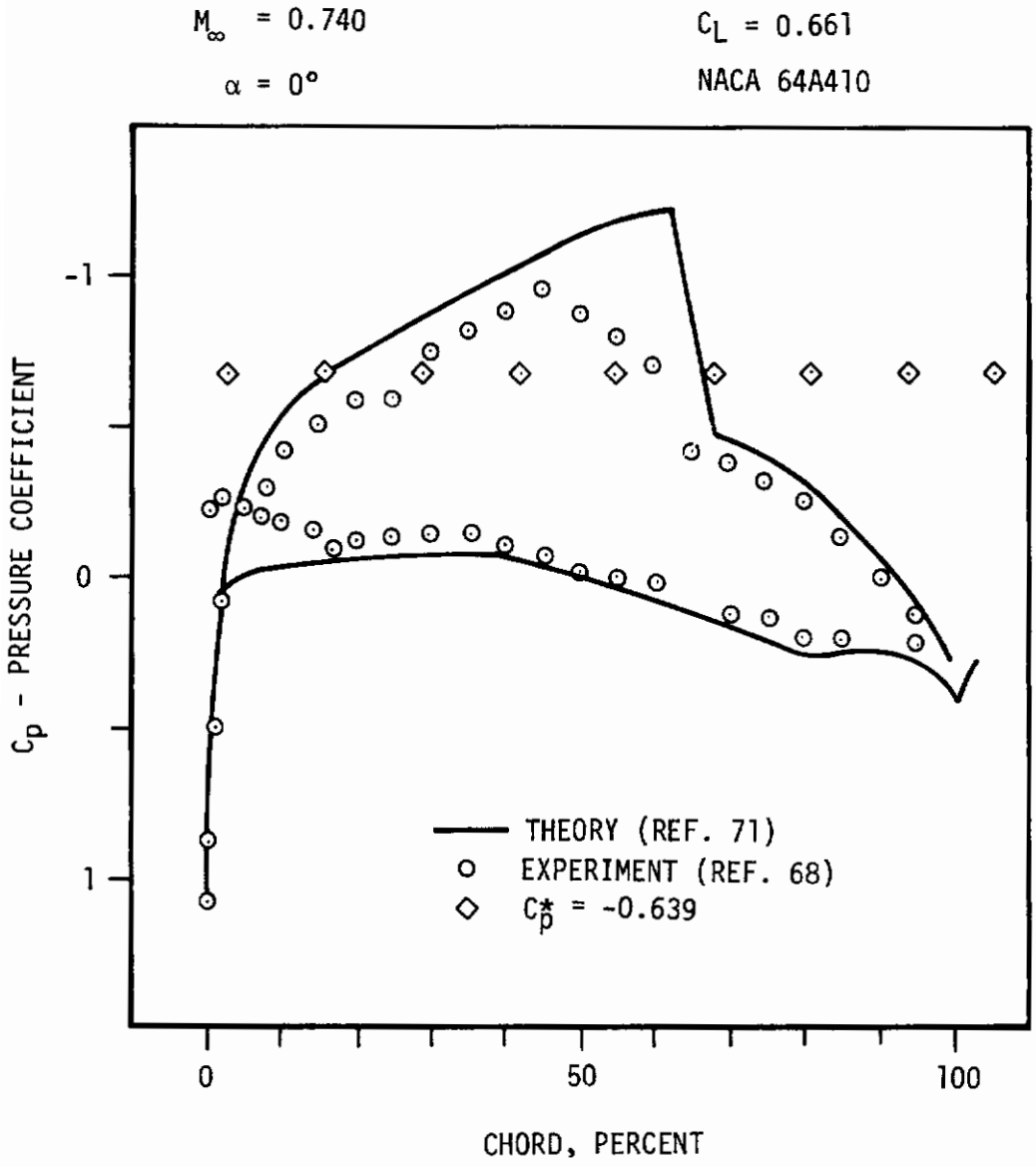

Figure 35. Comparison of Theory With Experiment (From Ref. 71)

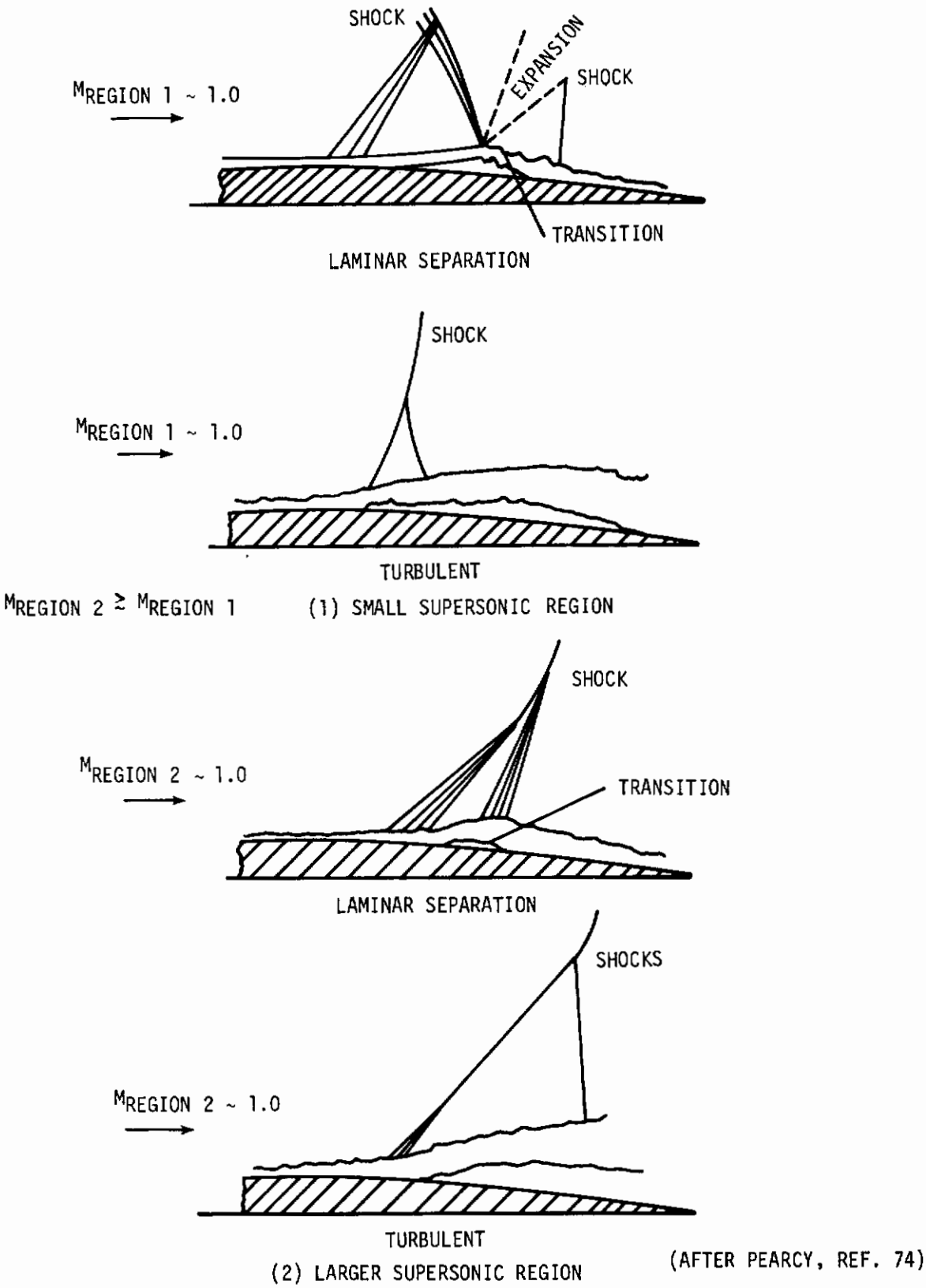

Figure 36. Illustration of Shock-Boundary Layer Interaction (From Ref. 73)

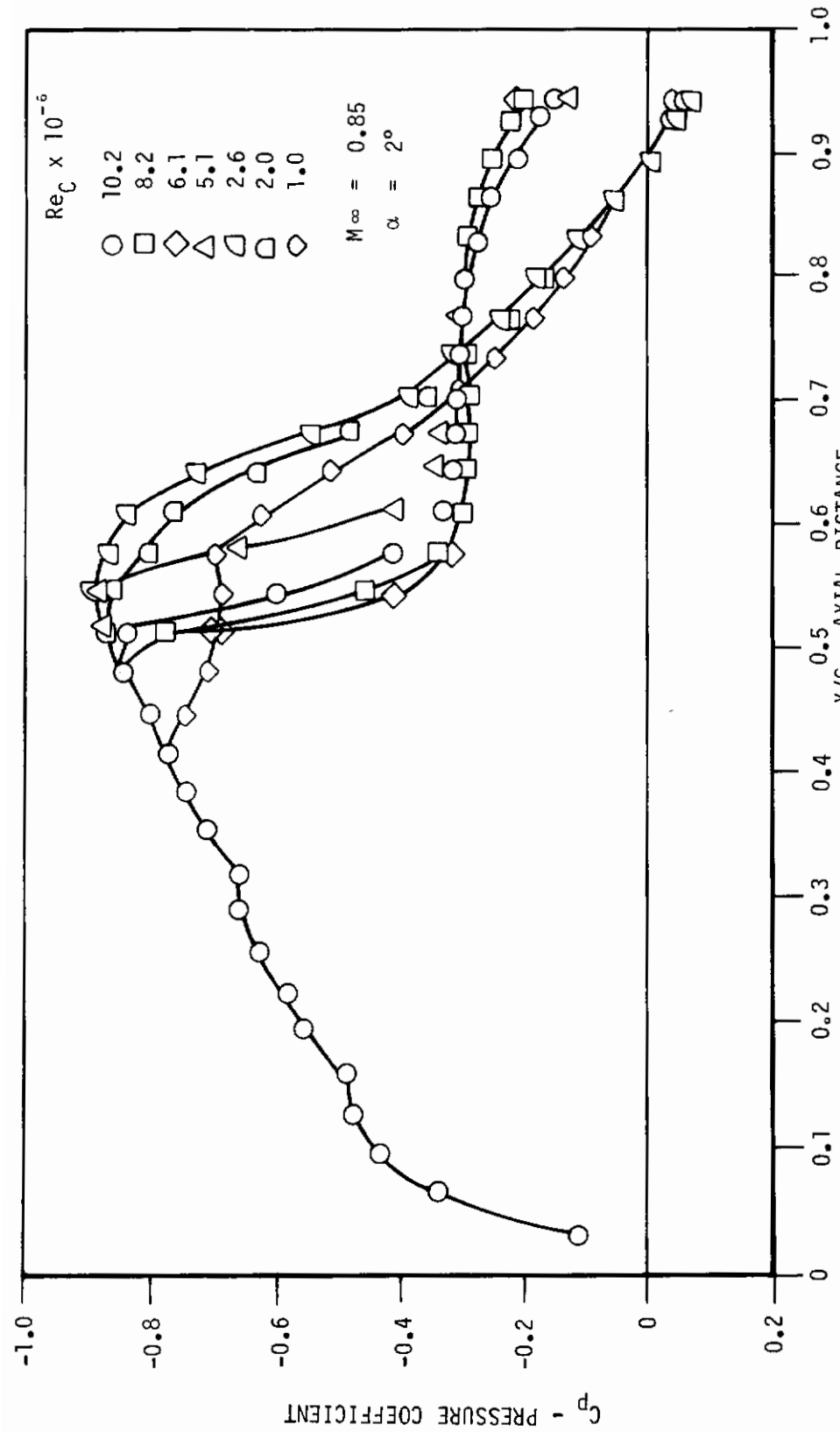

Figure 37. Reynolds Number Effects on Pressure Coefficient of Upper Surface (From Ref. 75)

Blackwell (Ref. 76) tries to find a correlation between wind tunnel and flight tests to minimize the Reynolds number effects. His 2-D investigation proves that, in order to obtain the same shock location and pressure distribution in wind tunnel tests as in flight, despite the different Reynolds number, the boundary layer transition in the wind tunnel must be set in such a way to obtain the same total pressure profile in the boundary layer at the airfoil trailing edge (Figs. 38-39).

Shock-boundary layer interaction has been and still is a problem area. The flow field is quite complex and consequently it is difficult to set up an adequate analytical model which would give good results when compared with experimental data. For instance, the estimated drag obtained from the strength of the shock wave itself can be seen in Figure 40 to be much smaller than the measured one. The additional drag is mostly due to the interaction of the shock wave with the boundary layer. Wind tunnel and flight tests have been compared to empirical criteria but the results most of the time are not satisfactory.

Thomas (Ref. 78) approach to the problem consists of using boundary layer theory. Once the transonic pressure distribution is obtained on the airfoil, the boundary layer theory can calculate the separation points as functions of Mach number and location of the separation, and the Reynolds number effect on the buffet onset can then be obtained.

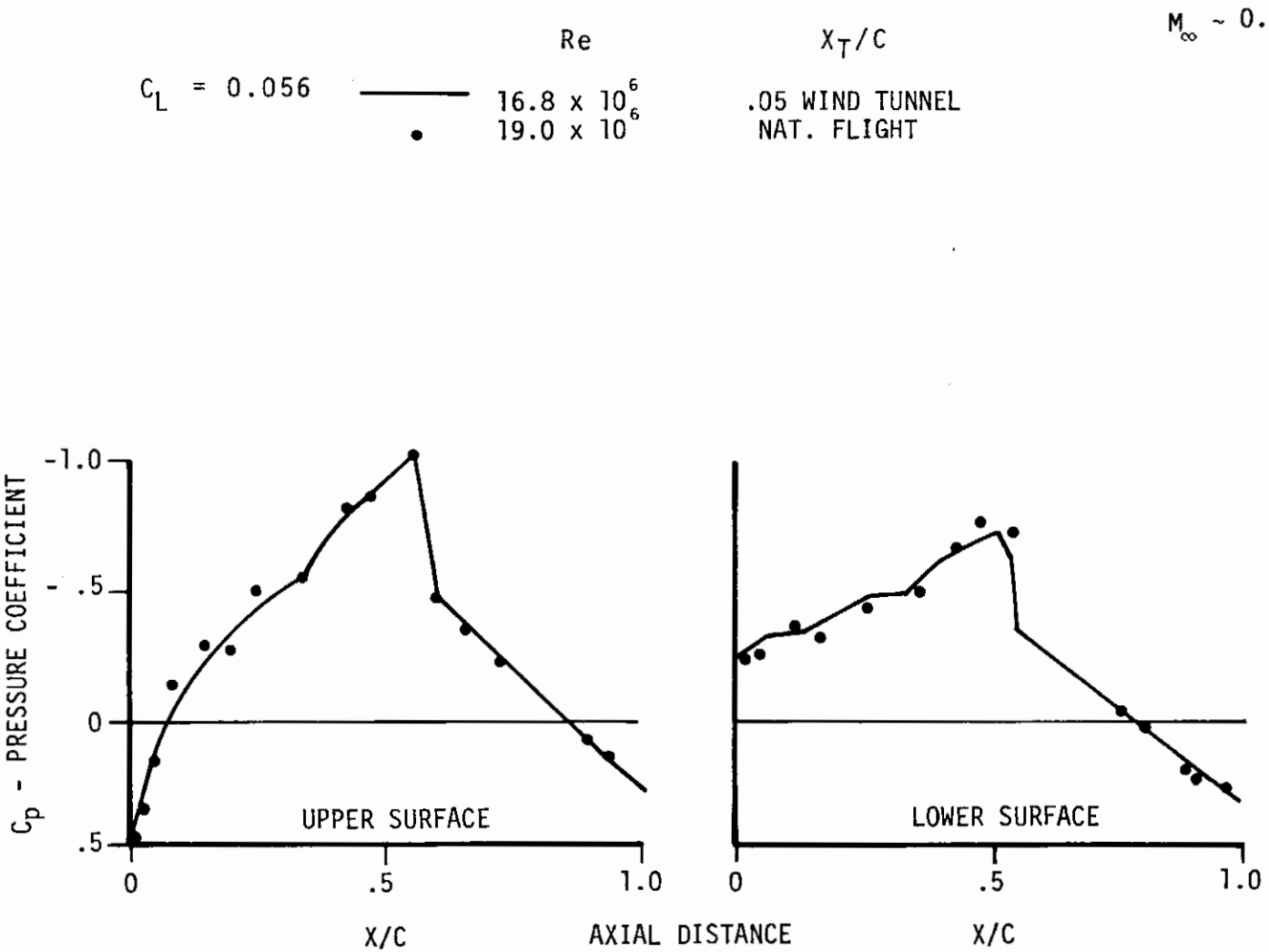

Figure 38. Correlation of Wind-Tunnel - Flight Results (From Ref. 76)

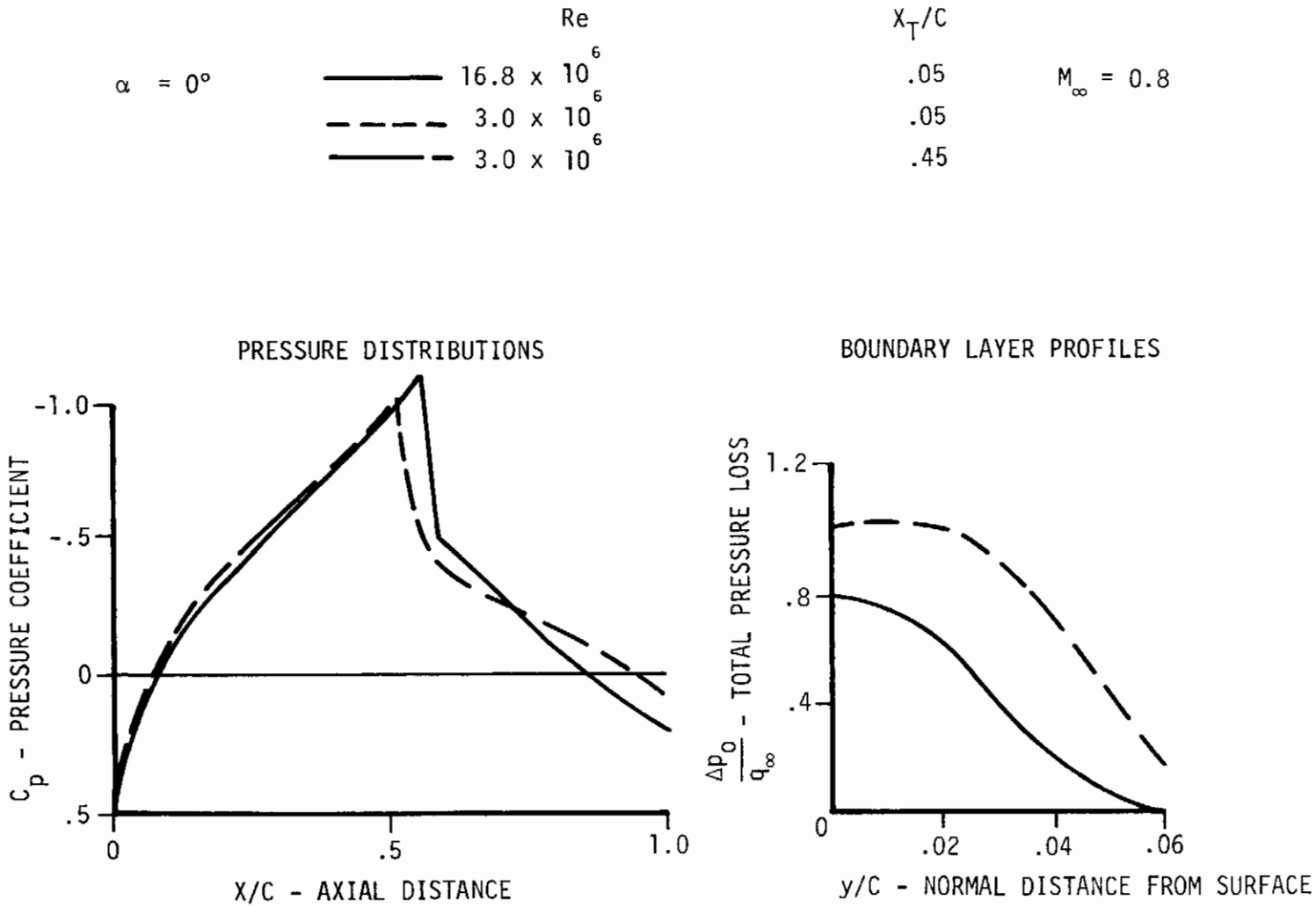

Figure 39. Effect of Reynolds Number and Transition Location (From Ref. 76)

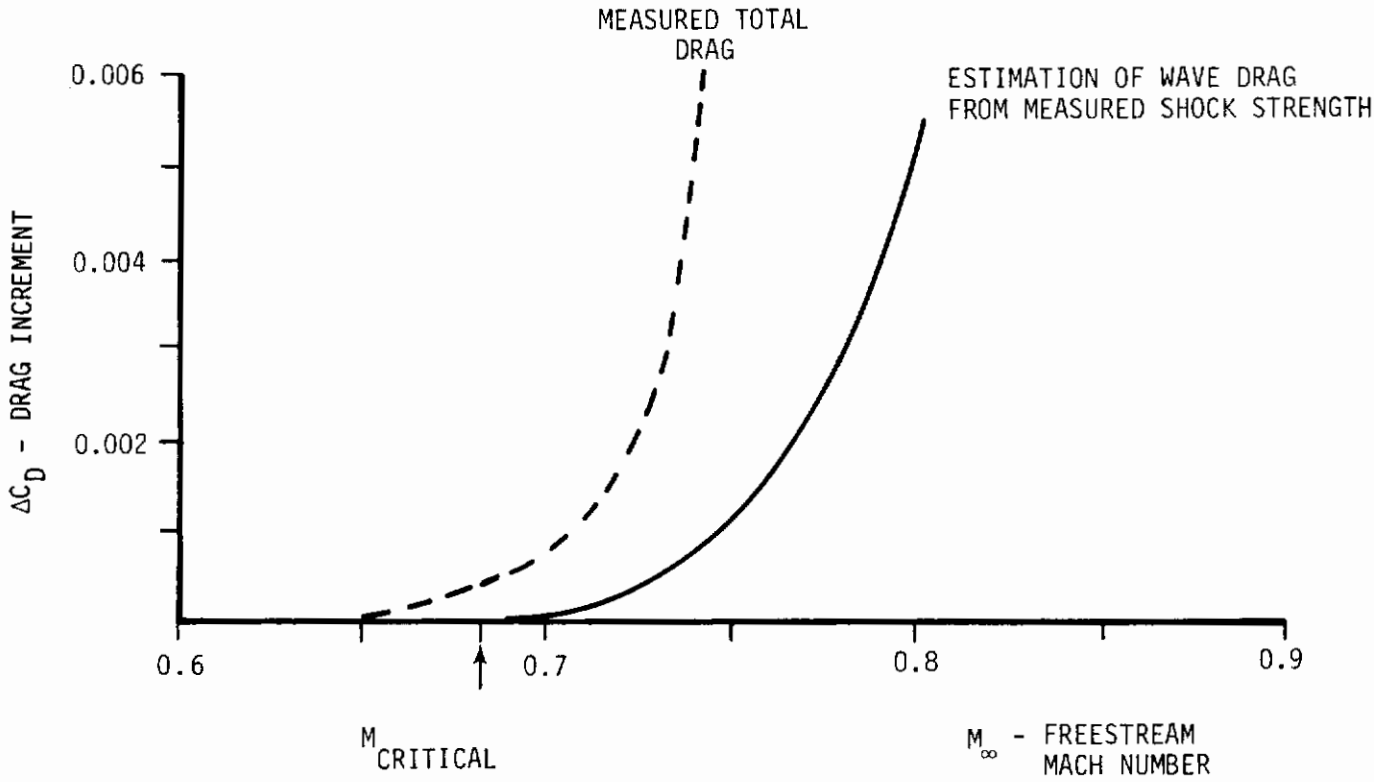

Figure 40. Breakdown of Drag Components in Transonic Flow (From Ref. 77)

Seddon (Ref. 79) proves by means of his experimental investigation on a flat plate that the shock-induced separation region has velocity profiles that are close to the profiles calculated analytically by Coles' wake hypothesis (Ref. 80) but with a degree of distortion in the vicinity of the shock wave where a very strong pressure gradient exists (Figs. 41-42). The validity of the Coles' hypothesis over the greater part of the separation region, and the suggestion of an empirical correction to account for the observed variations, enables us to obtain a solution of the flow field in the viscous-inviscid interaction region.

There is still a lot of work to be done in the transonic shock-boundary layer interaction region, experimentally and analytically. For example, boattail bleed could be tried when shock induced separation is present to ascertain whether the high drag rise can be reduced. Analytically new flow models should be devised when large separated regions are present on the boattail. The Reynolds number effect on shock location should be further investigated.

4. Internal Flow

The internal flow is analyzed with a time-dependent technique by Wehofer and Moger (Ref. 81). This technique includes the effects of nonuniform profiles of total pressure, total temperature and gas properties on the flow in convergent and C-D nozzles in the transonic regime. The assumption is that the gas is inviscid and non-heat conducting. The unsteady axisymmetric continuity equation,

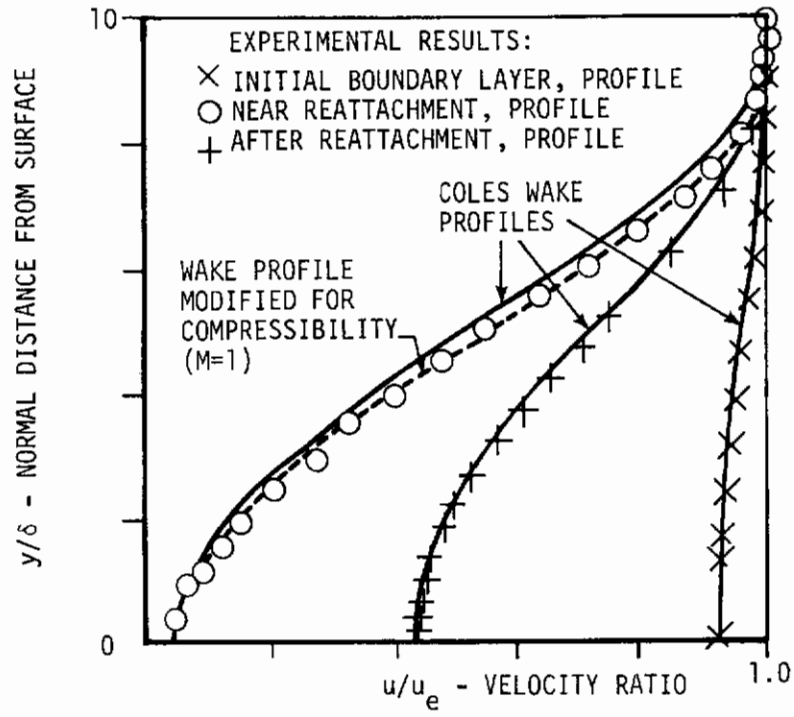

Figure 41. Conforming Wakes (From Ref. 79)

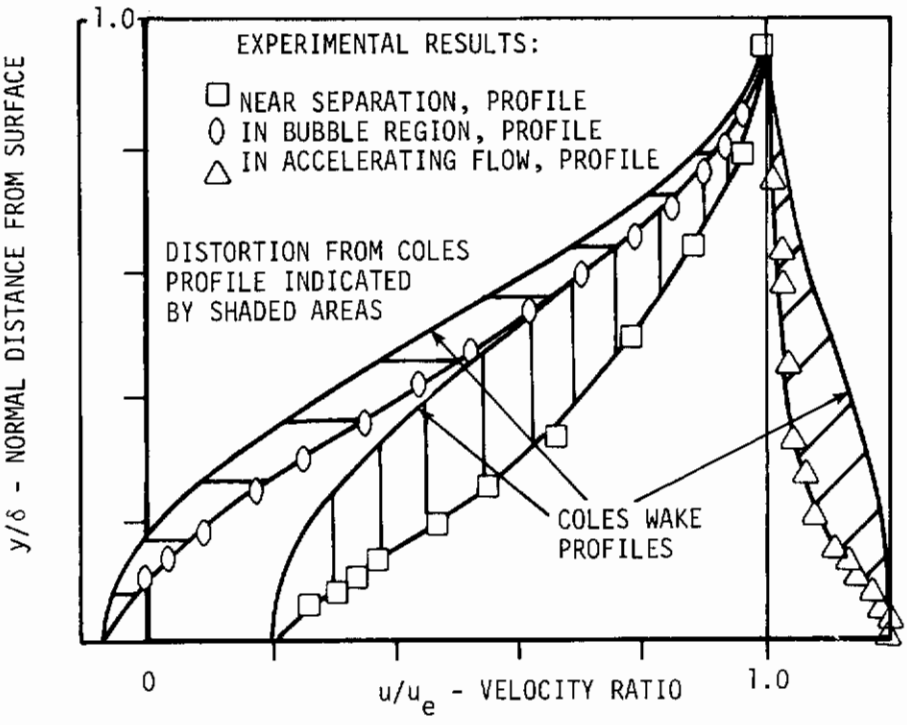

Figure 42. Distorted Wakes (From Ref. 79)

the momentum equations in the axial, radial, and peripheral direction, and the energy equation are written in "Conservation Law" form with the help of the equation of state written as a second order polynomial representing the relation between specific heat and temperature. The final result is a vector equation

$$\frac{\partial W}{\partial t} + \frac{\partial F(W)}{\partial X} + \frac{\partial H(W)}{\partial R} + I(W) = 0 \qquad (21)$$

where F, H, I, are functions of a vector W in a five-dimensional space. A coordinate transformation is applied in order to maintain the same grid size for the whole nozzle flow field in the Lax-Wendroff type of numerical calculations used to solve the above vector equation. Its solution is performed using a nine-point forward difference scheme with differences centered at $(t + \Delta t/2, Y, X)$. The scheme does not give the values at the mesh points lying on the boundary but these values can be obtained by extrapolation from the internal flow field. The wall pressure distribution can also be obtained by parabolic extrapolation from the internal flow field values and, together with the known values of the stagnation temperature, stagnation pressure, and wall inclination yields the values of the components of the vector W.

The analysis just described is applicable to twin nozzles and is quite accurate as substantiated in Figure 43.

Prozan's error minimization technique (Ref. 83) is used in Reference 7 to solve the transonic flow field in a nozzle. This is a relaxation method which reduces the error in the unsteady flow

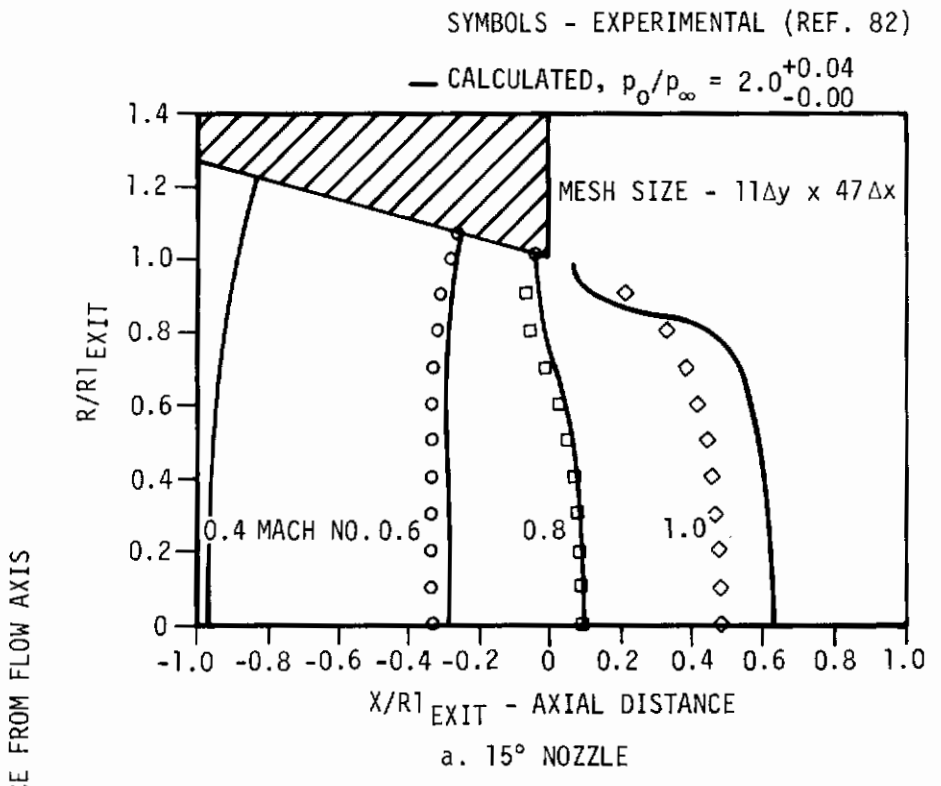

a. 15° NOZZLE

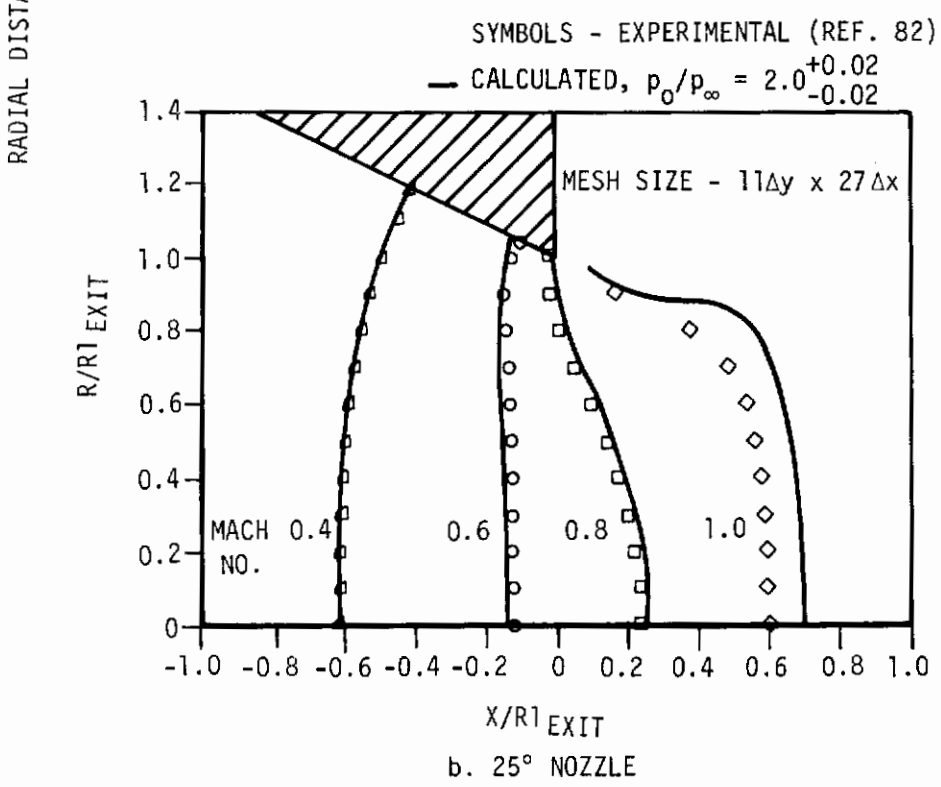

b. 25° NOZZLE

RADIAL DISTANCE FROM FLOW AXIS

Figure 43. Mach Number Distribution (From Ref. 81)

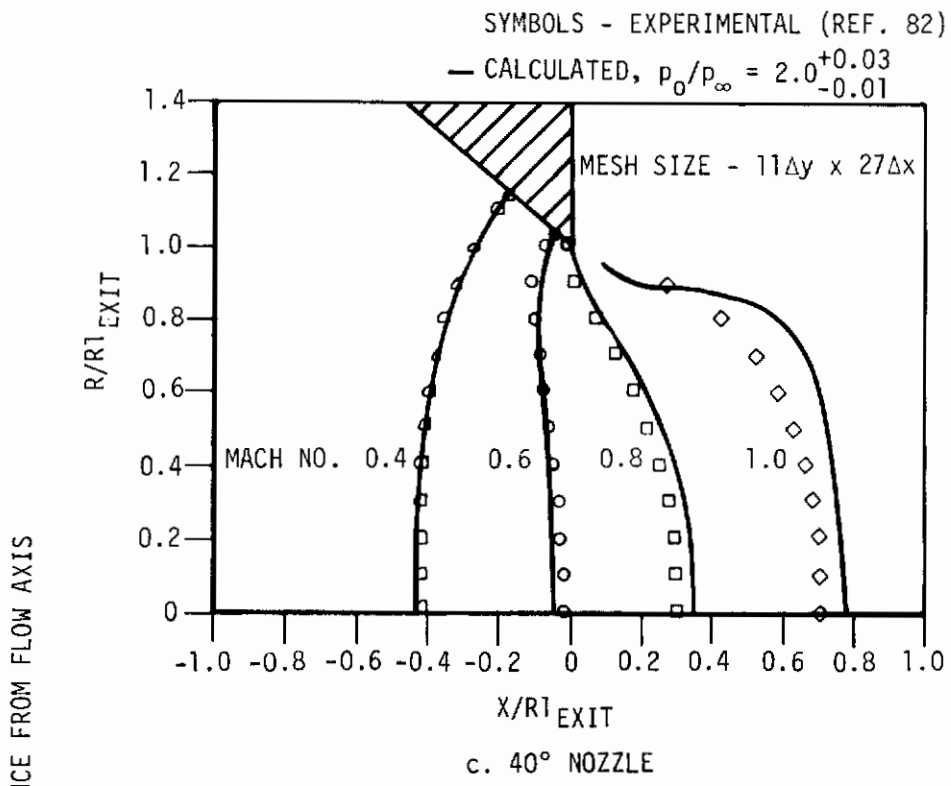

c. 40° NOZZLE

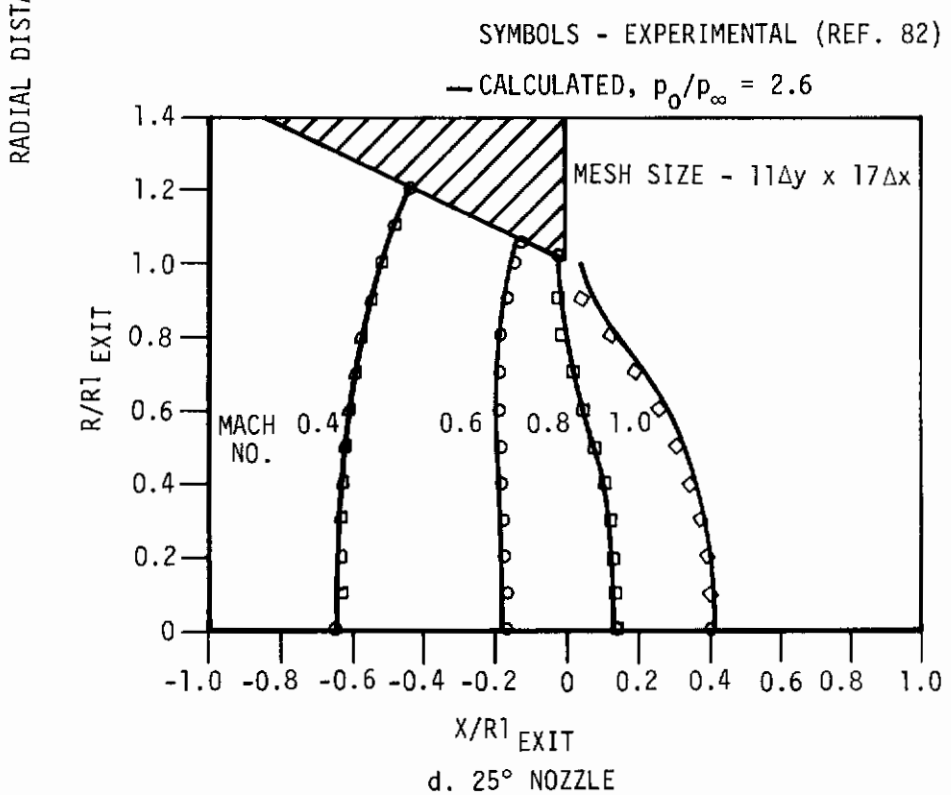

d. 25° NOZZLE

RADIAL DISTANCE FROM FLOW AXIS

Figure 43 (Concluded)

equations until they converge to a steady state solution. This method has not been as successful as time-dependent methods in predicting the correct flow properties. Figure 44 shows that the method gives at best results comparable to the simpler 1-D analysis.

Numerical techniques are applied to internal transonic flow solutions and they give nozzle performance coefficients which are usually close to experimental values. At the present time, the Lax-Wendroff type of analysis seems the most reliable.

5. Jet Plumes

Love et al (Ref. 84) devote considerable effort in the understanding of the mechanism regulating free jets exhausting from sonic and supersonic nozzles into still air or supersonic external streams. The effects of jet Mach number, free stream Mach number, jet static pressure ratio, nozzle divergence angle, ratio of specific heats of the jet, and boattail angle on the jet structure and on the shape and curvature of the jet boundary are considered. This investigation permits the evaluation of the jet interference.

The exhaust jet exhibits a periodic structure which depends on the jet pressure ratio. Inside the jet a series of expansions and compressions takes place. At the jet boundary the external flow mixes with the jet and penetrates it since the jet is not a solid body. The coalescence of characteristic lines creates shock waves, the pattern of which is regulated by the jet pressure ratio. With increasing jet pressure ratio, these shocks grow in strength from intersecting shocks to strong shocks that require a Mach reflection.

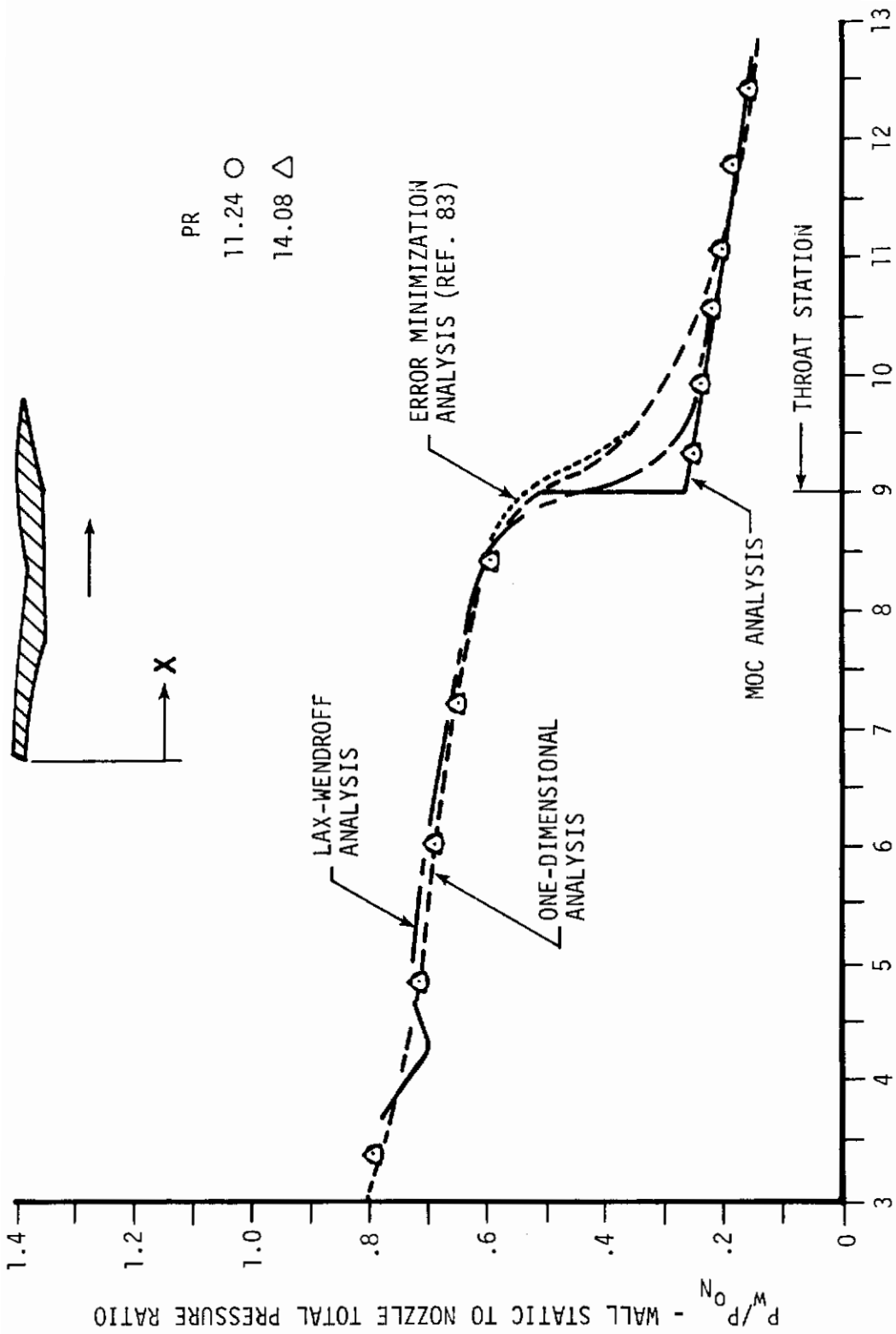

Figure 44. Nozzle Predicted and Experimental Internal Pressure Profile (From Ref. 7)

The normal shocks are the familiar Riemann waves and their location or the location of the focal point for intersecting shocks, which determines the primary wavelength of the periodic phenomenon, is of particular interest. The jet structure deflects from the jet axis due to the aerodynamic forces acting on it, and breaks down into a vortex street and a region of turbulent diffusion. For an axisymmetric jet, a semiempirical solution is obtained for the variation of primary wavelength to jet diameter ratio with jet pressure ratio (Ref. 1).

Deep and Henderson (Ref.85) consider the effects of the plume on the afterbody and surrounding flow field. In their investigation they show that the jet thrust has a strong effect on the base pressure. It was shown by Lockheed California (Ref. 43) that base pressures decrease with increasing nozzle pressure ratio but, for high nozzle pressure ratios, they become independent of it, i.e. maintain a locked-in constant value (Fig. 45). Deep and Henderson present a correlation that gives a complete picture of the jet and thrust effects on base pressures for cylindrical afterbodies (Fig. 46). Boattail pressures exhibit a different behavior; they usually increase with increasing nozzle pressure ratio (Fig. 47). The exit and free stream Mach numbers also affect the value of the base and boattail pressures. A sonic jet, for a fixed thrust coefficient C_T, usually creates a higher base pressure than a supersonic jet, with consequent decrease in base drag (Fig. 48). A jet issuing in a sonic external flow field creates a larger separation on the boattail than the separation occurring for a

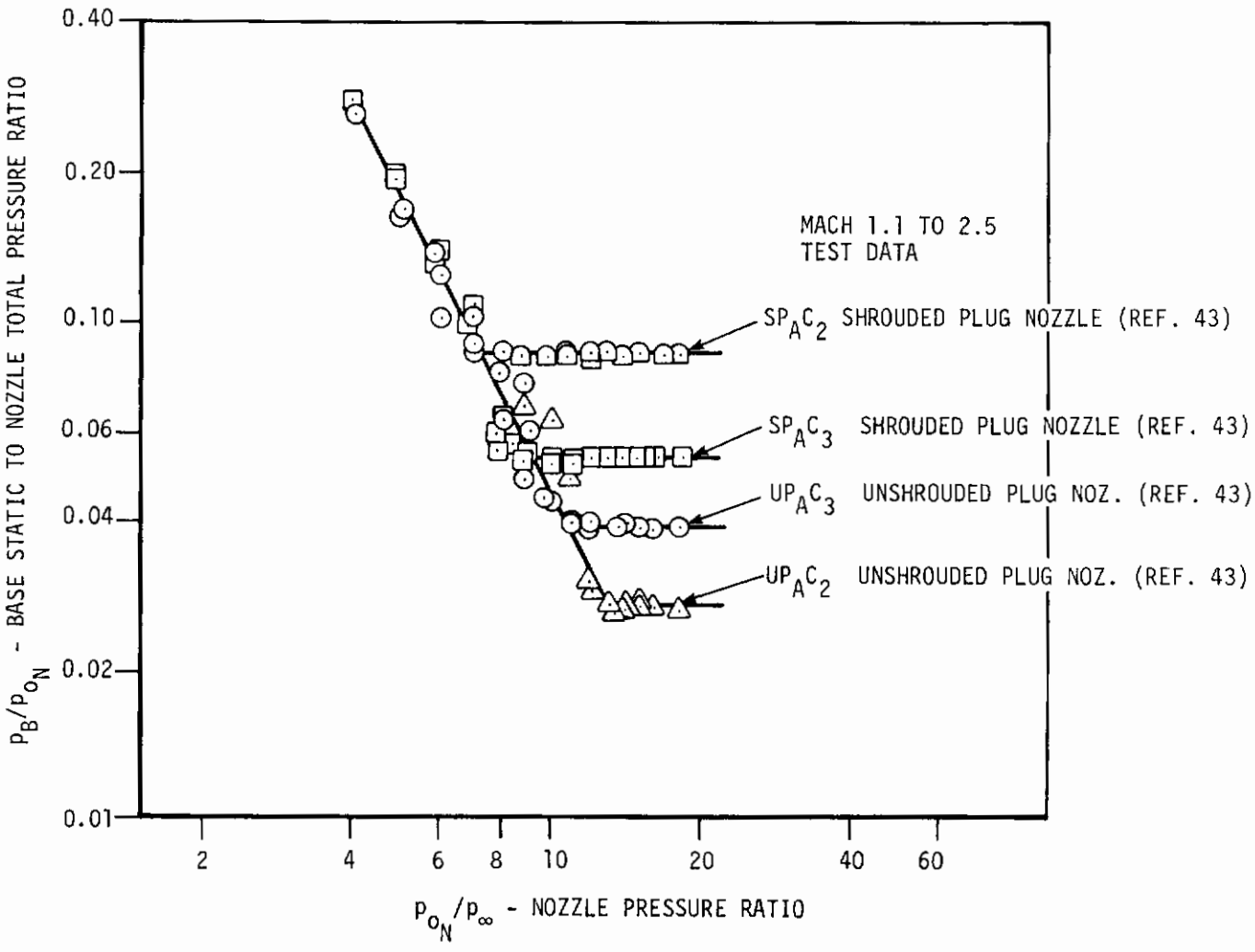

Figure 45. Isolated Plug Nozzle Base Pressure Correlation - 15° Plug (From Ref. 43)

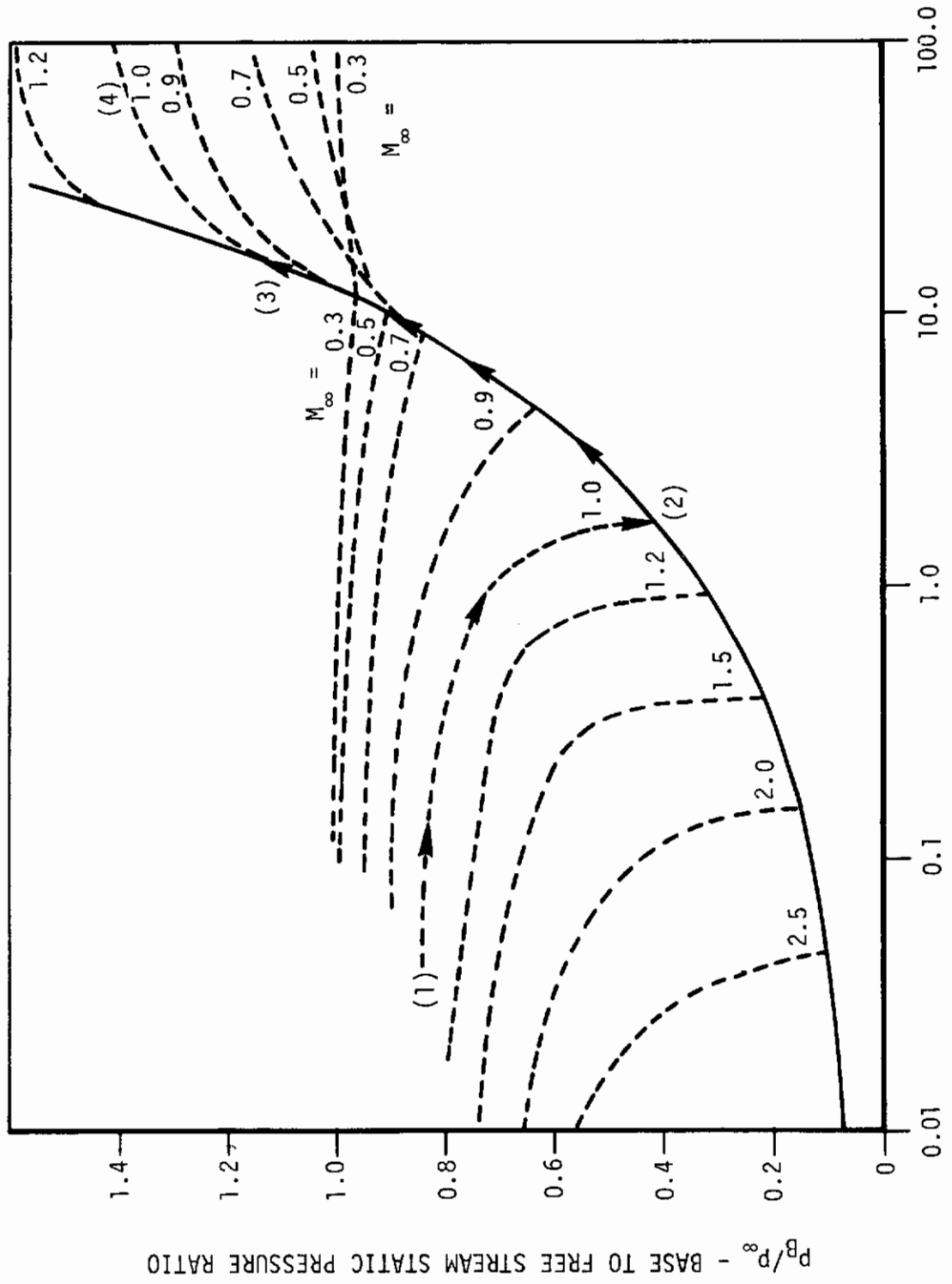

Figure 46. Base Pressure Variation With Thrust for a Cylindrical Afterbody With a Nozzle Flush With Base, Cold Air, $M_j = 2.7$, $\theta_N = 20°$ (From Ref. 85)

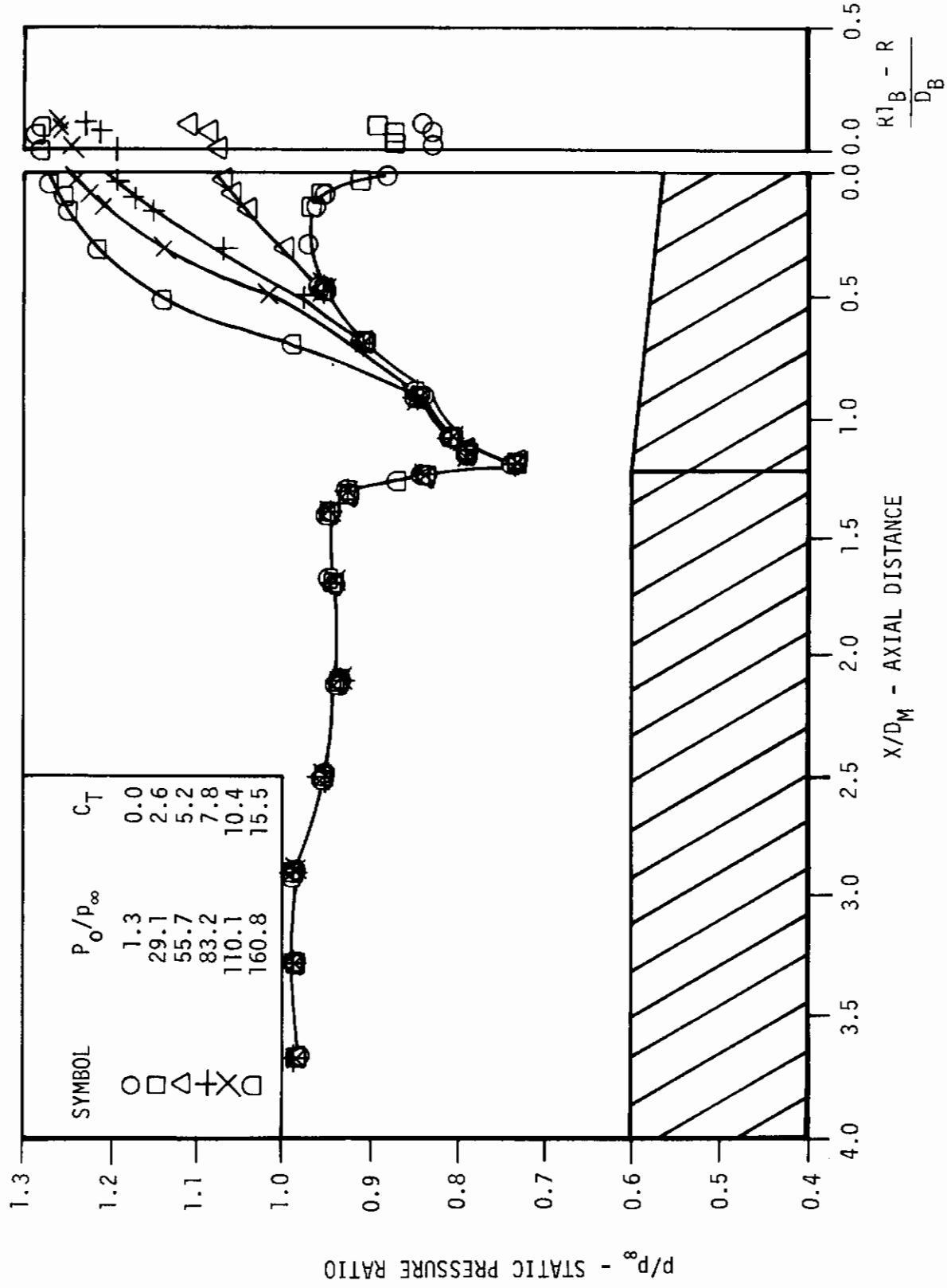

Figure 47. Thrust Effects on Pressure Distribution of Various Boattailed Afterbodies at M_∞ = 1.2 (From Ref. 85)

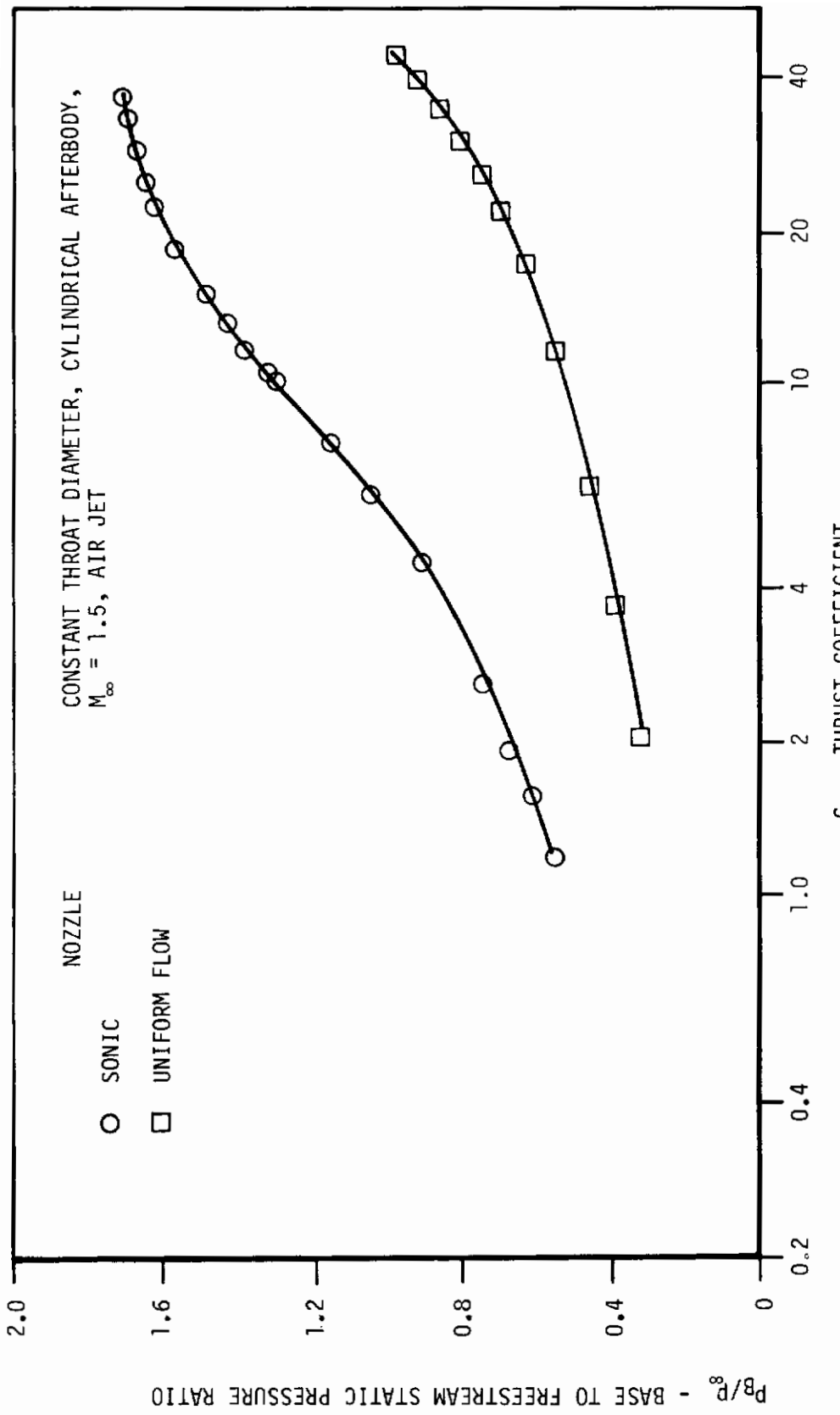

Figure 48. Comparison of Thrust Effects on Base Pressure of a Sonic Nozzle and a Uniform Flow Nozzle (M_j=2.7) (From Ref. 85)

supersonic free stream Mach number, with consequent increase in boattail drag. To achieve the optimum condition for low overall drag values a trade off is usually necessary between boattail and base drag.

6. Base Flow

The two stream base pressure for transonic and supersonic flow is obtained with the method developed by Korst et al (Ref. 86) which is based on Korst's base theory (Ref. 87). The method can calculate the base pressure also for the nonisoenergetic case between two streams, which then have different stagnation pressures and stagnation temperatures. The flow model is described in Figure 49. In the overall model, the continuity and energy equations are satisfied. The amount of mass and energy entrained in the base region from the internal and external stream and base bleed must match the amount escaping this region through the recompression at the beginning of the wake.

$$G_B + G_I + G_e = 0 \quad \text{(Mass Balance)} \tag{22}$$

$$E_B + E_I + E_e = 0 \quad \text{(Energy Balance)} \tag{23}$$

The mixing between the two streams is considered a constant pressure process with a thin initial boundary layer at the separation point. The pressure rise at the end of the base region, so called "dead air" region, generated the idea of the discriminating streamline, i.e. a streamline with sufficient mechanical energy to penetrate

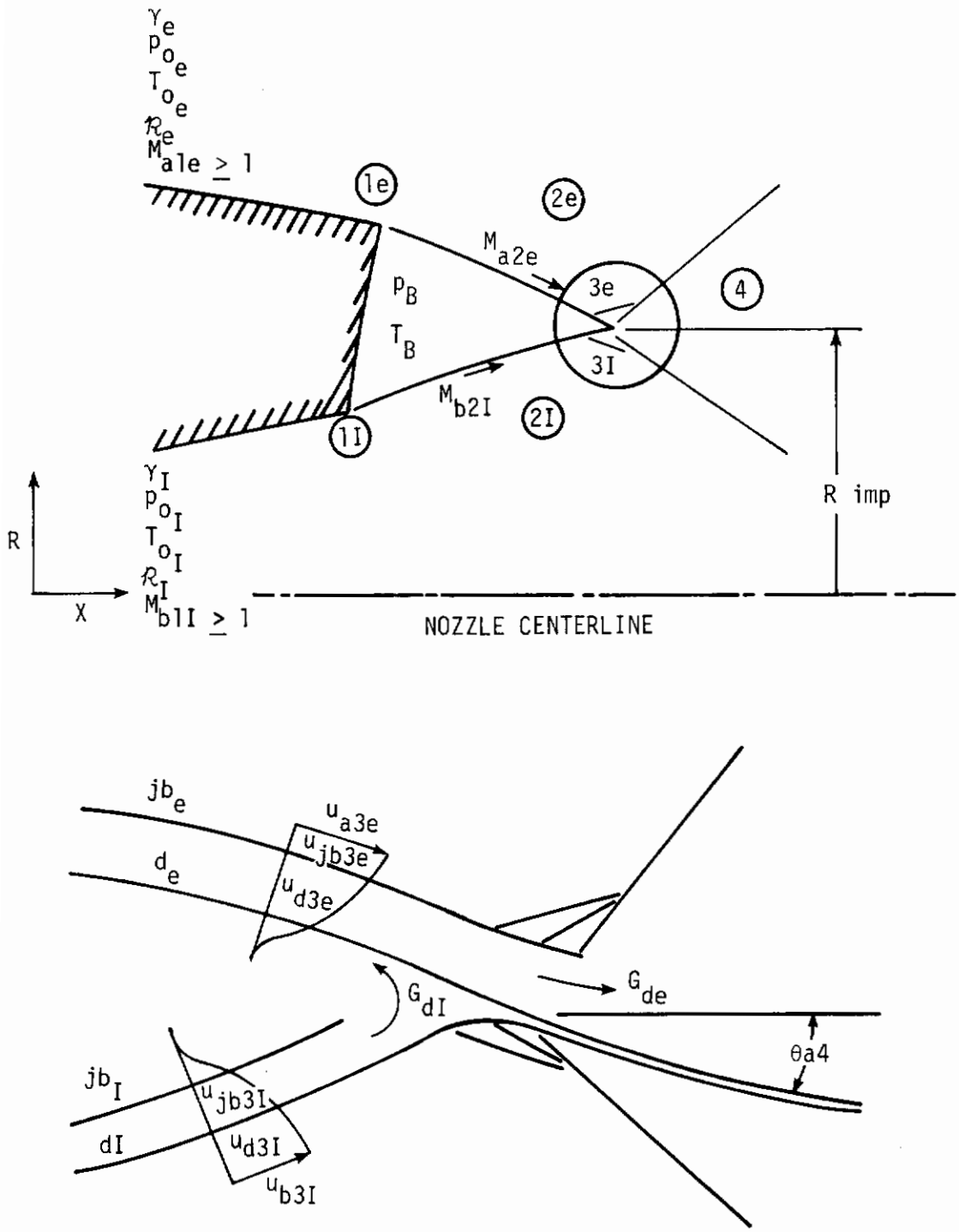

Figure 49. Two-Stream Base Pressure Model (From Ref. 3)

the high pressure behind the "dead air" region. This concept is called the escape criterion. The pressure rise is determined by a momentum integral method assuming an error function velocity profile in the mixing region. A simplified momentum equation for the mixing at constant pressure is set up and, applying mass and energy conservation principles, auxiliary integrals are obtained in terms of velocity and temperature ratios. Assuming a base pressure and a base temperature, the mass flow rate G_B and the energy rate E_B can be evaluated. In case the mass and energy balance equations are not satisfied, new values of p_B and T_B are assumed and iterated until the solution converges.

The analytical approach to the base pressure problem is simple and has been used extensively. Some corrections have been made to account for thick initial boundary layers at the separation point. Figure 50 shows the accuracy of the method by comparison with experimental data for supersonic Mach numbers.

7. Summary

The transonic flow theories applied to the afterbody/exhaust nozzle external flow fields as well as the transonic airfoil theories are consistent with experimental data with some discrepancies at the rear section of the body considered. However, no wall corrections have been applied so far to wind tunnel experiments. The classical methods of solution, e.g. local linearization, parabolic, etc., are currently used in axisymmetric and 3-D nozzle flow applications while the relatively new relaxation techniques have been applied to lifting and nonlifting airfoils. But relaxa-

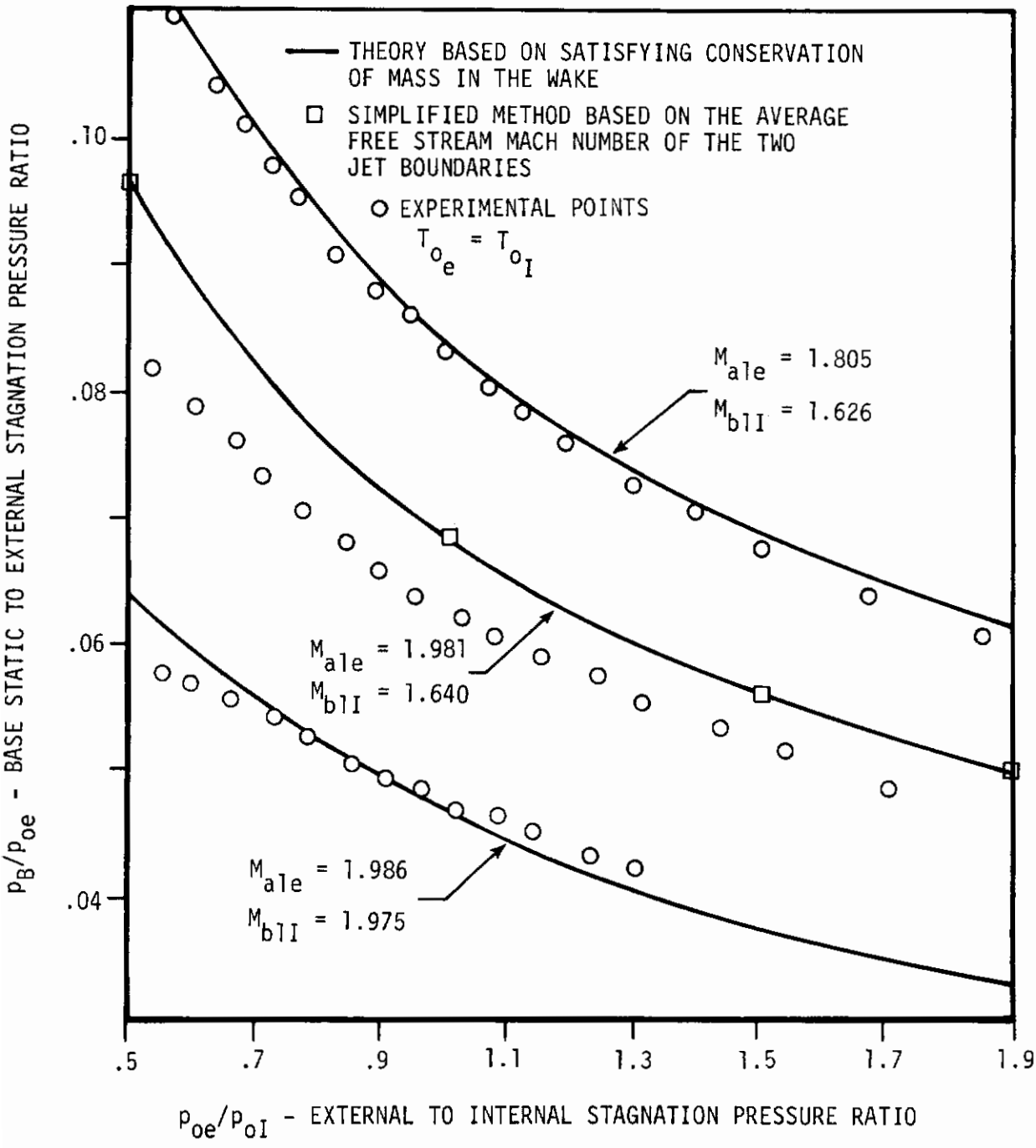

Figure 50. Base Pressure Ratios as Functions of Stagnation Pressure Ratios and Mach Numbers of the Approaching Streams. The Flow Configuration is Depicted in Figure 49. (From Ref. 86)

tion techniques have now been extended to 3-D and used more extensively. It seems that these powerful techniques will be used consistently for the solution of uniform and nonuniform transonic aft-end flow fields.

Shock-boundary layer interaction and Reynolds number effects on shock location are important factors in the determination of the aft-end transonic drag and additional research in this area should be performed on axisymmetric and 3-D configurations. New techniques should also be developed to analyze large separated regions on aircraft boattails.

The internal flow numerical analyses are well formulated and capable of a good flow description with accurate quantitative results.

The Korst base theory applied to two stream flows is very effective in the solution of the base pressure problem.

C. Supersonic Flow

1. External Flow

The supersonic external flow is calculated by Rakich and others (Refs. 88-90) using the 3-D method of characteristics. The 3-D inviscid, rotational, nonreacting compressible flow equations are used in Reference 88 to obtain compatibility equations valid along characteristic surfaces. The equations are complicated by the presence of cross derivatives and by the fact that 2-parameter interpolations are needed for data in the initial data surface, since bicharacteristics emanating from a general mesh point do not

pass usually through mesh points in the initial data surface. These complications are reduced considerably if reference planes in the longitudinal directions are considered. Therefore compatibility equations along the projections of bicharacteristics and streamlines onto the reference planes are derived. In this case, only, 1-parameter interpolations are needed.

The energy equation and the equation of state complete the set of equations necessary for the solution. The standard Euler predictor-corrector method, in which the coefficients are held constant locally and then considered equal to their average value over the step, is used to numerically solve the equations written in finite difference form. Iterations are used until convergence is reached. This method gives a second order accuracy.

In case large radial gradients of density or large cross flows develop in the vortical or entropy layer, a smoothing technique of the Lax-Wendroff type is used. This has the effect of smoothing the value of the density gradients and of stabilizing the difference scheme. The general stability criterion of C-F-L is followed.

The method just illustrated gives good results when compared with experimental data obtained for pointed and blunt cones at angle of attack and hypersonic Mach numbers (Figs. 51-52). It can be extended with some modifications to compute external flow fields over nonaxisymmetric boattails and the jet flow field and boundaries for twin-nozzle aircraft.

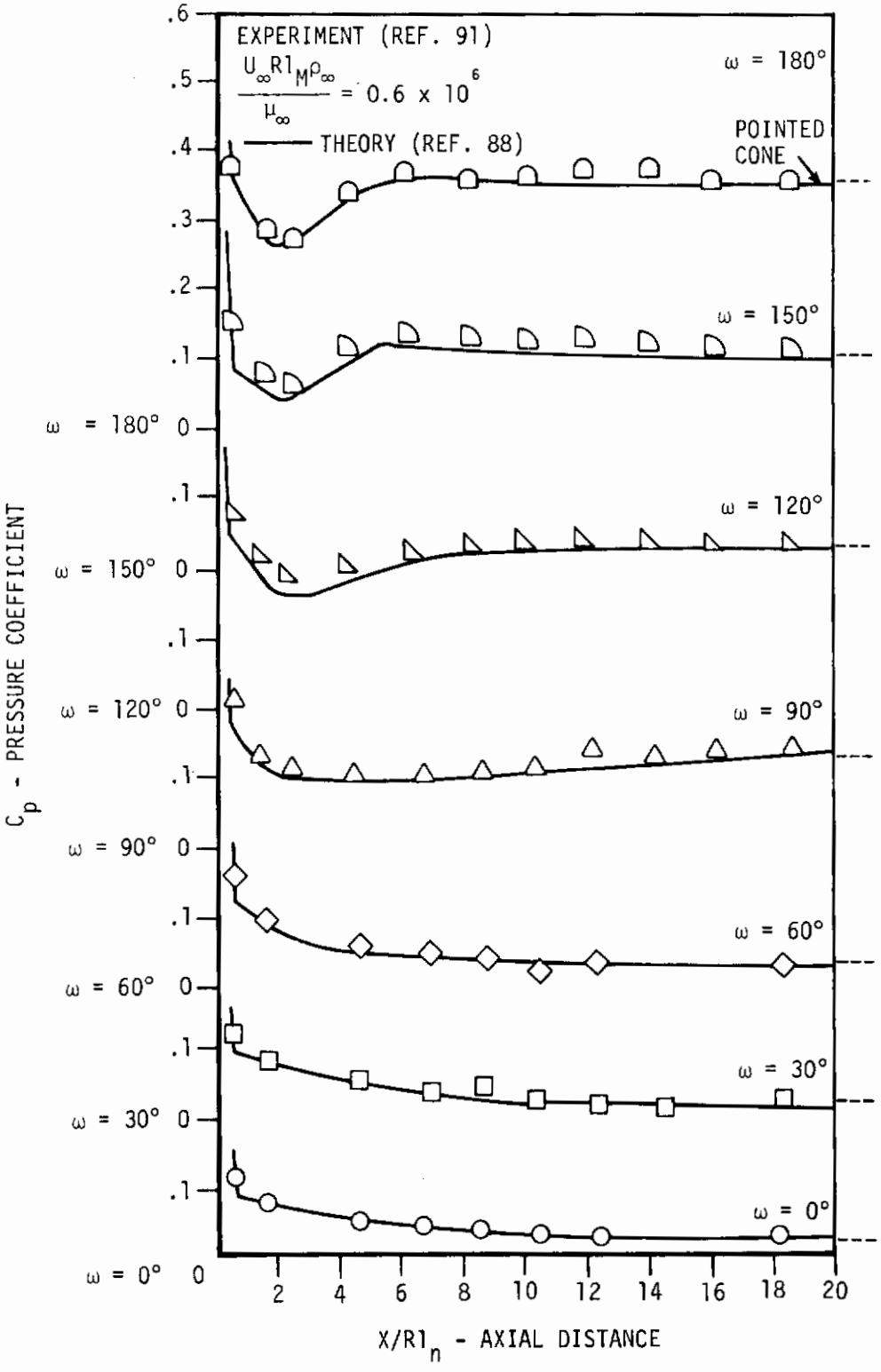

Figure 51. Surface Pressure Distribution, 15° Sphere-Cone, M_∞ = 10° (From Ref. 88)

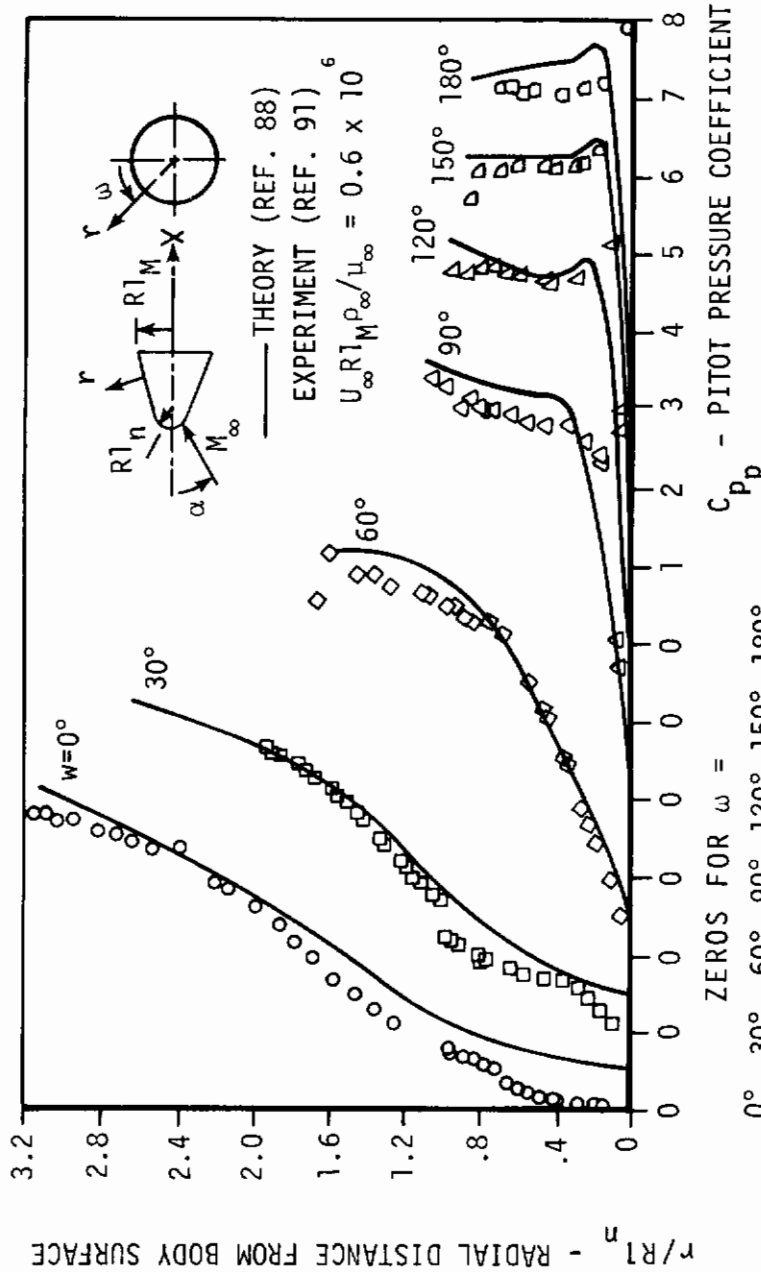

Figure 52. Shock-Layer Pitot-Pressure Distribution; 15° Sphere-Cone, $M_\infty = 10$, $\alpha = 10°$, $X/R1_n = 16.7$ (From Ref. 88)

Strom (Ref. 89) uses the 3-D method of characteristics and a different numerical scheme to calculate supersonic flow fields for nonequilibrium, steady, inviscid flow.

Besides the usual equations of conservation of mass, momentum, energy, and the equation of state, the species conservation and the vibrational energy equations are used to obtain the compatibility equations valid on characteristic surfaces in order to account for the nonequilibrium properties of the flow field. The compatibility equations are solved numerically. The stability criterion is the usual C-F-L condition.

The numerical procedure consists of a marching technique which allows finding the flow properties on a reference plane perpendicular to the streamline direction through numerical integration of the compatibility equations along the streamline direction and the bicharacteristics using known flow properties at a previous reference plane (Fig. 53). A mesh of nine points is used and the C-F-L criterion insures that the domain of dependence of the differential equation is contained in the domain of dependence of the difference network.

Strom's analysis allows, in principle, the calculation of 3-D flow fields in the vicinity of a smooth body including nonequilibrium thermochemical effects of a reacting real gas. Since the unsteady flow equations are used in the derivation, the analysis could be applied to nonequilibrium nozzle flows, asymmetric blunt bodies or sharp cones at angle of attack. However Strom

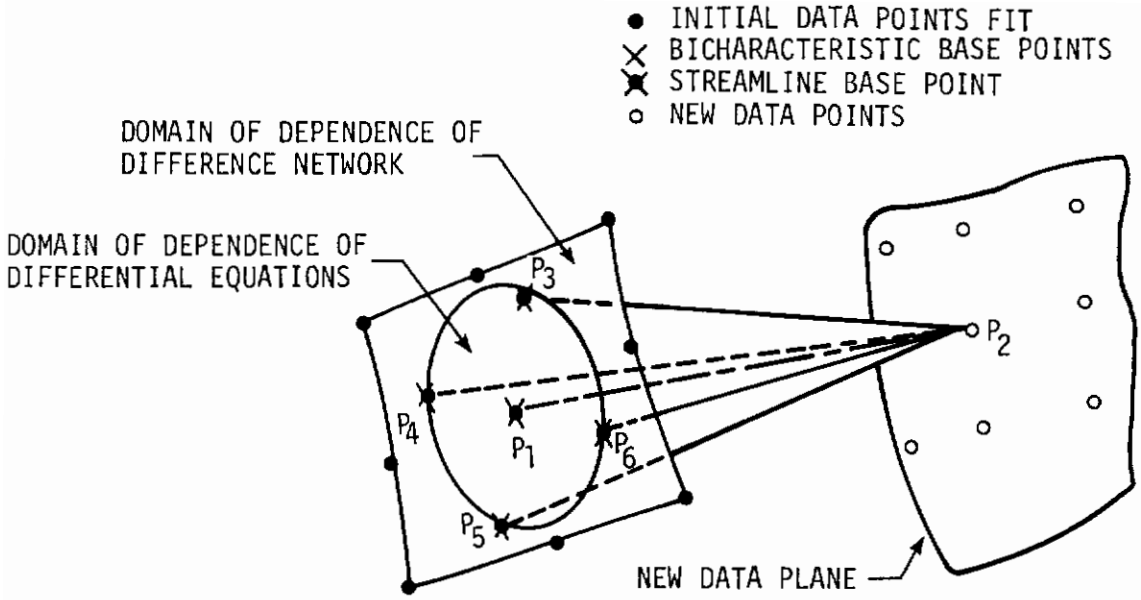

Figure 53. Proposed Field Point Network, Three Independent Variables (From Ref. 89)

develops a computer program to solve the steady, 3-D, frozen-inhomogeneous or ideal gas flows.

Korst and Divita (Ref. 92) develop a computer program, called the Rocketdyne program, to solve boattail flow fields. They use the axisymmetric method of characteristics applied to the steady, irrotational, isentropic flow of a perfect gas. The boattail pressure coefficient is calculated with good approximation except for the pressure rise at the end of the boattail where, instead of a shock, a Prandtl-Meyer compression is used and therefore some disagreement with experimental data is found (Figs. 54-55). The discrepancy is more pronounced at lower supersonic Mach numbers where a higher value of the drag is experienced, while it disappears at higher supersonic Mach numbers where the wake (trailing) shock is pushed further downstream and the drag is consequently lower. In this case the theoretical assumption of isentropic compression is justified.

Maslowe and Benson (Ref. 95) use also the method of characteristics for the solution of the axisymmetric external supersonic flow field but they try to improve their results over previous analyses by retaining in the compatibility equations the rotational terms The bow shock is calculated exactly, moving from the body along left running characteristics but subsequent shocks are approximated by a coalescing technique (isentropic shock). The inviscid flow properties obtained at a body station are used to calculate laminar or turbulent boundary layer properties and the displacement thickness

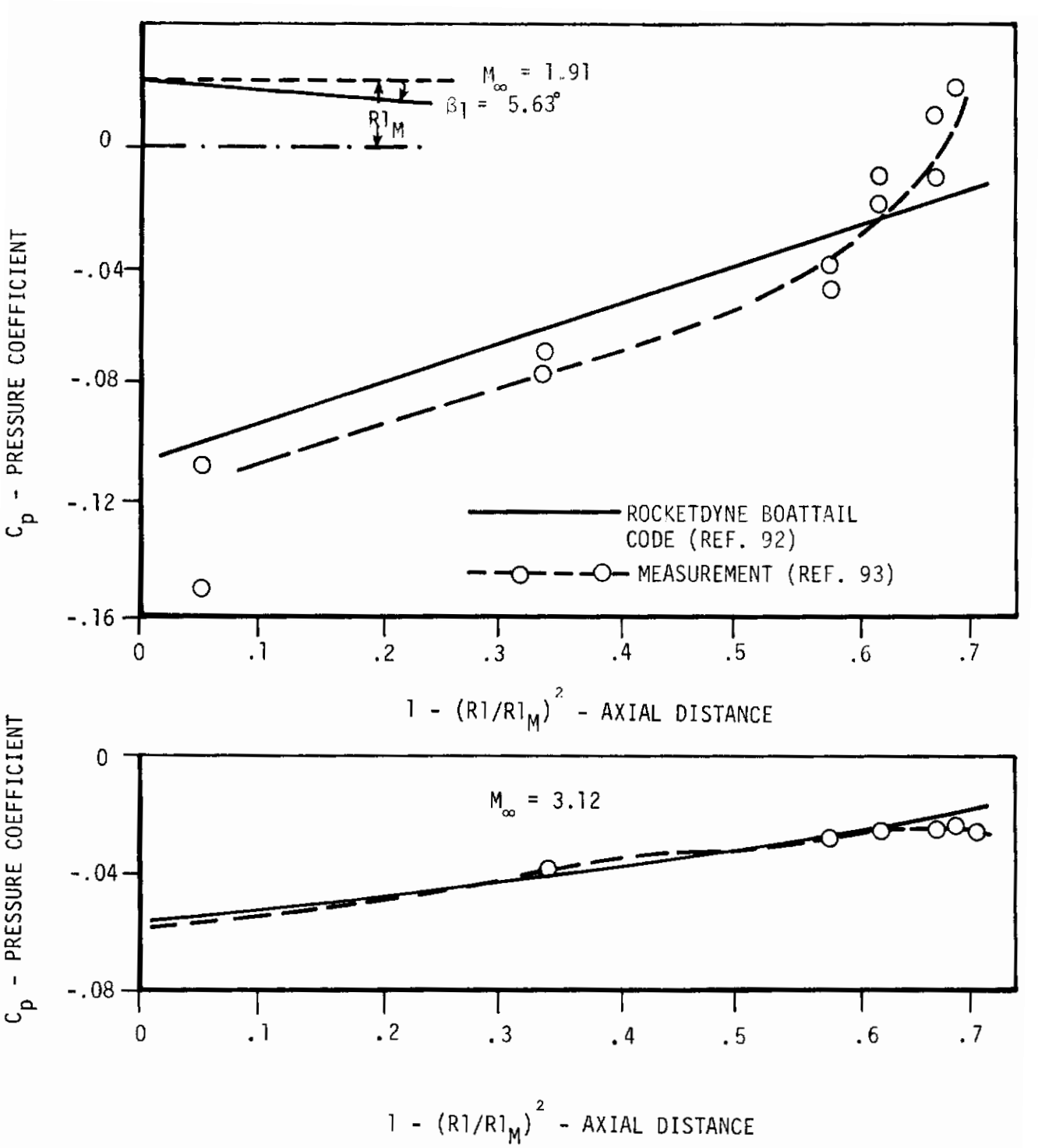

Figure 54. Conical Boattail With Boattail Angle of 5.63°; Comparison Between Calculation and Measurement; Jet Off (From Ref. 3)

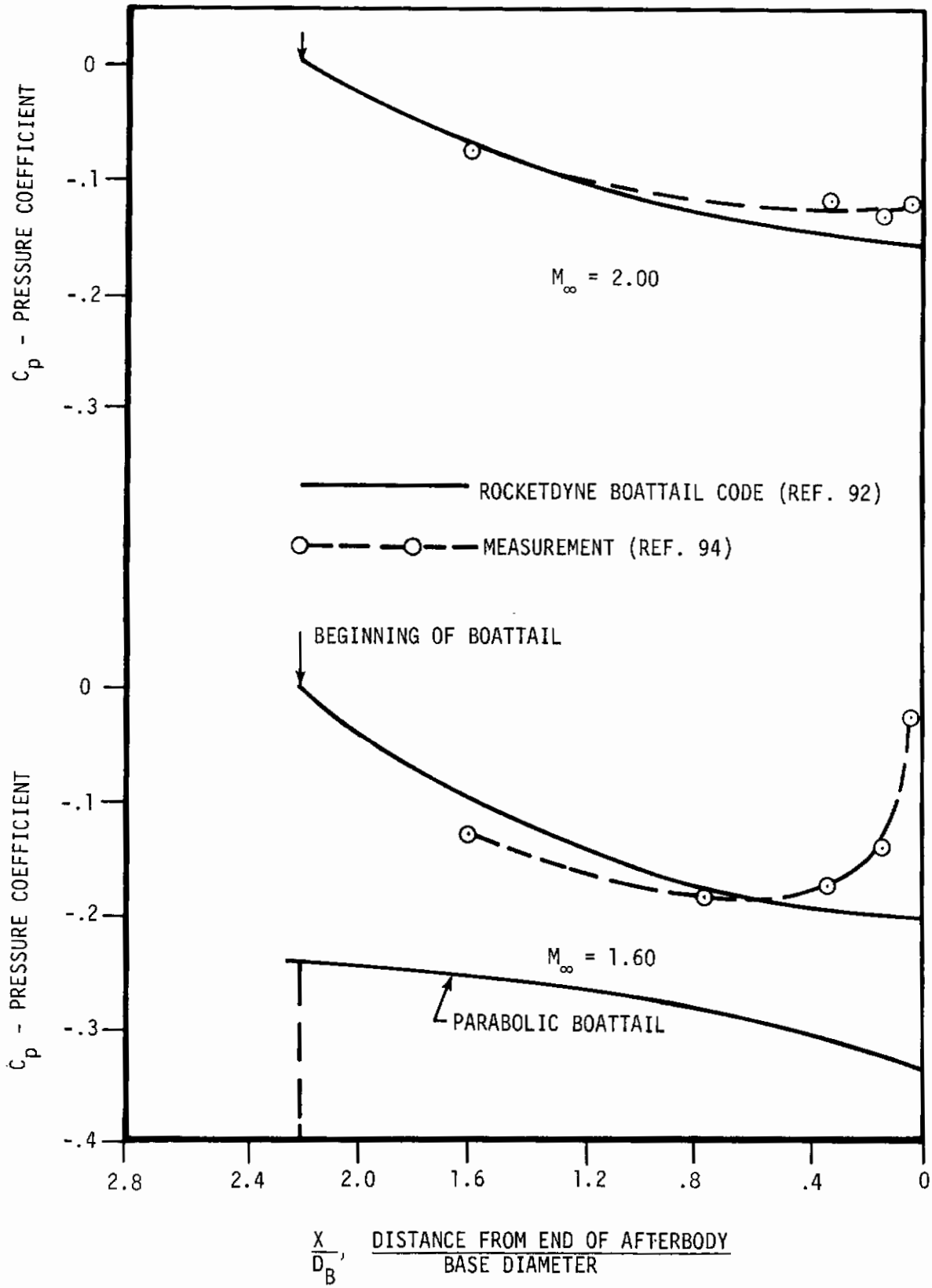

Figure 55. Afterbody for Nozzle B of Ref. 94; Comparison Between Calculation and Measurement; Jet Off (From Ref. 3)

which is added to the body geometry. Then a new solution is obtained on the displaced body. Successive iterations are made to correct for the initially assumed values and to reach convergence. Maslowe and Benson calculate the laminar boundary layer with the method of Reference 96 and the turbulent boundary layer with the method of Miller (Ref. 97). These methods account for real gas effects and are valid for frozen and equilibrium laminar, and equilibrium turbulent flows. For the laminar boundary layer, a set of third order ordinary differential equations is obtained for the momentum and energy equations through a transformation of independent variables. The momentum and energy equations are solved simultaneously by means of an iteration procedure. For the turbulent boundary layer, the momentum and energy equations are integrated throughout the boundary layer and solved numerically. A velocity power law and a modified Crocco relation are used together with a reference temperature method (Ref. 98) and a modified Reynolds analogy for the calculation of the skin friction and heat transfer. The method of Maslowe and Benson can be applied to isolated and twin jet bodies. The pressure distribution for three different boattail configurations is shown in Figures 56-58. The method gives good results for the C-D and plug nozzles but fails to predict the nozzle boattail recompression for the convergent iris nozzle which is due to axisymmetric effects. The method instead predicts a continuous expansion on the supersonic boattail. Reynolds number effects are shown in Figures 59-60. The experimental pressure distributions on the afterbody/nozzle boattails decrease with increasing Reynolds numbers, indicating an increasing drag trend.

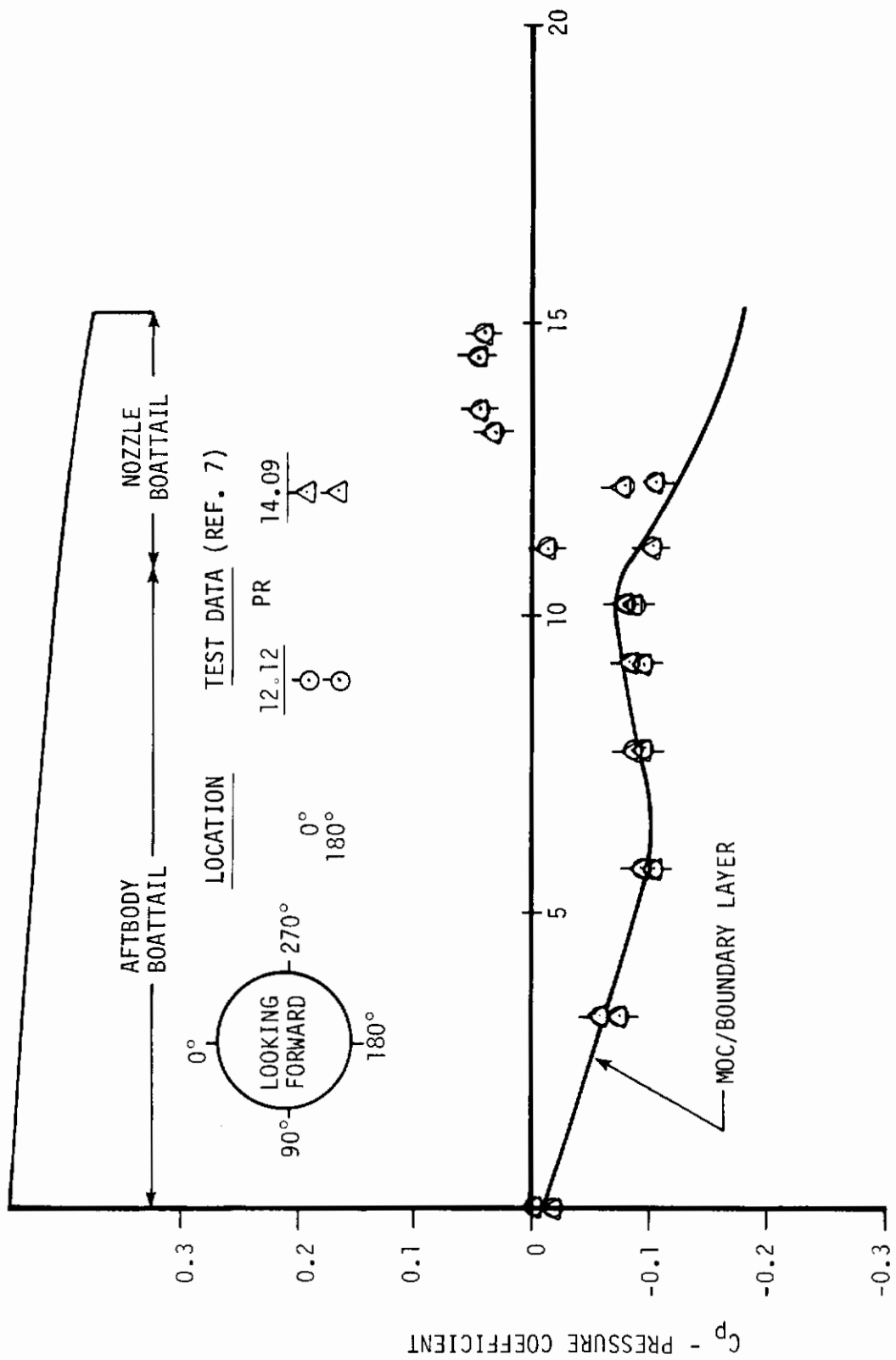

Figure 56. Convergent Iris Aftbody and Nozzle Boattail Predicted and Experimental Pressure Profiles - Mach 2.0 (From Ref. 7)

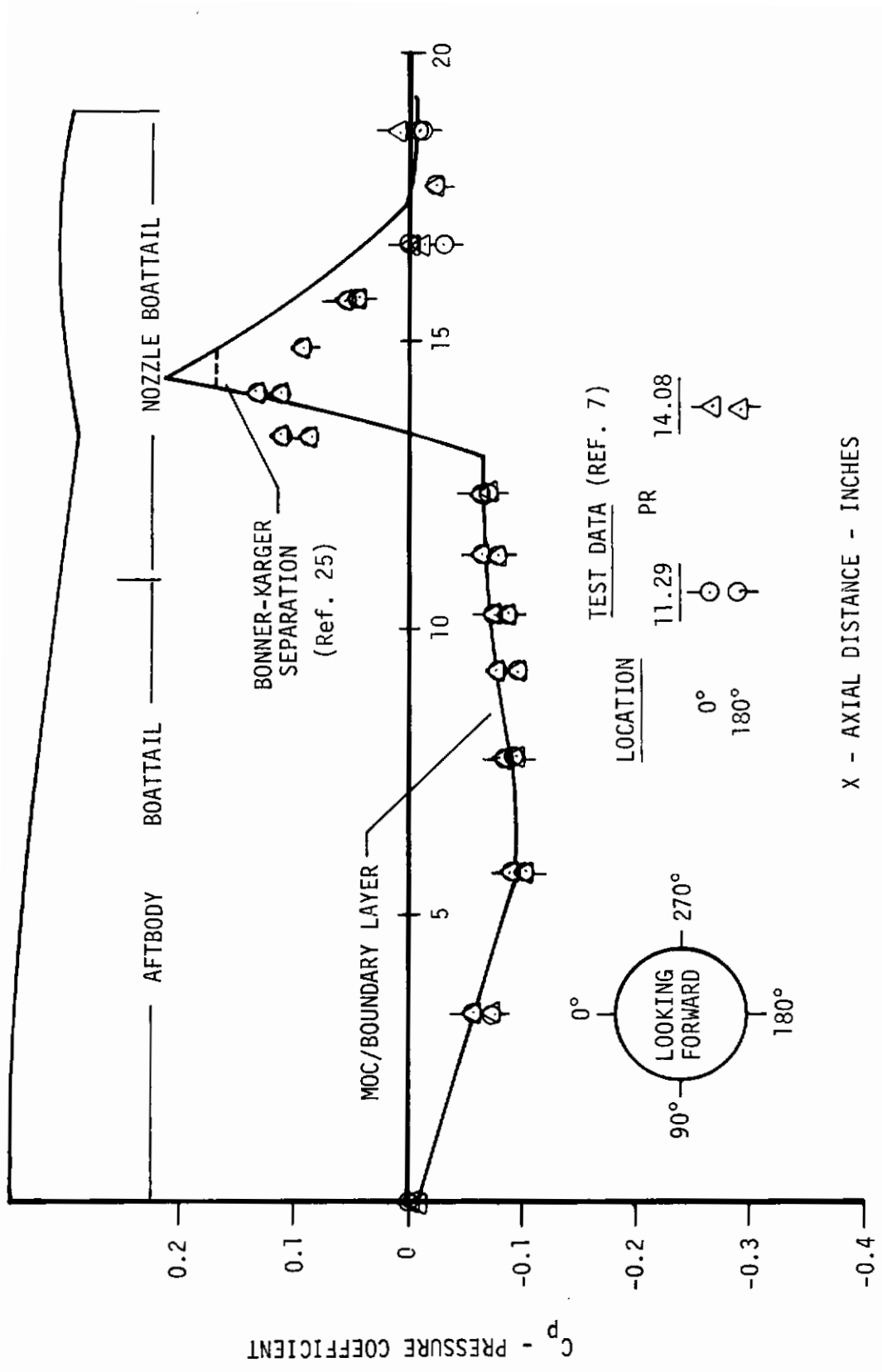

Figure 57. C-D Aftbody and Nozzle Boattail Predicted and Experimental Pressure Profiles - Mach 2.0 (From Ref. 7)

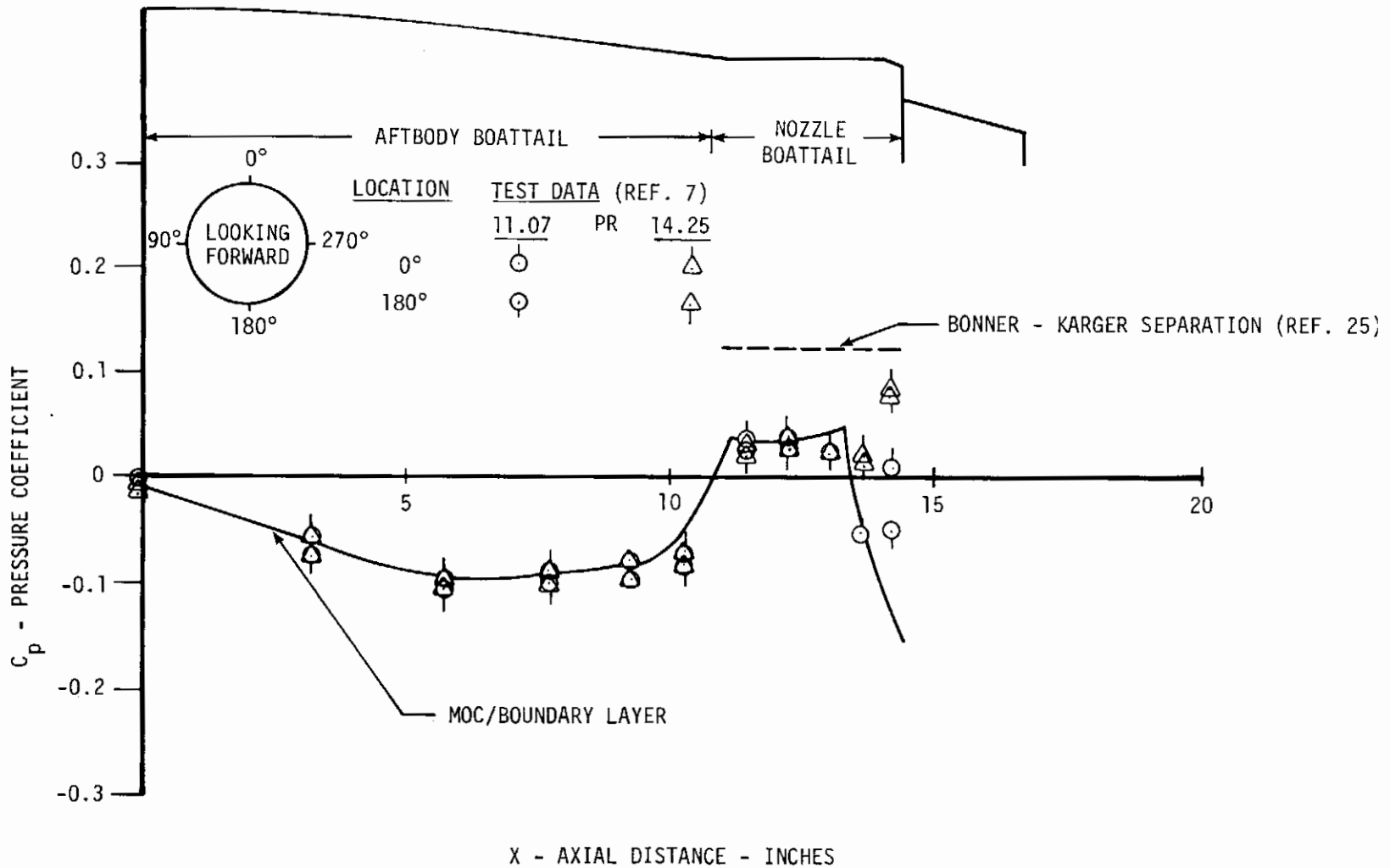

Figure 58. Plug Aftbody and Nozzle Boattail Predicted and Experimental Pressure Profiles - Mach 2.0 (From Ref. 7)

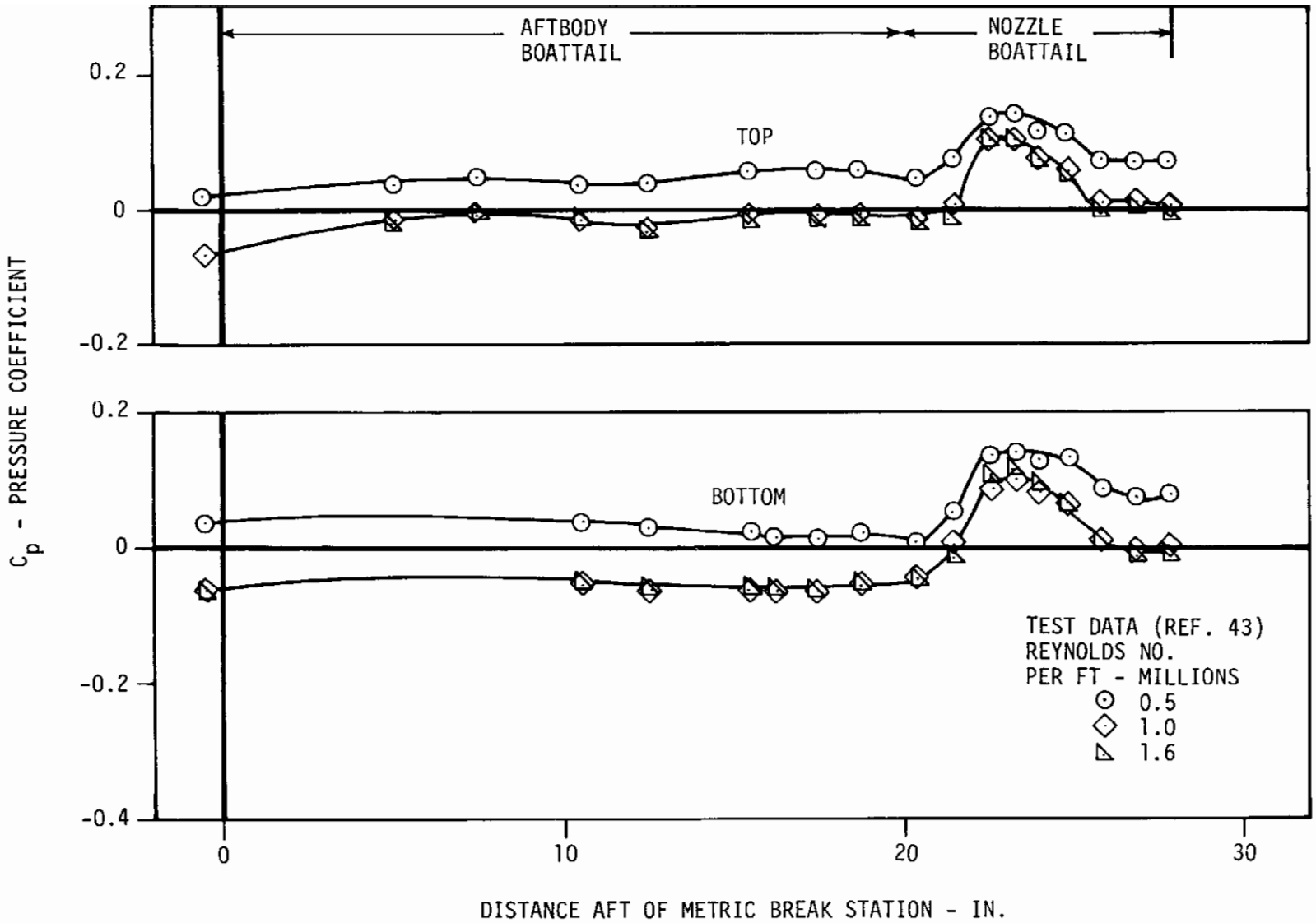

Figure 59. Effect of Reynolds Number on Aftbody/Nozzle Boattail Pressure Distributions - C-D Nozzle - Mach 2.0 (From Ref. 43)

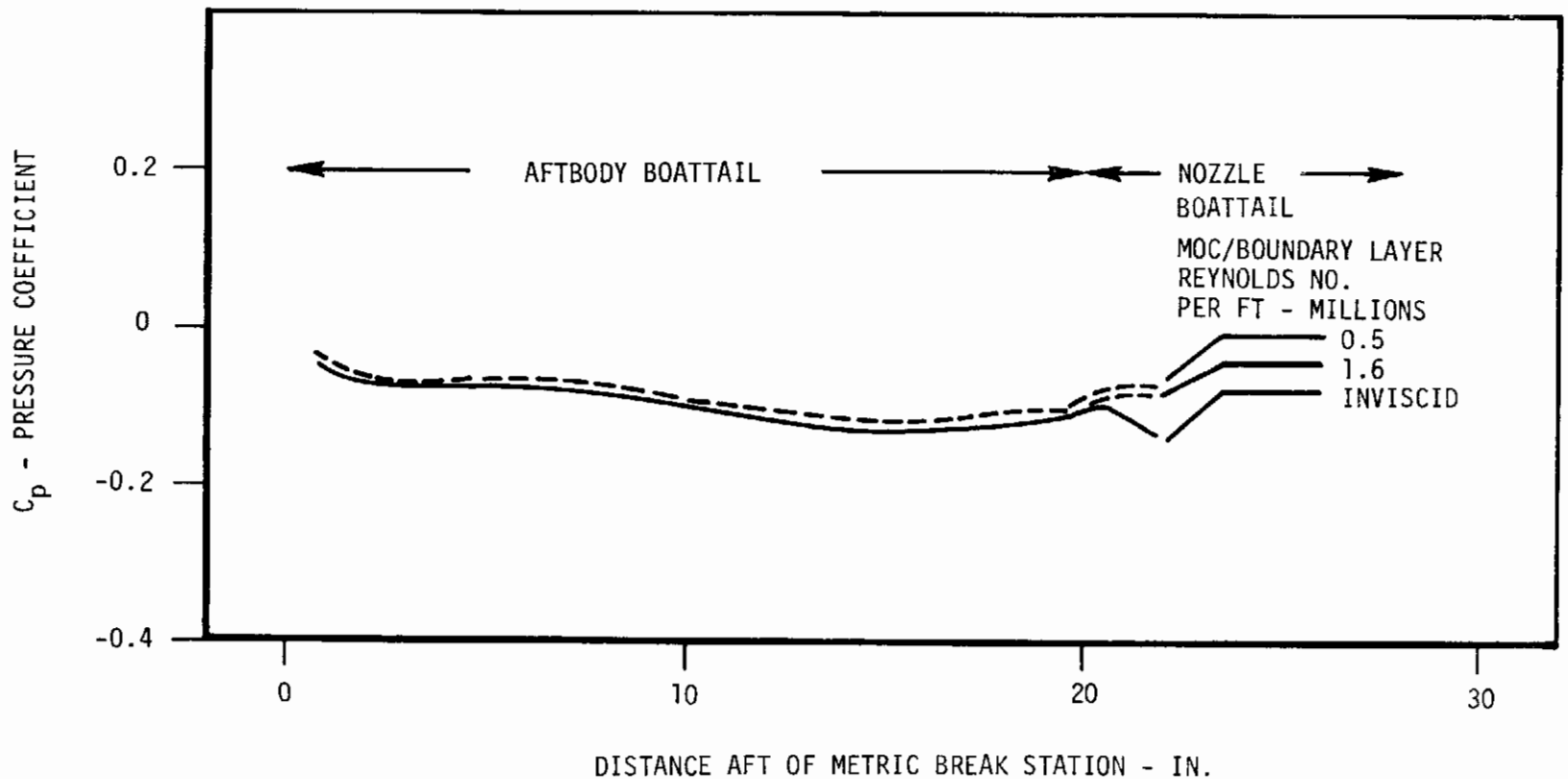

Figure 60. Effect of Reynolds Number on Aftbody/Nozzle Boattail Pressure Distributions - MOC/Boundary Layer Analysis on Equivalent Body - Mach 2.0 (From Ref. 43)

The analytical pressure distributions on an equivalent body with a convergent iris nozzle follow the same trend as in the experiment but the Reynolds number effect is much smaller. It would be interesting to study the effects of much higher Reynolds numbers to ascertain whether the differences between theory and experiment increase or decrease. Mach number effects are shown in Figure 61. The theoretical boattail drag of a body equivalent to the twin jet body shown in the figure decreases with increasing Mach number but it is 20 to 25% higher than the experimental data would indicate for the Mach number range considered.

3-D methods of characteristics have not yet been applied to the solution of the afterbody problem even when the flow analyzed is nonuniform and the configuration is nonaxisymmetric as in the case of twin jet aircraft. So far sector analyses and empirical correlations have been used instead. The 3-D MOC presented are certainly very accurate in the analysis of supersonic flow fields but large computer time is necessary to obtain solutions.

Time-dependent and relaxation techniques are used extensively in supersonic external flow. Time-dependent methods, e.g. Moretti's solution (Ref. 10), make use of the unsteady equations of motion where the steady state solution is obtained asymptotically for large values of time. Moretti treats the shocks present in the flow field as discontinuities and considers them as a part of the boundaries. His method consists of estimating the location of coalescence of

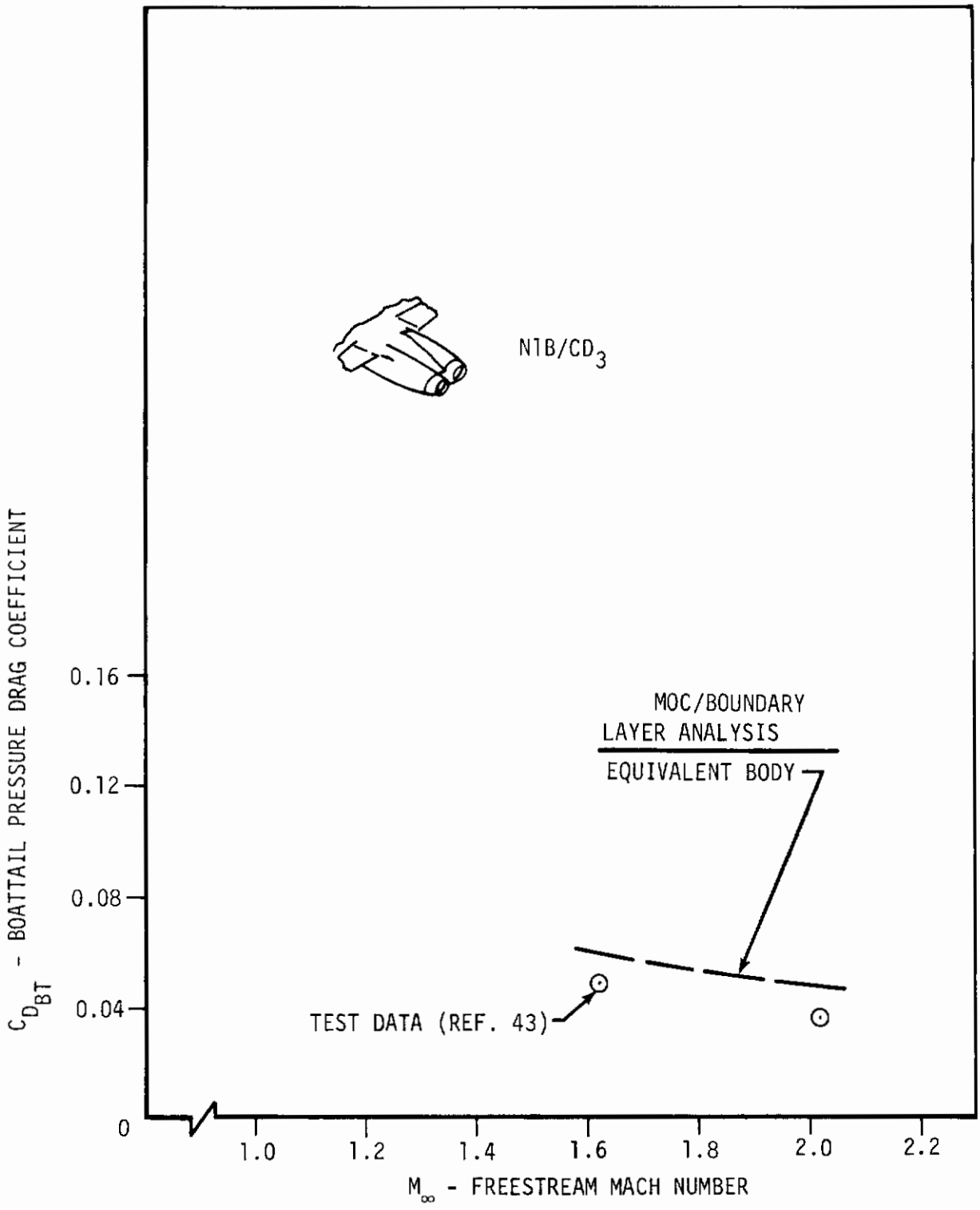

Figure 61. Comparison of Predicted and Measured Boattail Drag; N1B/CD_3 Configuration, Twin Jet Body, Horizontal Wedge Interfairing, Supersonic External Flow (From Ref. 43)

characteristic lines and fitting the shock at this position. Even if the position is not correct, the shock will oscillate back and forth until it will lock itself in the proper position when the flow becomes steady. Then two computational regions are considered, the regions ahead and behind the shock, and solved independently.

Relaxation methods are applied in the same way as in subsonic and transonic flow. No provisions are made for shocks present in the flow field since shocks appear automatically as part of the solution. As already mentioned, these numerical techniques are very powerful.

Another technique to compute the boattail drag is the wave drag method (Ref. 99). This method consists of calculating the pressure differential and the momentum deficit due to the presence of waves in the supersonic flow field. When applied to a twin body, together with boundary layer analysis to add the friction drag, the method gives drag values in poor agreement with the experiments and wrong trends are obtained, e.g. increasing drag with increasing Mach numbers (Fig. 62).

The external separation in supersonic flow is handled using the Bonner-Karger criterion (Ref. 25) (see Fig. 63). This criterion is based on the tangent wedge similarity for oblique shock waves, i.e.

$$\frac{p-p_e}{p_e} = \frac{\gamma M_e^2}{\sqrt{M_e^2-1}}\ \theta \qquad (24)$$

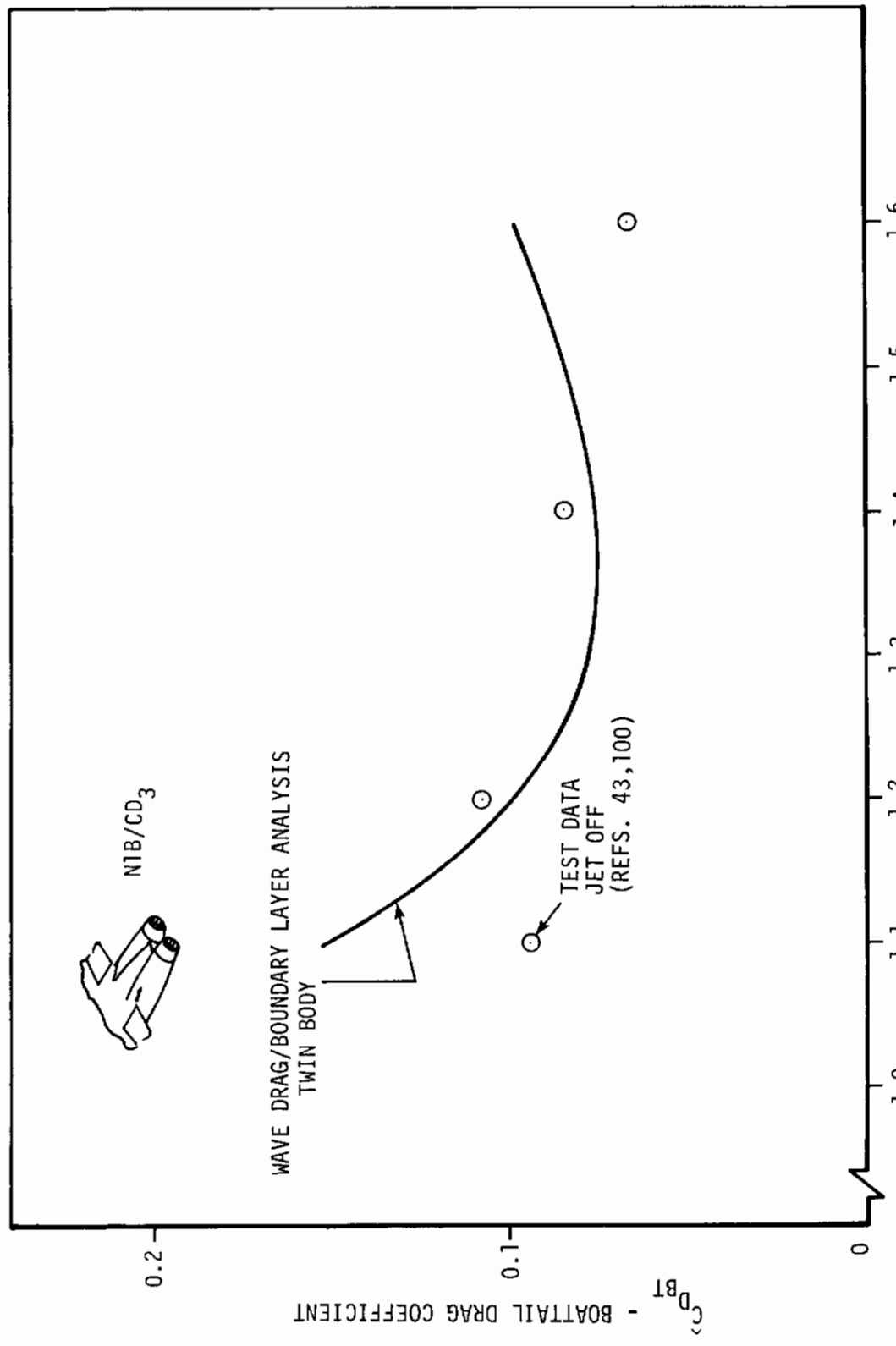

Figure 62. Comparison of Predicted and Measured Boattail Drag; N1B/CD_3 Configuration With Empennage (From Ref. 43)

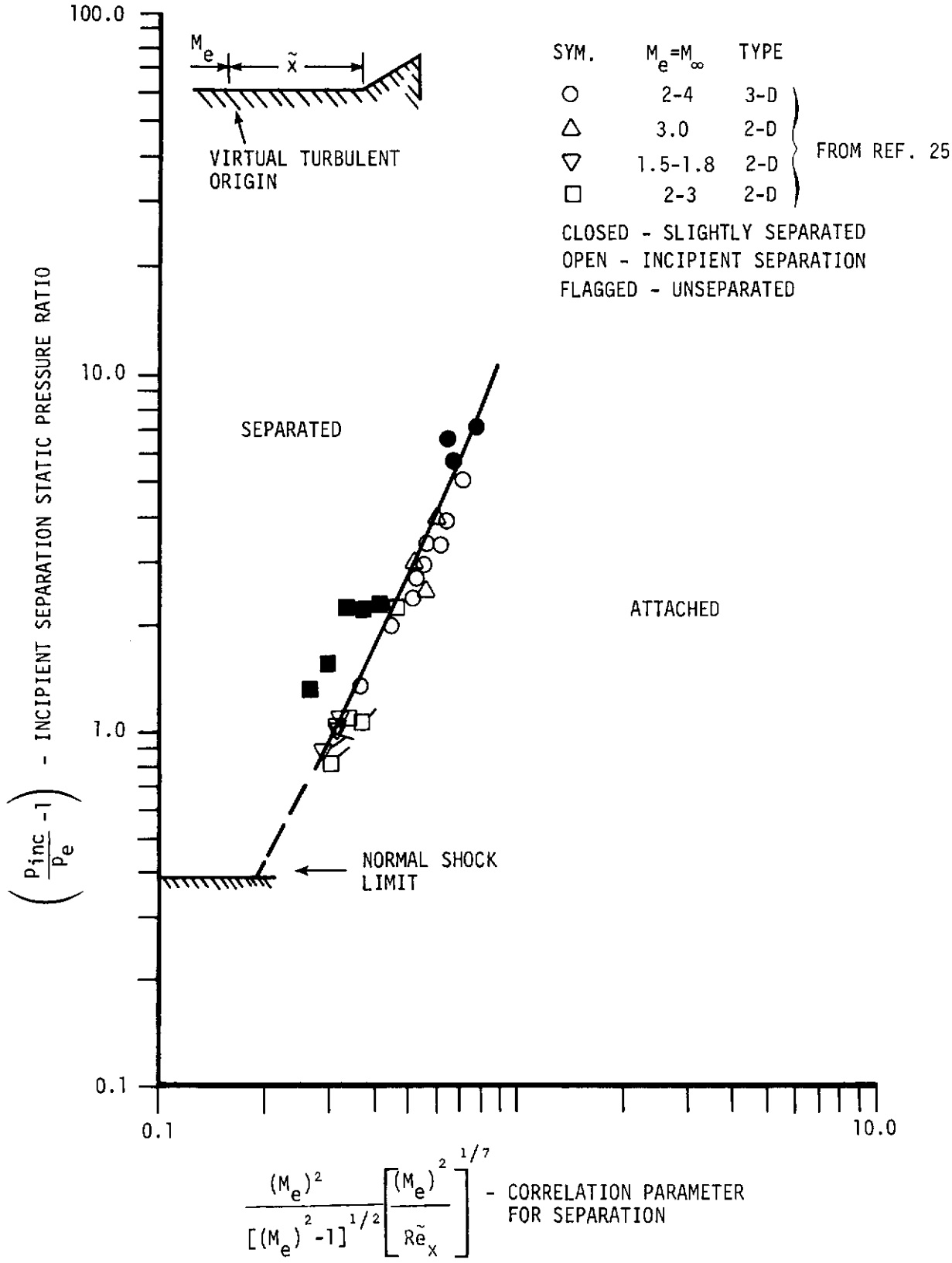

Figure 63. Criteria for Incipient Separation (From Ref. 25)

where θ is the angle of deflection relative to the free stream direction. θ can be considered as given by the rate of change of the displacement thickness at the separation point, i.e.

$$\theta \sim \frac{d\delta^*}{dx} \sim \left[\frac{CM_e^2}{R_{e_{\tilde{x}}}} \right]^{1/7} \tag{25}$$

Therefore

$$\frac{p_{inc}}{p_e} - 1 = f \left\{ \left[\frac{M_e^2}{\sqrt{M_e^2 - 1}} \right] \left[\frac{M_e^2}{R_{e_{\tilde{x}}}} \right]^{1/7} \right\} \tag{26}$$

$R_{e_{\tilde{x}}}$ is defined as the Reynolds number based on the equivalent flat plate length $\tilde{x}$ that would give the same momentum thickness existing at the separation point of the body considered.

The shock-boundary layer interaction is treated by Erdos and Pallone (Ref. 101) and Lees and Reeves (Ref. 102) using integral methods which allow the coupling of the boundary layer equations, valid in the interaction region, with an external inviscid flow solution. Erdos uses the momentum equation of a nearly isentropic inviscid flow coupled with the boundary layer momentum equation in the longitudinal direction to obtain the surface pressure distribution in the free interaction region, with provisions for both laminar and turbulent boundary layers. The concept of the near-wake solution is utilized, together with the dividing streamline assumption to obtain the location of the separation and reattachment points. The final expression for the surface pressure coefficient is a function of local Mach number, Reynolds number, skin friction and of a universal function obtained from experi-

ments (Ref. 103) for both laminar and turbulent flow. The results are consistent with experimental data (Figs 64-65).

Lees and Reeves utilize the integral momentum and moment of momentum equations and, through Stewartson transformations and the use of continuity, they obtain three simultaneous first-order non-linear differential equations for three variables, namely the local external Mach number, the displacement thickness, and the velocity profile parameter for attached and separated flow. With this method the velocity and enthalpy profiles are determined by a single parameter, which is not related to the local pressure gradient. The pressure distribution in the separated region is predicted accurately (Fig. 66).

The external supersonic flow is calculated efficiently with the techniques presented. This is due to the fact that the supersonic flow is "clean", i.e. nonlinear effects are negligible. Therefore simple linearized theory could be applied. For axisymmetric flow, obviously the solutions are consistent with experimental data using the method of characteristics with boundary layer corrections. The discrepancies still existing are attributed to Reynolds number effects. The Bonner-Karger separation criterion seems sufficient to give a good preliminary estimate of large separated regions. This criterion is of the same order of approximation as the shock-boundary layer interaction theories presented.

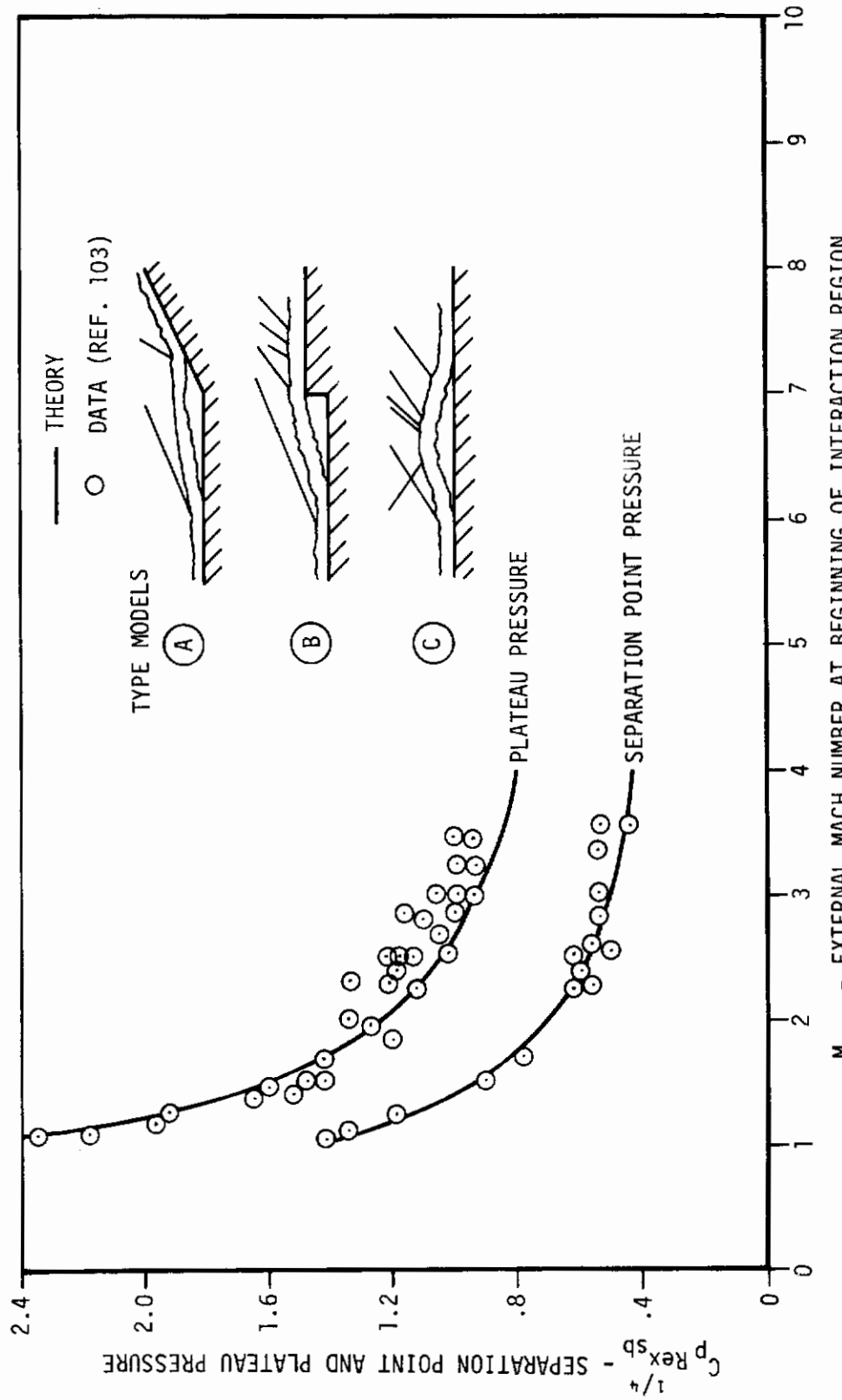

Figure 64. Separation Point and Plateau Pressure, Insulated Laminar Flow (From Ref. 101)

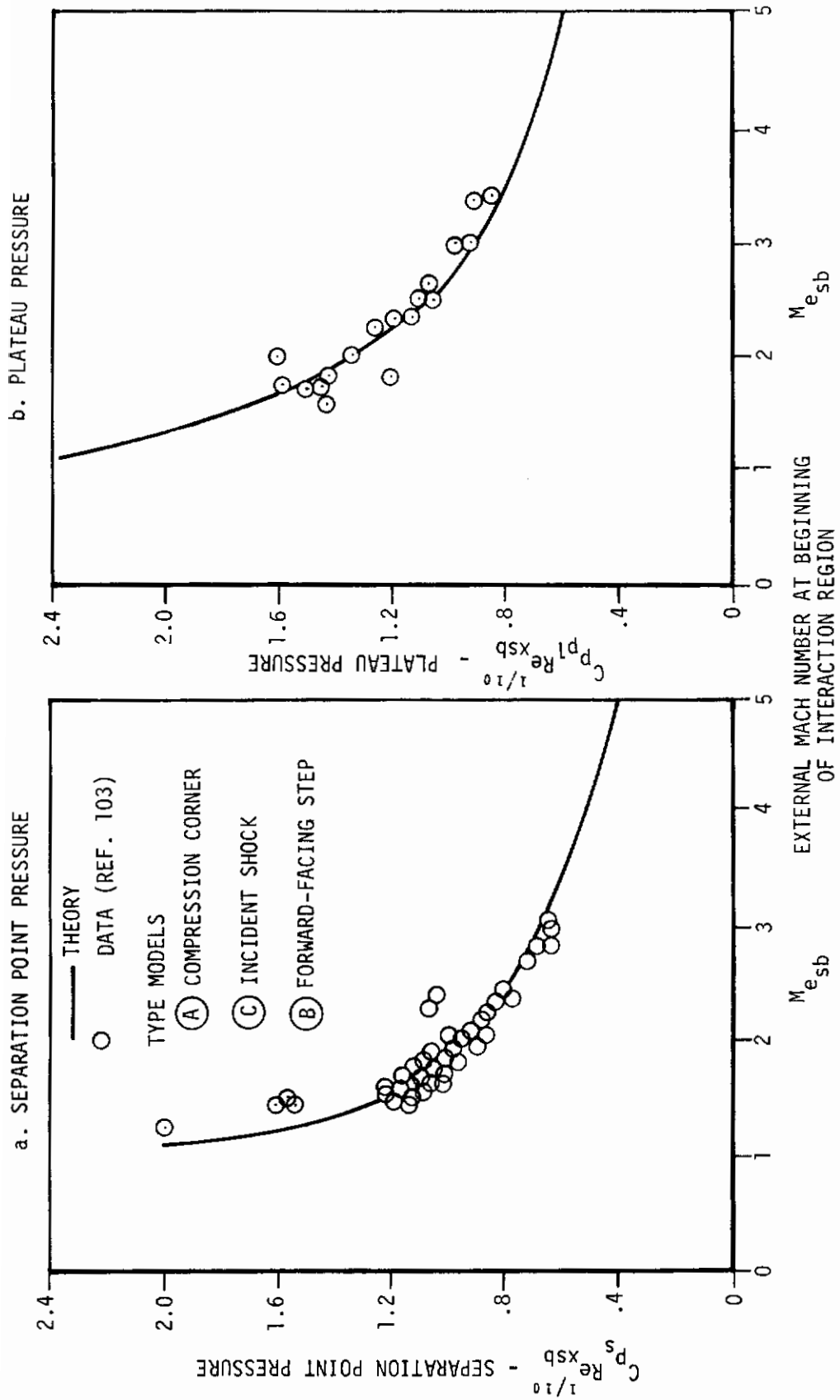

Figure 65. Separation Point and Plateau Pressure, Insulated Turbulent Flow (From Ref. 101)

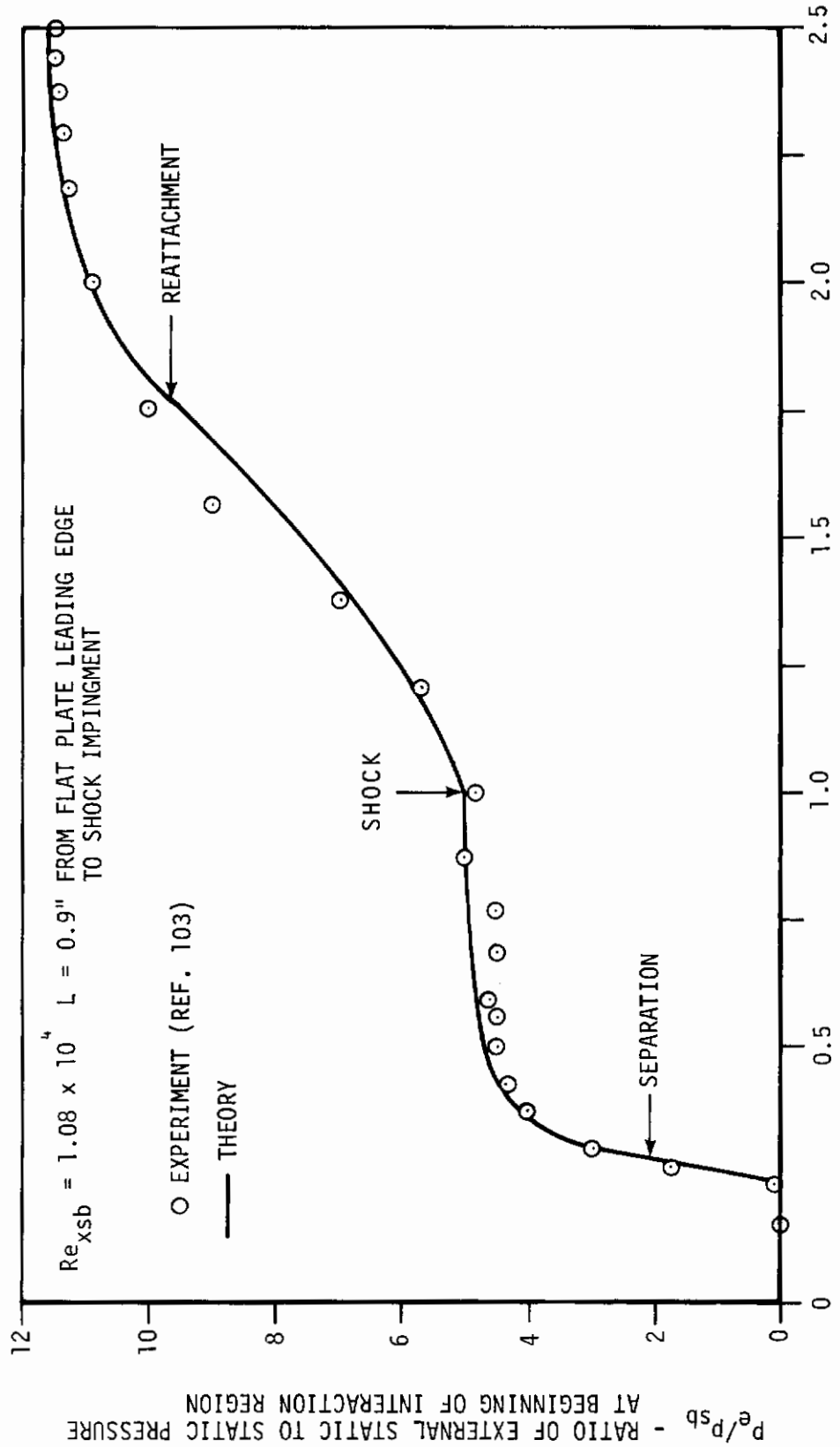

Figure 66. Experimental and Theoretical Pressure Distribution for a Shock Wave/Boundary-Layer Interaction at M_∞ = 2.45 (From Ref. 102)

2. Internal Flow

The method of characteristics is applied in the solution of internal supersonic flow fields. One application of the method is due to Prozan (Ref. 104). It refers to 2-D or axisymmetric, rotational, inviscid, compressible flow. The divergent part of a C-D nozzle or a plug nozzle can be investigated. If a shock is imbedded in the flow field, the flow properties are computed by oblique shock relations and by linear interpolation of the properties across the shock until convergence is reached. Figure 67 shows the plug pressure for isolated unshrouded nozzles obtained with this method, together with experimental data (Ref. 105). The discrepancy is probably due to the fact that the analysis does not account for the smoothing effect of the boundary layer. The analysis is also applicable to twin nozzles and to twin plug nozzles if the nozzle pressure ratios are above a value of 4 to 5, since, in this case, the plug surface pressure is not affected by the interaction between the exhaust jet and the external flow, being shielded by the shroud; for nozzle pressure ratio values less than 5 the plug pressure is unsymmetrical (Ref. 43, Fig. 68) and therefore the axisymmetric analysis does not approximate well enough the experimental values (Fig. 69). The discrepancy is possibly accentuated by boundary layer separation on the plug.

Time-dependent and relaxation methods, e.g. Lax-Wendroff method, error minimization method, etc., can of course be used for the solution of the internal supersonic flow field of C-D and plug nozzles.

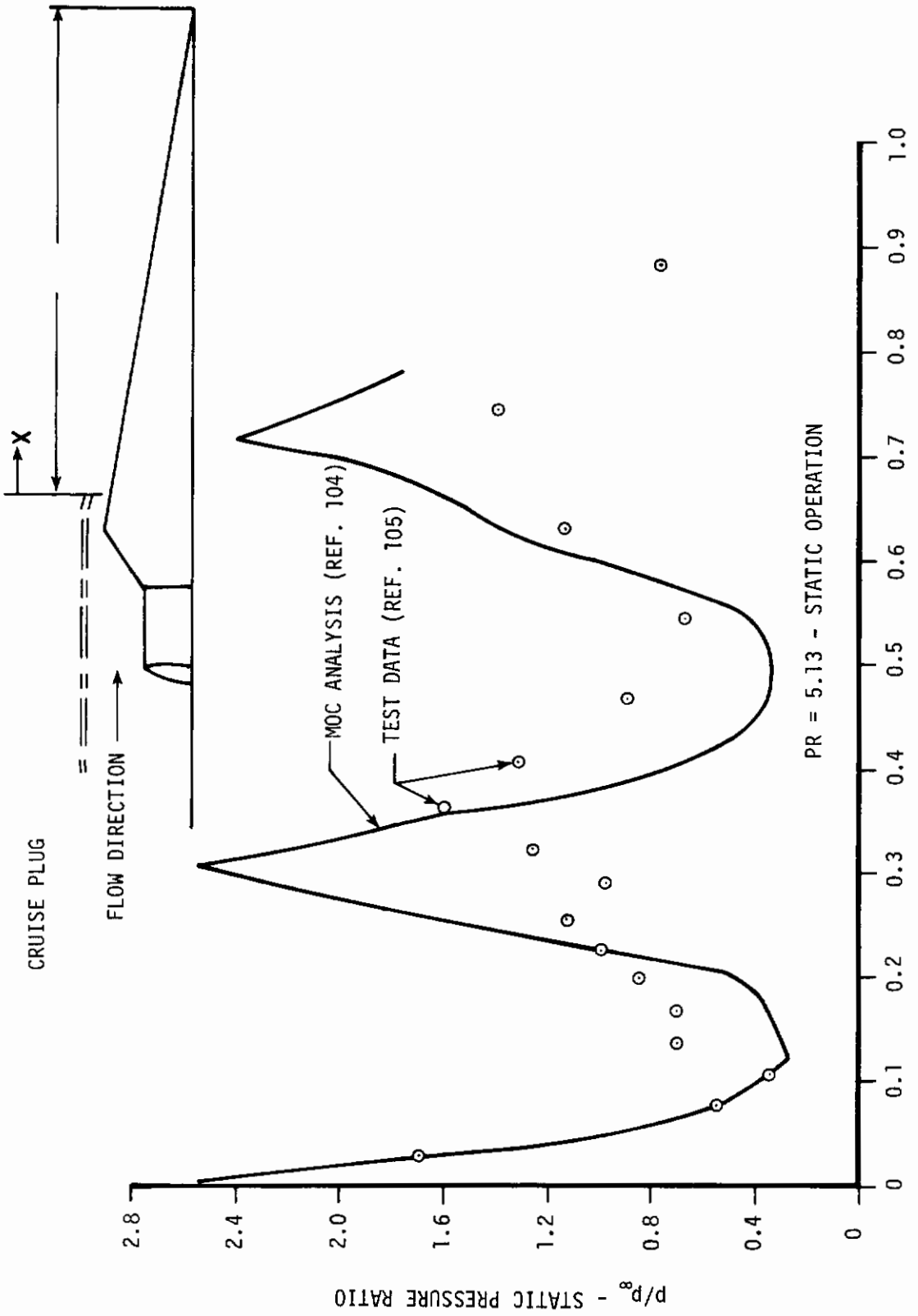

Figure 67. Plug Pressure Distribution for Unshrouded Nozzle (From Ref. 7)

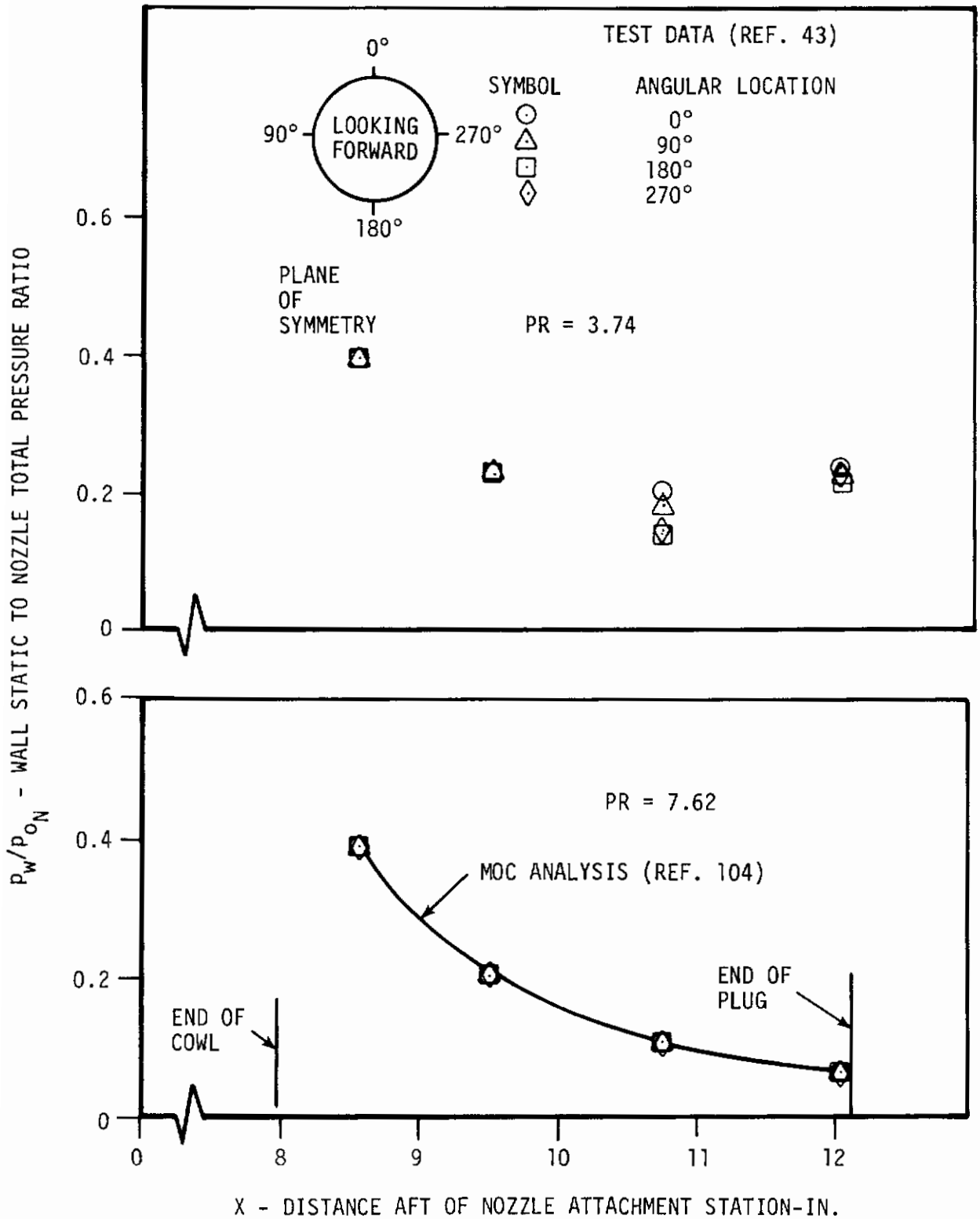

Figure 68. Comparison of Predicted and Measured Plug Surface Pressure Distributions, Unshrouded Nozzle, Mach 1.6 (From Ref. 43)

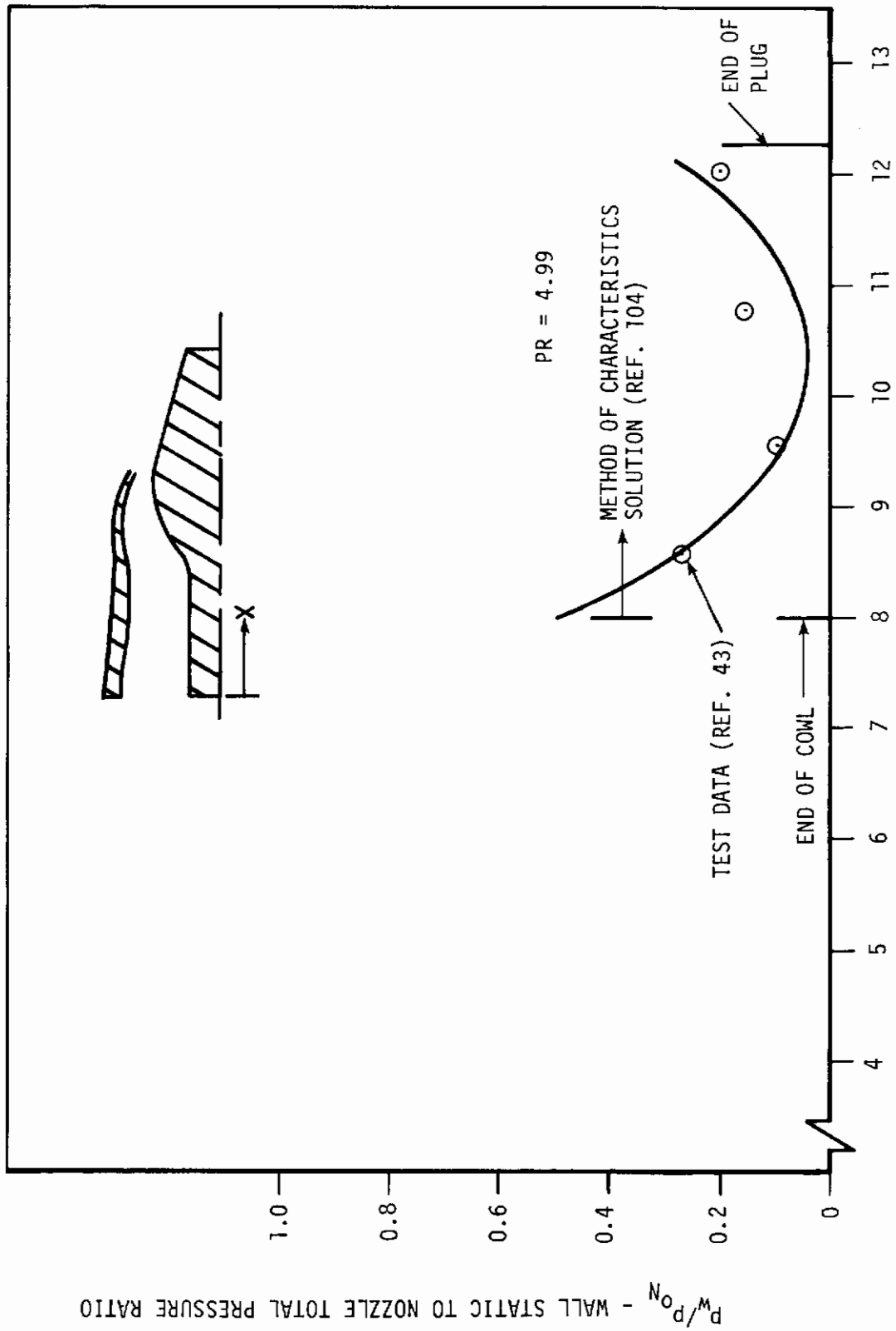

Figure 69. Comparison of Predicted and Measured Plug and Internal Cowl Pressure Distributions - Unshrouded Nozzle - Mach 0.0 (From Ref. 43)

Due to the importance of plug nozzles which have a marked advantage on conventional C-D nozzles, such as thrust control, and shorter length for the same expansion ratio of an axisymmetric nozzle, some authors have recently tried to optimize their performance. Reference 106 uses the method of characteristics to compute the flow field over the plug, the calculus of variation to ascertain whether the thrust is maximized, and a relaxation technique to change the wall contour if optimization is not achieved. Reference 107 analyzes the nonuniform flow field for a truncated plug nozzle. Two basic problems are considered: (1) the near wake-like flow which is solved with an analysis that includes base bleed, nonisoenergetic mixing and a finite approaching B.L.; (2) the inviscid adjacent flow which is solved by using the rotational method of characteristics. Reference 108 presents an analysis by the method of characteristics for the optimum design of plug nozzles which then yield uniform and axial flow.

Chow and Eddy (Ref. 109) analyze C-D ejector nozzle flow fields. They solve the primary flow with the method of characteristics and the secondary flow with 1-D isentropic theory. The analysis refers, in general, to cylindrical-shroud ejector nozzles but can also be used for different shroud shapes. In the event of large secondary flows, the inviscid interaction between the two streams is considered of primary importance and a viscous correction is simply superimposed on the solution (Region II of Fig. 70). For small secondary flow rates viscous interaction effects are too large to justify the use of the superposition principle and

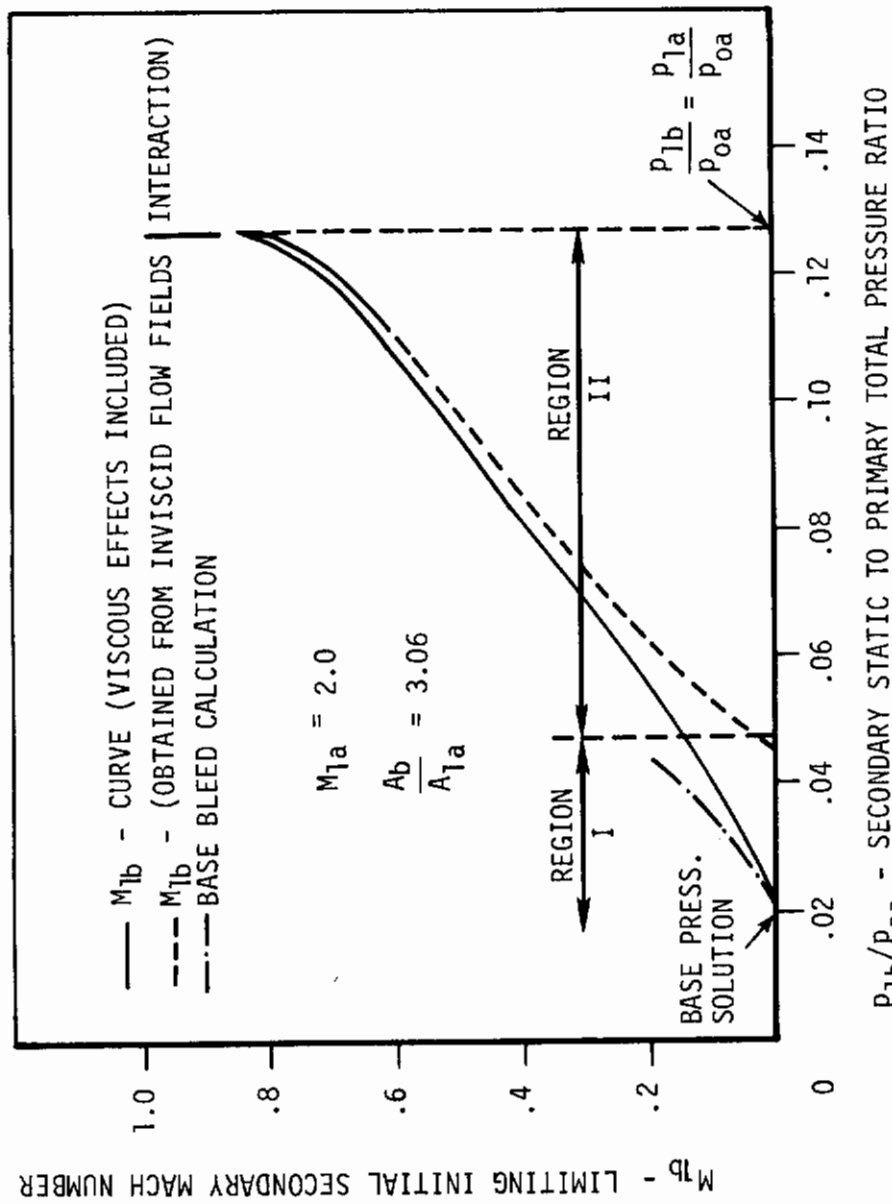

Figure 70. Limiting Initial Mach Number of the Secondary Flow as a Function of Secondary Static Pressure to Primary Total Pressure Ratio (From Ref. 109)

a solution similar to the base flow solution of Reference 87 is used (Region I of Fig. 70).

The internal flow is mostly analyzed with the method of characteristics because of its inherent accuracy. The method gives good results for 2-D and axisymmetric flows with nozzle pressure ratios above approximately 5.

Nozzle flow separation is predicted empirically and analytically (Ref. 27-30). Chamay (Ref. 110) found experimentally that the separation pressure ratio in ejector nozzles is mainly a function of the secondary to primary corrected mass flow ratio. He derives the following equation

$$\frac{p_1}{p_B} = 0.63 + 0.04 \ln \left[\frac{\dot{w}_b \sqrt{T_{o_b}}}{\dot{w}_a \sqrt{T_{o_a}}} + 0.01 \right] \qquad (27)$$

Arens and Spiegler (Ref. 27) instead solve the nozzle flow separation problem with a simple analytical formulation. With the assumption that the pressure rise in the nozzle is sufficient to stagnate a characteristic velocity, u_s^*, in the boundary layer, that the stagnation temperature is constant, that the flow is isentropic up to the separation point, and neglecting the pressure rise in the mixing region, the following equation for the ratio of the separation to ambient pressure in terms of nozzle pressure ratio is obtained

$$\frac{p_s}{p_{am}} = \frac{p_{oN}/p_{am}}{\left[\frac{(p_{oN}/p_{am})-(u_s^*/u_{sb})}{1-(u_s^*/u_{sb})^2}\right]^{\frac{\gamma}{\gamma-1}}} \qquad (28)$$

where the ratio u_s^*/u_{sb} assumes a value of 0.56. This formulation does not consider the effect of the nozzle divergence angle which affects the value of the separation pressure ratio as reported in Reference 28, and Reference 30.

The separation criteria of the cited references have been used by Lockheed California in their investigation of airframe/exhaust nozzle integration. Knowing the separation location, it is possible to calculate the nozzle performance; however these theories do not account for the pressure recovery that occurs in the flow after separation.

3. Jet Plumes

Plumes with supersonic internal flow are analyzed with various techniques, e.g. 1-D theory, shock-expansion theory, method of characteristics, Newtonian impact theory, time-dependent techniques. Various combinations of external and internal flow techniques are used to calculate the plume shape, depending on whether the external flow is subsonic or supersonic.

Lockheed California (Ref. 7) tried different techniques and compared them to the accurate method of characteristics. The reason was to find a technique as accurate but faster than the method of characteristics. The shock-expansion 1-D theory is selected for jets issuing in subsonic and supersonic external flows.

The method for the latter case consists of calculating the initial Prandtl-Meyer expansion at the cowl lip to match the external pressure at this point; then the jet boundary is extrapolated for a short distance downstream, and 1-D expansion is used to obtain the pressure at this new location. This pressure is considered as the upstream pressure, and the local external pressure as the downstream pressure, and oblique shock relations are applied to obtain the jet boundary inclination just downstream of the new location. Continuing the calculation downstream, the entire jet boundary is obtained. For subsonic external flow, the method involves iterations of the internal and external flow fields until the pressure matches on the plume boundary.

Benson et al (Ref. 15) use the same method but they simplify the calculation of the subsonic external flow field by assuming that the pressure is known at the cowl lip. For supersonic external flow an estimated value of the initial turning angle at the cowl lip is used. Conical shock relations are then used to find the external pressure distribution behind the shock. Subsequent segments of the jet boundary are found using Prandtl-Meyer expansions. The total extent of the jet boundary is found by a series of straight segments. For an external flow with M>3, they apply the Newtonian impact theory which relates the local pressure and flow angle to the pressure, Mach number, and flow angle just upstream of the plume through a relation involving the sine square of the flow angle.

Rudman and Maise (Ref. 8) balance the pressure decrease in the jet plume due to expansion and the pressure increase on the jet boundary due to turning to match the local ambient pressure. For subsonic external flow the basic assumptions are: (1) the jet boundary, over a distance of Δx, is a circular arc, (2) knowing the jet flow conditions at the cowl lip and assuming a pressure drop due to area increase, a new area can be computed at a distance Δx downstream using 1-D compressible flow properties. The new area determines uniquely the jet boundary inclination θ. The complete jet boundary can therefore be computed by partial calculation on successive Δx.

Love et al (Ref. 84) compute the jet boundary with the method of characteristics. The method follows the principle of successive iterations. In case of coalescence of characteristic lines, which leads to shock formation, the foldback procedure is followed, i.e. the characteristic equations are permitted to ignore the intersection of characteristics of the same family, so that calculations proceed. Then the shock location is given by the inner envelope of the intersections of characteristics of the same family. The flow field between the shock and the jet boundary is obtained by means of the characteristic net remaining after deleting the foldback part of the net.

Bastianon (Ref. 111) uses a Lax-Wendroff time-dependent technique to calculate supersonic 3-D jet plumes. The time-dependent governing equations, written in finite difference form, are transformed and the flow field is divided into two separate regions, (1) the inner region bounded by the shock wave surface and (2) the outer

region between the shock and the jet boundary surfaces. Sample calculations of axisymmetric flow fields compared favorably with the method of characteristics solutions (Fig. 71).

All the methods described give plume solutions fairly close to each other. From Schlieren photographs taken during the experiments of Love et al (Ref. 84), there is indication that the shape of the boundary from nozzle exit to maximum diameter can be approximated fairly well by a circular arc.

4. Base Flow

The supersonic base flow has been studied and solved with both analytical and empirical methods.

The base flow model of Chapman (Ref. 112) gives qualitative flow characteristics for the viscous flow in the base region. The flow undergoes an expansion at the point of separation from the body which is function of Mach number, pressure, boundary layer thickness, and profile shape. This separation causes the formation of the so-called "dead air" region behind the base. At a certain distance from the base the flow reattaches and goes through a reattachment shock. In the calculation of the base pressure, a mass balance is required, i.e. the mass flow scavenged from the "dead air" region must be replaced by the pressure rise at the reattachment zone. The base pressure is obtained by requiring that the total pressure of the dividing streamline, i.e. the streamline that divides the recirculation flow in the "dead air" region from the flow that goes through the recompression oblique shock at reattachment, be equal to the static pressure behind the recompression shock. In

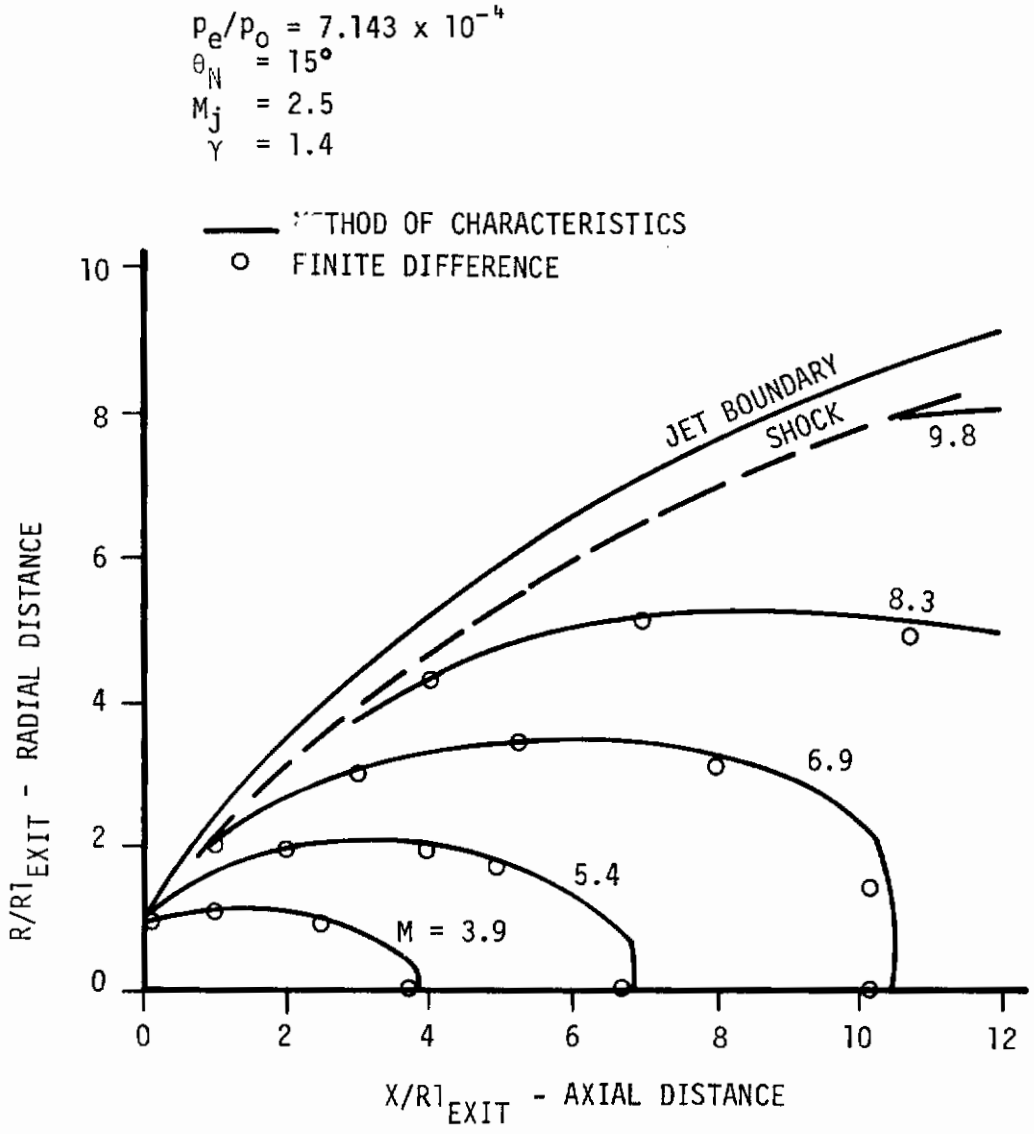

Figure 71. Comparison of Lines of Constant Mach Number, Axisymmetric Case (From Ref. 111)

other words, as mentioned in the Transonic Section, the dividing or discriminating streamline in the shear flow region has just enough mechanical energy to penetrate the region of high pressure behind the recompression shock. This mechanical energy derives from an almost complete conversion of its kinetic energy.

The viscous mixing process causes the shear flow region to thicken as it approaches the recompression shock. In axisymmetric flows, (since the mean radius of a stream decreases while approaching the trailing shock), the spreading of the shear flow region is also caused by the requirement to keep the cross-sectional area of the stream tube constant.

Based on this flow model, the base pressure is obtained from simple interaction between the laminar or turbulent boundary layer and the external flow, assuming Blasius boundary layer profiles for the laminar case, and correlation parameters, like the ratio of boundary layer thickness to base diameter for both laminar and turbulent cases.

The various theories developed do not account for viscous effects or for compression along the dividing streamline. They assume zero boundary layer thickness at the separation point, a linear relation between viscosity and temperature in the wake, and constant pressure in the mixing region. The influence of the vortex street on the base pressure is not accounted for. Nevertheless, they give a clear insight of the mechanism of the wake flow and base pressure, and some quantitative results.

More sophisticated analyses (see Refs. 109, 113, 114, etc.) make use of a simplified equation of motion for the shear region and of mixing integrals, already mentioned, to take care of the viscous mixing process. The base pressure is obtained by a mass balance in the "dead air" region, which actually has finite velocities that allow heat exchange between the wake flow and the boundary walls.

The method of Reference 86 is the Korst et al base pressure analytical method already discussed in transonic flow which is also valid in supersonic flow.

Korst and Chow (Ref. 113) account for the initial boundary layer thickness at the separation point with the concept of an equivalent bleed flow. This is based on the realization that in the integral equations developed to solve the base flow, the terms for the boundary layer and the base bleed can be added. Therefore a change of one quantity can be replaced by a corresponding change in the other. In the case that both an initial boundary layer and mass bleed are present, the mixing integral for the discriminating streamline contains both boundary layer momentum thickness and mass bleed. In this way the disturbance caused by an initial boundary layer is taken into consideration.

Another concept to account for the initial boundary layer thickness at the separation point can be found in Reference 115. The method consists of shifting the origin of the jet upstream a distance $\tilde{X}$ to an imaginary jet with no initial boundary layer (Fig. 72). To find this distance the assumption is that the mass

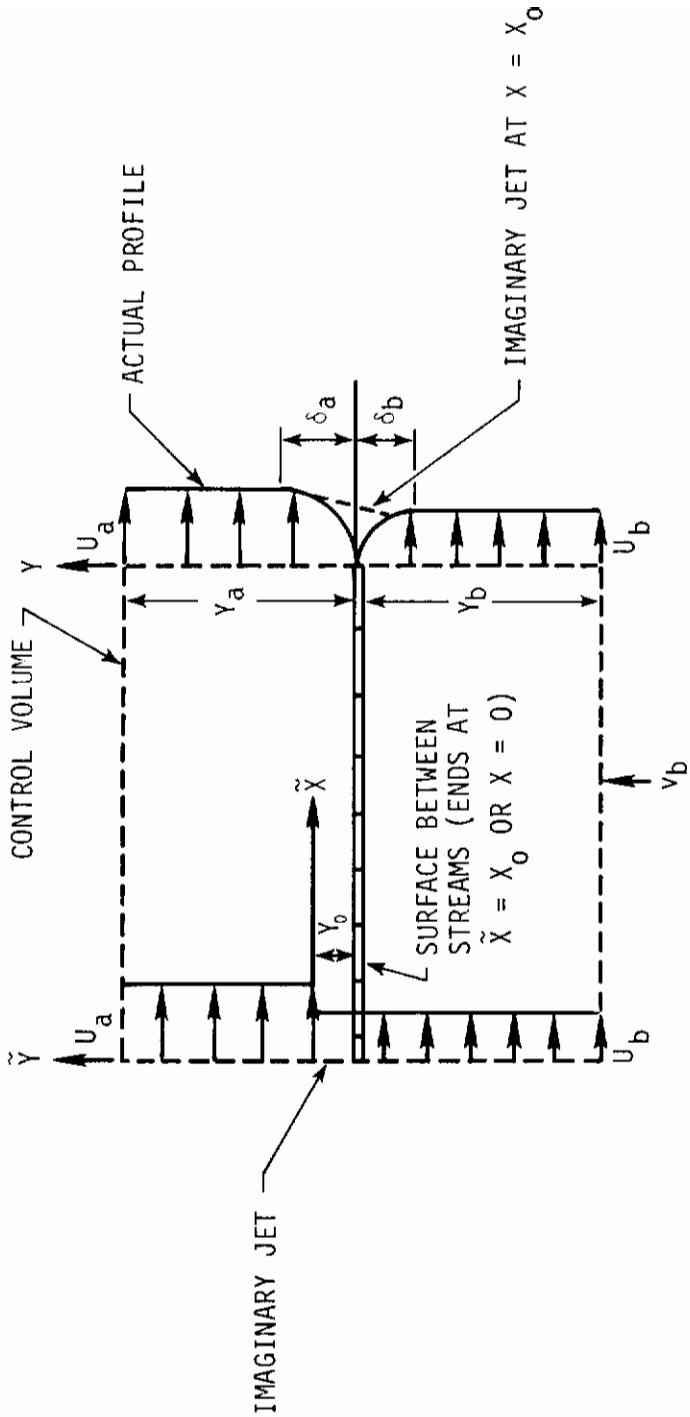

Figure 72. Determination of Origin Displacement (From Ref. 115)

flow and momentum of the imaginary jet at $\tilde{X}$ are the same as those of the actual boundary layer. Continuity and momentum are applied to a control volume to obtain the value of $\tilde{X}$ and also the corresponding shift in the Y direction. Once this is accomplished the theory of Korst and Chow (Ref. 113) can be used to obtain the velocity distribution in the mixing region and determine the base pressure.

Reeves and Lees (Ref. 116) and Alber and Lees (Ref. 117) develop an integral near-wake analysis for supersonic laminar and turbulent base flows. The solution for the free shear layer is joined with the one for the wake to get the conditions near the body. Using a modified version of the Stewartson transformation (Ref. 118), a set of boundary layer continuity and momentum equations is used to obtain the familiar Blasius equation for laminar flow, ($f''' + ff'' = 0$) which gives the spreading of the shear layer. Then from continuity and momentum, three integral conservation equations are obtained for the local external Mach number, the ratio of centerline velocity to external velocity, and the displacement thickness. The equations are integrated upstream from the rear stagnation point. This procedure is similar to that used by the same authors in the shock-boundary layer investigation. For the turbulent case, the basic assumption is that the eddy viscosity can be described by one incompressible constant, derived from the average incompressible spreading parameter used to scale the error function velocity profile, and one reference density. Other authors (Refs. 119, 120) assume that the turbulent shear stress is locally proportional to the turbulent intensity of kinetic energy.

Erdos and Zakkay (Ref. 121) consider the base problem as an inviscid interaction of the mixed supersonic-subsonic type and obtain a solution for the base pressure and centerline pressure distribution in the wake on a time-dependent basis using a two-step Lax-Wendroff technique which gives the time derivatives in terms of centered differences of spatial derivatives evaluated at the midpoint of the time interval (Ref. 13). This solution can be regarded as a first approximation in an asymptotic expansion in inverse powers of Reynolds number by which viscous effects due to the interaction can be subsequently obtained.

Brazzel and Henderson (Ref. 38) develop an empirical correlation for the base pressure which considers the effects of various influencing parameters such as jet to free stream momentum flux ratio, jet temperature, boattail area ratio, free stream Mach number, and nozzle position relative to the body base. The correlation for cylindrical afterbodies with flush nozzles and sonic jet flows is plotted in Figure 73.

The supersonic base flow has been analyzed extensively and the theories available give results consistent with experimental data. The Korst model with variations to include initial boundary layer and base bleed effects is reliable when applied to the solution of the aft-end flow field.

5. Summary

Good solutions are available in supersonic flow. The most accurate, the method of characteristics, is used for both external

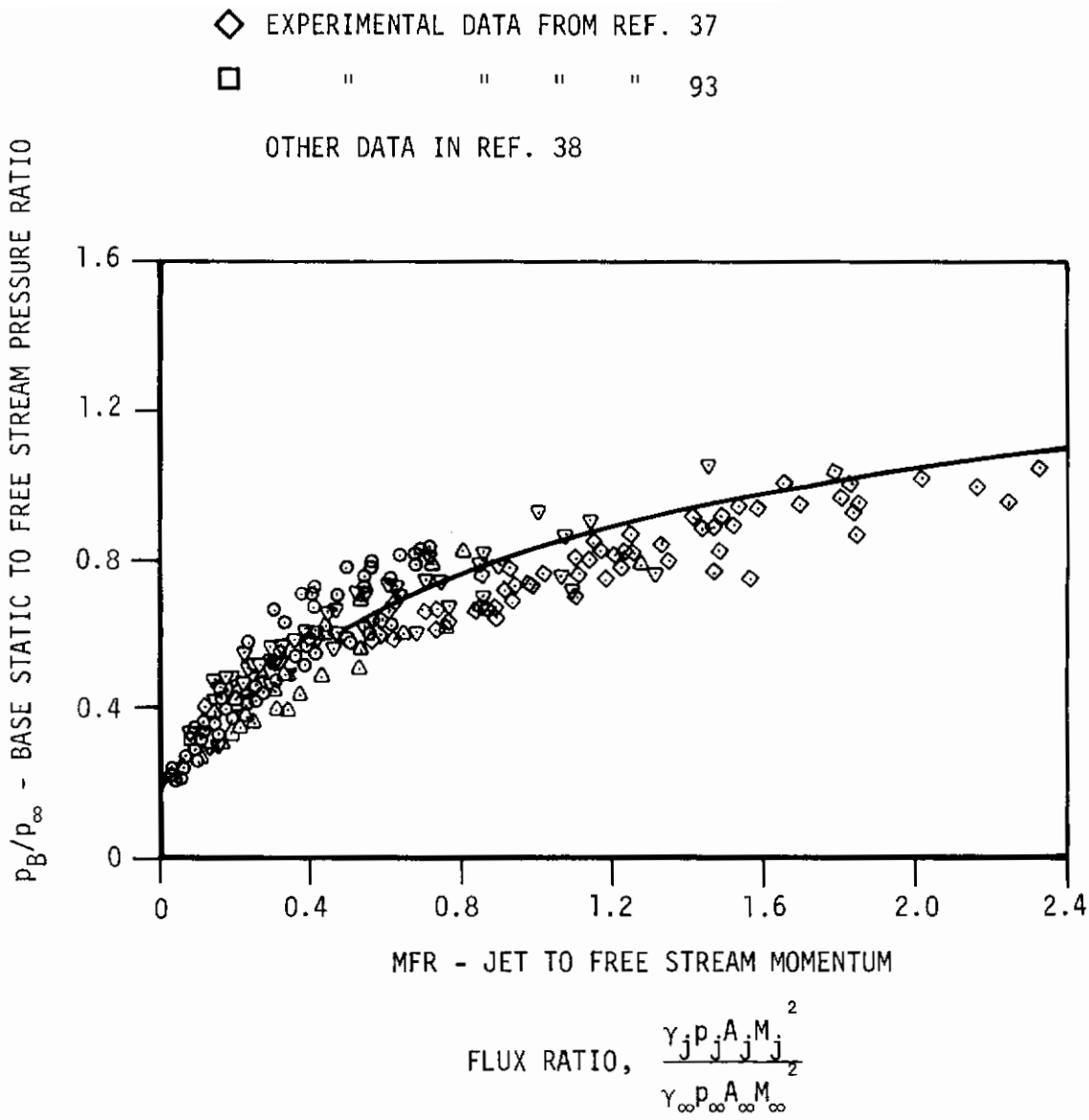

Figure 73. Normalized Base Pressure Data for Cylindrical Bodies With Flush Nozzles (From Ref. 38)

and internal flow problems, but numerical techniques are also applied efficiently. More effort should be devoted to obtain correct plug pressure distributions for unshrouded plug nozzles. Boattail separation flow fields should be solved analytically since only empirical techniques are now available. Also the influence of high Reynolds numbers on supersonic boattail drag should be investigated.

CONCLUSIONS

A critical review of some analytical methods for the solution of the afterbody/exhaust nozzle flow fields has been presented.

The various techniques treated for the analysis of subsonic flow fields, namely potential theory and numerical methods, are effective but develop some computational problems at the body/plume junction and in the presence of body slope discontinuities. Additional work in this area should be performed. The subsonic jet plume and its effects on base pressure and boattail separation point should be further analyzed and compared with experimental results. The boattail empirical separation criterion currently used should be checked against experimental data at subcritical Mach numbers to ascertain its validity. Also the analytical investigation of the subsonic base drag and wake characteristics should be initiated.

The most critical situation is the one related to transonic flight regimes. The gap between the theories and experiments is still present. Besides errors due to theoretical and numerical approximations, it is possible that errors are introduced in experimental data obtained by wind tunnel testing because of Reynolds number and wall effects. Transonic studies have lately acquired new impetus with the use of time-dependent and relaxation techniques. Further studies in this area should improve the predictions of aircraft aft-end drag. 3-D investigations should be used to study the unsymmetric flow fields. To overcome the prob-

lems created by large separated regions due to jet plume and shock-boundary layer interaction effects some empirical techniques might be used in absence of complete analytical solutions. Base flow and free mixing in the wake of axisymmetric bodies are analyzed in detail and are consistent with experimental data in transonic and supersonic flow as well.

The supersonic flow investigations present no difficulties up to the terminal section of the boattail and time-dependent and relaxation methods have supplemented the method of characteristics. However, at low supersonic Mach numbers, the theories do not predict properly the recompression effects at the boattail end. Correction factors could eliminate the problem. The shock-boundary layer investigations and separation criteria are consistent with experimental evidence. Investigations could be undertaken to solve analytically the supersonic boattail separation at high Reynolds numbers in order to predict its effect on the boattail drag.

REFERENCES

1. Calarese, W., "Critical Review of Analytical Investigations of Airframe-Exhaust Nozzle Integration", AFFDL TM 72-35 FX, August 1972.

2. Hess, J.L., and Smith, A.M.O., "Calculation of Potential Flow about Arbitrary Bodies", Progress in Aeronautical Sciences, Vol. 8, Pergamon Press, 1967.

3. Goebel, T.P. and Divita, J.S., "Analytical Investigation of Aircraft Exhaust Nozzle Performance", Technical Report, AFFDL-TR-70-28-Vol. 1, March 1970.

4. Smith, A.M.O., and Pierce J., "Exact Solution of the Neumann Problem Calculation of Non-Circulatory Plane and Axially Symmetric Flows About or Within Arbitrary Boundaries", Douglas Report ES-26988, April 1958.

5. Hess, J.L., "Calculation of Potential Flow About Bodies of Revolution Having Axes Perpendicular to the Free Stream Direction", Douglas Report ES-29812, October 1960.

6. Henry, B.Z., Jr. and Cahn, M.S., "Pressure Distributions Over a Series of Related Afterbody Shapes as Affected by a Propulsive Jet at Transonic Speeds", NACA RM-L56K05, January 1957.

7. Lockheed-California Company, "Phase I Test Plan of Program for Experimental and Analytical Determination of Integrated Airframe-Nozzle Performance", LR 24183 18 December 1970.

8. Rudman, S. and Maise, G., "Afterbody Performance Prediction in Subsonic and Supersonic Flight Including the Effects of Boundary Layer", Grumman Advanced Development Program, Report No. 01-03-70.2, June 1970.

9. Shrewsbury, G., "Effect of Boattail Juncture Shape on Pressure Drag Coefficients of Isolated Afterbodies", Lewis Research Center, Cleveland, Ohio, NASA TMX-1517, 1967.

10. Moretti, G., "Time-Dependent Techniques for the Computation of Nozzles, Boattails and Airfoils", Grumman Aerospace Corp., Advanced Development, Report No. ADR 01-03-69.4, April 1969.

11. Grossman, B., "Time-Dependent Calculation of Subsonic Flow Over Aircraft Aft-End Configurations", Grumman Aerospace Corp., Advanced Development, Report No. ADR 01-03-70.3, December 1970.

12. Grossman, B., and Moretti, G., "New Techniques for the Time-Dependent Computation of Transonic Flows", Grumman Aerospace Corp., Advanced Development, Report No. ADR 01-03-70.4, December 1970.

13. Richtmyer, R.D. and Morton, K.W., "Difference Methods for Initial-Value Problems", Interscience Publishers, 2nd Edition, 1967.

14. Steger, J.L. and Lomax, H., "Numerical Calculation of Transonic Flow About Two-Dimensional Airfoils by Relaxation Procedures", AIAA Paper No. 71-569, June 1971.

15. Benson, J.L., Miller, L.D., and Horie G., "Theoretical Study of Engine Exhaust Nozzle Airframe Integration", Lockheed-California Company, Arnold Engineering Development Center, AEDC-TR-67-214, October 1967.

16. Silhan, F.V., and Cubbage, J.M., Jr., "Drag of Conical and Circular-Arc Boattail Afterbodies at Mach Numbers from 0.6 to 1.3", NACA RM L56K22, January 1957.

17. Cohen, C.B. and Reshotko, E., "Similar Solutions for the Compressible Laminar Boundary Layer with Heat Transfer and Pressure Gradient", NACA Report No. 1293, 1956.

18. Wazzan, A.R. and Ball, W.H., "Body Shape Effects on Skin Friction in Supersonic Flows", AIAA Journal pp 1770 - 1772, September 1965.

19. Reshotko, E. and Tucker, M., "Approximate Calculation of the Compressible Turbulent Boundary Layer with Heat Transfer and Arbitrary Pressure Gradient", NACA TN 4154, 1957.

20. Sasman, P.K., and Cresci, R.J., "Compressible Turbulent Boundary Layer with Pressure Gradient and Heat Transfer", AIAA Journal, Volume 4, No. 1, January 1966.

21. Ludwieg, H., and Tillman, W., "Investigations of the Wall-Shearing Stress in Turbulent Boundary Layers", NACA TM 1285, 1950.

22. Eckert, E.R.G., "Survey on Heat Transfer at High Speeds", WADC, TR 54-70, 1954.

23. Allen, J.M. and Monta, W.J., "Turbulent-Boundary-Layer Characteristics of Pointed Slender Bodies of Revolution at Supersonic Speeds", NASA TN D-4193, October 1967.

24. Goldschmied, F.R., "An Approach to Turbulent Incompressible Separation and the Determination of Skin Friction Under Adverse Pressure Gradients", AIAA Paper 64-465, July 1964.

25. Bonner, E. and Nixon, J.A., "Wind Tunnel Testing Techniques for Integrated Airframe-Exhaust Nozzle Systems", AFFDL-TR-68-94, July 1968.

26. Wehofer, S., and Moger, W.C., "Analysis and Computer Program for Evaluation of Air Breathing Propulsion Exhaust Nozzle Performance", AEDC-TR-73-29, May 1973.

27. Arens, M. and Spiegler, E., "Shock-Induced Boundary Layer Separation in Overexpanded Conical Exhaust Nozzles", AIAA Journal, Vol. 1, No. 3, March 1963.

28. Summerfield, M., Foster, C.R., and Swan, W.C., "Flow Separation in Overexpanded Supersonic Exhaust Nozzles", Princeton University, Princeton, N.J., and California Institute of Technology, Pasadena, California, September-October 1954. (Jet Propulsion)

29. Green, L., Jr., "Flow Separation in Rocket Nozzles", ARS Journal, January-February 1953.

30. Scheller, K, and Bierlein, J.A., "Some Experiments on Flow Separation in Rocket Nozzles, Wright Air Development Center, Dayton, Ohio, November 30, 1950.

31. Vick, A.R., Cubbage, J.M., and Andrews, E.H., Jr., "Rocket Exhaust - Plume Problems and Some Recent Related Research," AGARD Specialist Meeting on Fluid Dynamic Aspects of Space Flight, Gordon and Breach Science Publishers, New York, 1964.

32. Fetterman, D.E., Jr., "Effects of Simulated Rocket-Jet Exhaust on Stability and Control of a Research-Type Airplane Configuration at a Mach Number of 6.86", Lewis Research Center, Cleveland, Ohio, 1959, NASA TM X-127.

33. Dryer, M., and North, W.J., "Preliminary Analysis of the Effect of Flow Separation Due to Rocket Jet Pluming on Aircraft Dynamic Stability During Atmospheric Exit", Lewis Research Center, Cleveland, Ohio, NASA Memo 4-22-59E.

34. Falanga, R.A., Hinson, W.F., and Crawford, D.H., "Exploratory Tests of the Effects of Jet Plumes on the Flow Over Cone-Cylinder-Flare Bodies", Langley Station, Hampton, Virginia, 1962, NASA TN D-1000.

35. Alpinieri, L.J., and Adams, R.H., "Flow Separation Due to Jet Pluming", AIAA Journal, Vol. 4, October 1966, pp. 1865-1866.

36. Nichols, M.R., "Aerodynamics of Airframe-Engine Integration of Supersonic Aircraft", NASA Technical Note, NASA TN D-3390, August, 1966.

37. Cubbage, J.M., Jr., "Jet Effects on Base and Afterbody Pressures of a Cylindrical Afterbody at Transonic Speeds", NACA RM L56C21, May 1956.

38. Brazzel, C.E. and Henderson, J.H., "An Empirical Technique for Estimating Power-On Base Drag of Bodies of Revolution with a Single Jet Exhaust", AGARD Conference Proceedings, No. 10, September 1966.

39. McDonald, H. and Hughes, P.F., "A Correlation of High Subsonic Afterbody Drag in the Presence of a Propulsive Jet or Support Sting", Journal of Aircraft, Vol. 2, No. 3, May-June 1965, pp 202-207.

40. Spreiter, J.R. and Alksne, A.Y., "Thin Airfoil Theory Based on Approximate Solution of the Transonic Flow Equation", NACA Rep. 1359, 1958, (Supercedes NACA TN 3970.)

41. Spreiter, J.R., and Alksne, A.Y., "Slender-Body Theory Based on Approximate Solution of the Transonic Flow Equation", National Aeronautics and Space Administration Technical Report R-2, 1959.

42. Pratt and Whitney Aircraft, "Experimental and Analytical Determination of Integrated Airframe-Nozzle Performance, Phase I Summary Report", Pratt and Whitney Aircraft Support Program, PWA-4065, November 1970.

43. Lockheed-California Company, "Experimental and Analytical Determination of Integrated Airframe-Nozzle Performance", Phase II Interim Report, Vols. II and III LR 24830, February 1972.

44. Presz, W., "Experimental and Analytical Determination of Integrated Airframe Nozzle Performance", Phase II, Summary Report, Pratt and Whitney Aircraft Support Program, PWA-4375, February 1972.

45. Presz, W., Konarski, M. and Grund, E., "Prediction of Installed Nozzle Flow Fields", AIAA Paper No. 70-700, June 1970.

46. Oswatitsch, K, and Keune, F., "The Flow Around Bodies of Revolution at Mach Number One", Proc. Conf. on High-Speed Aeronautics, Polytechnic Institute of Brooklyn, Brooklyn, New York, June 20-22, 1966, pp. 113-131.

47. Spreiter, J.R., and Stahara, S.S., "Calculative Techniques for Transonic Flows About Certain Classes of Airfoils and Slender Bodies", NASA Contractor Report, NASA CR-1722, April 1971.

48. Grund, E., Presz, W. Jr., and Konarski, M., "Predicting Airframe/Exhaust Nozzle Interactions at Transonic Mach Numbers", AIAA Paper No. 71-720, June 1971.

49. Epler, W.E., "Prediction of Boattail Drag Coefficients", Pratt & Whitney Aircraft, Florida SMR FR-3674, 1970.

50. Wu, J.M., Aoyama, K. and Moulden, T.H., "Transonic Flow Fields Around Various Bodies of Revolution Including Preliminary Studies on Viscous Effects With and Without Plume", U.S. Army Missile Command, 1971.

51. Hosokawa, I., "A Simplified Analysis for Transonic Flows Around Thin Bodies", Symposium Transonicum, Editor, K. Oswatitsch, Springer-Verlag, Berlin, 1964, pp. 184-199.

52. Crown, J.C., "Calculation of Transonic Flow Over Thick Airfoils by Integral Methods", AIAA J, Vol. 6, pp. 413-423, March 1968.

53. Ruppert, P.E., "Analysis of Transonic Flow by Means of Parametric Differentiation", Rept. 65-2, November 1965, Massachusetts Institute of Technology, Cambridge, Mass.

54. Knechtel, E.D., "Experimental Investigation at Transonic Speeds of Pressure Distributions Over Wedge and Circular Arc Airfoil Sections and Evaluation of Perforated-Wall Interference", NASA TN D-15, August 1959.

55. Erdos, J., Baronti, P., and Elzweig, S., "Transonic Viscous Flow Around Lifting Two-Dimensional Airfoils", AIAA Paper No. 72-678, June 1972.

56. Sichel, M., "Theory of Viscous Transonic Flow - A Survey", AGARD Conf. Proceed. No. 35, September 1968.

57. Lock, R.C., Powell, B.J., Sells, C.C.L., and Wilby, P.G., "The Prediction of Aerofoil Pressure Distributions for Sub-Critical Viscous Flows", AGARD Conf. Proceed. No. 35, September 1968.

58. Varga, R.S., "Matrix Iterative Analysis", Prentice-Hall, Inc., 1962.

59. Van Dyke, M.D., "Second Order Subsonic Aerofoil Theory Including Edge Effects", NACA Rep. 1274, 1956.

60. Nieuwland, G.Y., "Transonic Potential Flow Around a Family of Quasi-Elliptical Aerofoil Sections", N.L.R. Tech. Rep. 172 (1967).

61. Bagley, J.A., "Aerodynamic Principles for the Design of Swept Wings (Section 6.1)", Progress in Aeronautical Sciences, 3, 1-81, Pergamon Press, 1962.

62. Firmin, M.C.P., and Cook, T.A., "Detailed Exploration of the Compressible Viscous Flow over Two-Dimensional Aerofoils at High Reynolds Numbers", Paper presented at 6th I.C.A.S. Conference, Munich, September 1968.

63. LaBrujere, T.E., Loeve, W., and Slooff, J.W., "An Approximate Method for the Determination of the Pressure Distribution on Wings in the Lower Critical Speed Range", AGARD Conf. Proceed. No. 35, September 1968.

64. Garabedian, P.R., and Korn, D.G., "Analysis of Transonic Airfoils", Comm. on Pure and Applied Math., Vol. XXIV, 1971.

65. Kacprzynski, J.J., Ohman, L.H., Garabedian, P., and Korn, D.G., "Analysis of the Flow Past a Shockless Lifting Airfoil in Design and Off-Design Conditions", N.R.C. Report, Ottawa, To Appear.

66. Oswatitsch, K., "New Results on Steady, Two-Dimensional Transonic Flow", AGARD Conf. Proceed. No. 35, September 1968.

67. Magnus, R., and Yoshihara, H., "Inviscid Transonic Flow over Airfoils", AIAA J., Vol. 8, No. 12, December 1970.

68. Stivers, L., "Effects of Subsonic Mach Number on the Forces and Pressure Distribution of Four NACA 64A - Series Airfoil Sections", TN-3162, 1954, NACA.

69. Murman, E.M., and Cole, J.D., "Calculation of Plane Steady Transonic Flows", AIAA J., Vol. 9, No. 1, January 1971.

70. Bailey, F.R. and Steger, J., "Relaxation Techniques for Three-Dimensional Transonic Flow About Wings", AIAA Paper No. 72-189, January 1972.

71. Krupp, J.A. and Murman, E.M., "The Numerical Calculation of Plane Steady Transonic Flows Past Thin Lifting Airfoils", Boeing Scientific Research Laboratories.

72. Klunker, E.B., "Contribution to Methods for Calculating the Flow About Thin Lifting Wings at Transonic Speeds-Analytic Expressions for the Far Field", NASA TN D-6530, November 1971.

73. Wu, J.M., "Supplementary Material for the Short Course of Transonic Flow Problems", Univ. of Tenn. Space Institute, June 1973.

74. Pearcey, H.H., "Shock-Induced Separation and Its Prevention by Design and Boundary-Layer Control", Boundary Layer and Flow Control, Pergamon Press, 1961.

75. Antonatos, P.P., "Fundamental Influence of Reynolds Number", Lecture Notes, Univ. of Tenn. Space Institute Short Course on Transonic Flow Problems, June 1973.

76. Blackwell, J.A., Jr., "Effect of Reynolds Number and Boundary Layer Transition Location on Shock-Induced Separation", AGARD Conf. Proceed. No. 35, September 1968.

77. Moulden, T.H., "Physical Aspects of the Transonic Flow over Wings and Airfoils", Notes for Univ. of Tenn. Space Institute Short Course on Transonic Flow Problems, June 1973.

78. Thomas, F., "Die Ermittlung Der Schüttelgrenzen von Tragflügeln Im Transsonischen Geschwindigkeits Bereich", Jahrbuch, 1966.

79. Seddon, J., "The Flow Produced by Interaction of a Turbulent Boundary Layer with a Normal Shock Wave of Strength Sufficient to Cause Separation", Aeronautical Research Council R&M No. 3502, 1967.

80. Coles, D., "The Law of the Wake in the Turbulent Boundary Layer", J. Fluid Mech. Vol. I, pp. 191-226, 1956.

81. Wehofer, S., and Moger, W.C., "Transonic Flow in Conical Convergent and Convergent-Divergent Nozzles with Nonuniform Inlet Conditions", AIAA Paper No. 70-635, June 1970.

82. Thornock, R.L., "Experimental Investigation of the Flow Through Convergent Conical Nozzles", Document No. DG-20375, The Boeing Company, September 1968.

83. Prozan, R.J., "Transonic Flow in a Converging-Diverging Nozzle", LMSC/AREC D162177, 1969.

84. Love, E.S., Grigsby, C.E., Lee, L.P. and Woodling, M.J., "Experimental and Theoretical Studies of Axisymmetric Free Jets", NASA TR R-6, 1959.

85. Deep, R.A., and Henderson, J.H., "Exhaust Nozzle Integration Problems for Rockets and Aircraft at Transonic Speeds", U.S. Army Missile Research, Development, and Eng. Lab., Redstone Arsenal, Al., June 1973.

86. Korst, H., Chow, W., and Zumwalt, F., "Research on Transonic and Supersonic Flow of a Real Fluid at Abrupt Increases in Cross Section", University of Illinois Report ME TN 392-5, December 1959 (I Ed.), October 1964 (II Ed.).

87. Korst, H.H., "A Theory for Base Pressures in Transonic and Supersonic Flow", Journal of Applied Mech., December 23, 1956.

88. Rakich, J.V., "A Method of Characteristics for Steady Three-Dimensional Supersonic Flow with Application to Inclined Bodies of Revolution", NASA TN D 5341, October 1969.

89. Strom, C.R., "The Method of Characteristics for Three-Dimensional Real-Gas Flows", Air Force Flight Dynamics Laboratory, TR AFFDL-TR-67-47, July 1967.

90. Powers, S.A., Niemann, A.F., Jr., Der, J., Jr., et al, "A Numerical Procedure for Determining the Combined Viscid-Inviscid Flow Fields Over Generalized Three-Dimensional Bodies", TR AFFDL-TR-124, Vol. I and II, December 1967.

91. Cleary, J.W., "An Experimental and Theoretical Investigation of the Pressure Distribution and Flow Fields of Blunted Cones at Hypersonic Mach Numbers", NASA TN D-2969, 1965.

92. Korst, H.H., and Divita, J.S., "Investigation of Integrated Booster-Sustainer-Afterbody Design on Overall Vehicle Performance", Rocketdyne Internal Report LAP-69-204, March 1969.

93. Baughman, L.E., and Kochendorfer, F.O., "Jet Effects on Base Pressures of Conical Afterbodies at Mach 1.91 and 3.12", NACA RM E57E06, 1957.

94. Englert, G.W., Vargo, D.J., and Cubbison, R.W., "Effect of Jet Nozzle Expansion Ratio on Drag of Parabolic Afterbodies", NACA RM-E54B12, April 1954.

95. Maslowe, S.A. and Benson, J.L., "Computer Program for the Design and Analysis of Hypersonic Inlets-Final Report", Lockheed-California Company, 18079, March 1964.

96. Cohen, N.B., "Boundary-Layer Similar Solutions and Correlation Equations for Laminar Heat Transfer Distribution in Equilibrium Air at Velocities up to 41,000 Feet Per Second", NASA TR R-1118, 1961.

97. Miller, L.D., "A Machine Program for Computing a Turbulent Boundary Layer with Pressure Gradient and Dissociation", Lockeed Report 16103, November 1962.

98. Sommer, S.C., and Short, B.J., "Free Flight Measurements of Turbulent-Boundary-Layer Skin Friction in the Presence of Severe Aerodynamic Heating at Mach Number from 2.8 to 7.0" NACA TN 3391, March 1955.

99. Baxendale, M.L., Bruckman, F.A., and Shaar, R.H., "Wave Drag Computer Program", Lockheed Report No. 20553, March 1967.

100. Berrier, B.L., and Wood, F.H., Jr., "Effect of Jet Velocity and Axial Location of Nozzle Exit on the Performance of a Twin-Jet Aferbody Model at Mach Numbers up to 2.2", NASA TN D5393, September 1969.

101. Erdos, J. and Pallone, A., "Shock-Boundary Layer Interaction and Flow Separation", Proceedings of the 1962 Heat Transfer and Fluid Mechanics Institute", F. Edward Ehlers, et al, Editors, Stanford University Press 1962.

102 Lees, L. and Reeves, B.L., "Supersonic Separated and Re-Attaching Laminar Flows: I. General Theory and Application to Adiabatic Boundary Layer/Shockwave Interactions", AIAA J., Vol. 2, No. 11, November 1964, pp, 1907-1920.

103. Chapman, D.R., Kuehn, D.M., and Larson, H.K., "Investigation of Separated Flows in Supersonic and Subsonic Streams with Emphasis on the Effect of Transition", NACA TN No. 1356, 1958.

104. Prozan, R.J., "Development of a Method of Characteristics Solution for Supersonic Flow of an Ideal, Frozen, or Equilibrium Reacting Gas Mixture, LMSC/HREC", A782535, 1966.

105. Wasko, R.A., and Harrington, D.E., "Performance of a Collapsible Plug Nozzle Having Either Two Position Cylindrical or Variable Angle Floating Shrouds at Mach Numbers From 0 to 2.0", NASA TM X-1657, October 1968.

106. Humphreys, R.P., Thompson, H.D. and Hoffmann, J.D., "Design of Maximum Thrust Plug Nozzles for Fixed Inlet Geometry", AIAA Paper No. 71-40, January 1971.

107. Hall, C.R. and Mueller, T.J., "An Analytical and Experimental Study of Nonuniform Plug Nozzle Flow Fields", AIAA Paper No. 71-41, January 1971.

108. Migdal, D., "Supersonic Annular Nozzles", AIAA Paper No. 71-43, January 1971.

109. Chow, W.L. and Addy, A.L., "Interaction Between Primary and Secondary Streams of Supersonic Ejector Systems and Their Performance Characteristics", AIAA J., Vol. 2, pp. 686-695, April 1964.

110. Chamay, A.J. (Pratt and Whitney Aircraft), "Exploratory Research Program for Turbo-Propulsion Exhaust Systems", Volume II, "Advanced Concepts", AFFAPL-TR-68-103, Volume II, September 1968.

111. Bastianon, R.A., "Numerical Calculation of a Supersonic Three-Dimensional Jet Plume", Ph.D. Dissertation Published by University Microfilms Limited, High Wycomb, England, A Xerox Company, Ann Arbor, Michigan, USA, 1971.

112. Chapman, D.R., "An Analysis of Base Pressure at Supersonic Velocities and Comparison with Experiment", NACA, Report 1051, 1950.

113. Korst, W.H. and Chow, A.L., "Non-Isoenergetic Turbulent Jet Mixing Between Two Compressible Streams at Constant Pressure", NASA CR-419, 1966.

114. Street, T.A., "Base Pressure Program for a Body of Revolution with Nozzle Flow", U.S. Army Missile Command Report No. RF-TM-64-2, January 1964.

115. Kessler, T.J., "Two-Stream Mixing with Finite Initial Boundary Layers", AIAA J., Vol. 5, No. 2, February 1967, pp. 363-364.

116. Reeves, B.L., and Lees, L., "Theory of the Laminar Near Wake of Blunt Bodies in Hypersonic Flow", AIAA J., Vol. III, No. 11, November 1965, pp. 2061-2074.

117. Alber, I.E. and Lees, L., "Integral Theory for Supersonic Turbulent Base Flows", AIAA J., Vol. 6, No. 7, July 1968, pp. 1343-1351.

118. Stewartson, K., "Correlated Incompressible and Compressible Boundary Layer", Proc. Royal Society, Vol. 200, 1949, p. 84.

119. Lee, S.C. and Harsha, P.T., "The Use of Turbulent Kinetic Energy in Free Mixing Studies", ARO, Inc., Arnold Air Force Station, Tennessee, 1969.

120. Laster, M.L., and Snyder, W.T., "Characteristic Equations for Parallel Free Jet Turbulent Mixing", AEDC, April 1969.

121. Erdos, J. and Zakkay, V., "Numerical Solution of Several Steady Wake Flows of the Mixed Supersonic/Subsonic Type by a Time-Dependent Method and Comparison with Experimental Data", AIAA Paper No. 69-649, June 1969.

UNCLASSIFIED
Security Classification

DOCUMENT CONTROL DATA - R & D

(Security classification of title, body of abstract and indexing annotation must be entered when the overall report is classified)

1. ORIGINATING ACTIVITY *(Corporate author)* AFFDL Wright-Patterson AFB, Ohio 45433	2a. REPORT SECURITY CLASSIFICATION UNCLASSIFIED 2b. GROUP N/A

3. REPORT TITLE
REVIEW OF METHODS OF SOLUTION OF AFTERBODY/EXHAUST NOZZLE FLOW FIELDS

4. DESCRIPTIVE NOTES *(Type of report and inclusive dates)*

5. AUTHOR(S) *(First name, middle initial, last name)*
Dr. Wladimiro Calarese

6. REPORT DATE January 1974	7a. TOTAL NO. OF PAGES 160	7b. NO. OF REFS 121
8a. CONTRACT OR GRANT NO. b. PROJECT NO. 1476 c. Task 14760204 d.	9a. ORIGINATOR'S REPORT NUMBER(S) AFFDL-TR-74-108 9b. OTHER REPORT NO(S) *(Any other numbers that may be assigned this report)*	

10. DISTRIBUTION STATEMENT
Approved for public release; distribution unlimited

11. SUPPLEMENTARY NOTES None	12. SPONSORING MILITARY ACTIVITY AFFDL, WPAFB

13. ABSTRACT

The present work consists of a review of methods of solution of afterbody/exhaust nozzle flow fields for different flight regimes. For the transonic regime airfoil solutions are also presented. A comparison between various theories and experiments is made wherever considered necessary to show the state-of-the-art. Most of the available theories are selected and correlated.

DD FORM 1 NOV 65 1473

UNCLASSIFIED
Security Classification

14. KEY WORDS	LINK A		LINK B		LINK C	
	ROLE	WT	ROLE	WT	ROLE	WT
Subsonic Flow						
Transonic Flow						
Supersonic Flow						
Viscous/Inviscid Flow Fields						
Jet Plumes						
Base Flow						

☆U.S.Government Printing Office: 1974 — 657-013/100